LOAN DOCUMENT

PHOTOGRAPH THIS SHEET

DTIC ACCESSION NUMBER

LEVEL

INVENTORY

D

NRL-MR-1177

DOCUMENT IDENTIFICATION

Jul 61

Approved for public release
Distribution Unlimited

DISTRIBUTION STATEMENT

HANDLE WITH CARE

ACCESSION FOR

NTIS GRA&I ☒

DTIC TRAC ☐

UNANNOUNCED ☐

JUSTIFICATION

BY

DISTRIBUTION/

AVAILABILITY CODES

DISTRIBUTION	AVAILABILITY AND/OR SPECIAL	
A-1		

DISTRIBUTION STAMP

DATE ACCESSIONED

DATE RETURNED

19960625 188

DATE RECEIVED IN DTIC

REGISTERED OR CERTIFIED NUMBER

PHOTOGRAPH THIS SHEET AND RETURN TO DTIC-FDAC

DTIC FORM 70A JUN 90

DOCUMENT PROCESSING SHEET

PREVIOUS EDITIONS MAY BE USED UNTIL STOCK IS EXHAUSTED.

LOAN DOCUMENT

27 JUN 1996

1177

UNCLASSIFIED

NRL Memorandum Report 1177

STATUS REPORT ON THERMOELECTRICITY

Dr. J. W. Davisson and Joseph Pasternak

Solid State Division

In Collaboration With:
B. B. Rosenbaum (BuShips)

July 1961

U. S. NAVAL RESEARCH LABORATORY
Washington, D.C.

NRL Memorandum Report No. 1177

STATUS REPORT ON THERMOELECTRICITY

Dr. J. W. Davisson

and

Joseph Pasternak

In Collaboration with

B. B. Rosenbaum (BuShips)

Technical Editing by Robert Peden, C-E-I-R

Approved By:

Paul H. Egli
U. S. Naval Research Laboratory

CONTENTS

FOREWORD

This is the seventh report in a series of quarterly reviews on the state of the art on thermoelectricity. The previous reports were numbers 901, 940, 969, 1037, 1089, and 1127. Report 1037 contains a listing of government contracts on thermoelectricity. Subsequent reports list only new contracts.

The services of C-E-I-R have been retained to assist in the preparation of this report.

The contents of this report are restricted to efforts in the United States. Every effort has been made to give a full description of the work on thermoelectricity, but important contributions may have been overlooked. It is hoped that organizations with pertinent information do not wait for a specific invitation to cooperate in this report. Information may be sent to the Naval Research Laboratory, Code 6430, Washington 25, D. C.

AUTHORIZATION

NRL Problem No. 64P03-03

STATUS REPORT ON THERMOELECTRICITY

INTRODUCTION

Progress in Thermoelectricity continues on schedule. A gratifying number of materials improvements have appeared both in government sponsored and industry sponsored work. Some of the results are still proprietary such as the material that appears to have a Z that approaches 1×10^{-3} at 1800°C. Others have been announced such as the Bell Laboratory work that produced Z of 5×10^{-3} at 80°K. Some of the announcements (including some of the data in this issue concerning extremely high Z factors) are highly suspect but some very respectable gains have been confirmed. While it is encouraging that Z values continue to rise, some of the most important results are on materials with only moderate Z's at moderately high temperatures but with other virtues that make them extremely valuable.

It is important to recognize that efficiency per se is a dominating requirement in only a few power source requirements. It is widely accepted that efficiency can be sacrificed for weight, size, silence and long lived, unattended reliability in many military and commercial applications. It may be less obvious that a low efficiency results in no sacrifice in many applications. In waste heat utilization, capital investment is the important consideration. Installation and maintenance costs are the determining factors and the efficiency of thermoelectric materials is related only indirectly to these costs. With a more efficient material, fewer pounds of thermocouples are required to produce a kilowatt, but a less efficient material may cost so much less per pound that it is the better investment. For example, one design study showed that to produce a kilowatt generator for $100,

material with a Z of 1×10^{-3} would have to be produced for $5.00 per pound of thermocouples. A Z of 50×10^{-3} would allow spending $35.00 per pound, and otherwise it didn't matter which was used. For these reasons it is encouraging that materials are appearing without tellurium or other expensive ingredients.

With a broader spectrum of materials available, the problem of design and fabrication of devices becomes considerably more complex, and as indicated in the device discussions of this report, this whole facet of the problem is in a very primitive state. Despite the fact that commercially useful devices are in production, and that a number of military devices are in an advanced state of development, the whole present generation of devices barely hints at what can be achieved by improved engineering. The problems to be solved are unfortunately not easy, but neither are they unsoluble. Enough progress on various organizations to make it clear that compact, economical thermoelectric generators will be achieved.

To pursue this goal most efficiently is a difficult problem because of the many interrelated parameters. No general solutions are expected to the electrode problem or to materials fabrication techniques, or to encapsulation or to mechanical mounting details. Each will be a new problem with a new material, and each of these details can dominate the success of a design. Accordingly, module fabrication is likely to go through many generations of gradual improvement. In order to reduce duplication and waste motion to a minimum, it is hoped that the same excellent government industry collaboration that has occurred in materials development can be continued on the engineering problems.

THERMOELECTRIC MATERIALS DEVELOPMENT

Westinghouse Research Laboratories* has prepared and partially investigated the electrical properties of a number of compounds which had anistropic effective mass tensors or which had anions or cations that occurred in clusters. A survey was made of compounds having cubic or near cubic structures which included GeTe, PbTe and $AgSbTe_2$. The efficiency of MnTe was improved by dissolving up to 6% Li in it.

Prepared samples of $CoSb_3$ had a Seebeck coefficient of about + 120 μV/°C and a resistivity of 0.0055 ohm-cm. Those doped with 0.05 Te showed -163 μV/°C and a 0.0006 ohm-cm. Samples of $CoAs_3$ had +155 μV/°C and 0.008 ohm-cm. The density of these specimens were very poor.

$MoTe_2$ is p-type and has a resistivity of several hundred ohm-cm. $MoTe_{1.95}$ has a Seebeck coefficient of +70 μV/°C and a resistivity of about 200 ohm-cm.

Listed in Table I below are the structures, thermoelectric powers, and resistivity ranges for a number of transition metal ditellurides.

TABLE I

Ditelluride Periodic Chart

	Mn	Fe	Co	Ni
S (μV/°C)	Pyrite +200 - + 400	Marcastite +27 - + 59	Marcasite -20	CdL_2 +8
ρ (ohm-cm	2- .07	.05 - .004	.0001	.00006
		Ru	**Rh**	**Pd**
S		Pyrite	Pyrite	CdL_2
ρ		-140 - -180 02-03	-13 .0002	-2 .00007
	Re	**Os**	**Ir**	**Pt**
S	?	Pyrite	Pyrite	CdL_2
ρ	+487 20,000	-65 - -82 .008		-5 .006

*Department of the Navy contract NObs-78365. Quarterly Progress Report No. 3

The results of anti-doping Ru, Os and Co by adding Sb are given in Table II below:

TABLE II

	S (μV/°C)	ρ (ohm-cm)
$RuTe_{1.95}Sb_{.05}$	+232	2.1
$OsTe_{1.95}Sb_{.05}$	+113*	.007
$OsTe_{1.9}Sb_{.1}$	+105	-
$CoTe_{1.95}Sb_{.05}$	-14.7	.0001

*Erratic behavior at this composition. S as low as +2.6. Best value +113.

Anti-doping was successful in Ru and Os but not with Co indicating that $CoTe_2$ will probably not be a useful thermoelement. Cation doping apparently would not work in $OsTe_2$. Changes in the Os:Te ratio did not affect the electrical properties.

The results obtained on transition metal diantimonides and dibismuthides are given in Table III below:

TABLE III

Compound	Structure	S (μV/°C)	ρ (ohm-cm)
$PdSb_2$	Pyrite	+3 to + 17.6	1.3×10^{-4}
$PtSb_2$	Pyrite	+ 25 to + 54	1.2×10^{-3}
$PtBi_2$	Pyrite	- 1 to + 7	1.4×10^{-3}
$CrSb_2$	Marcasite	- 12 to - 25	6×10^{-4} to 1.3×10^{-3}
$FeSb_2$	Marcasite	+ 32 to + 35	1.2×10^{-3}

$PtSb_2$ was anti-doped successfully by a substitution of .05 Te giving S = -53.1 and ρ = .0015. The compound $PtSb_2$ is one of the few congruent melting pyrites (m.p. 1226°C). With .05 Te the sample appeared to melt between 600 and 700°C.

Seebeck and resistivity measurements made on titanium sulfide compounds in the compositional range $TiS_{1.93}$ - $TiS_{1.99}$ showed that S decreased and ρ increased as the sulfur concentration was lowered. Maximum values of S and ρ of titanium disulfide are reached at approximately 300°C. At high temperatures ρ drops rapidly, See Figure 1.

Room temperature resistivities and Seebeck coefficients of a number of prepared cubic compounds are given in Table IV below:

TABLE IV

Room Temperature Electrical Properties of Cubic Compounds

	$\rho \times 10^4$ (ohm-cm)	S (μV/°C)
	Rock Salt or Distorted Rock Salt	
Sn_3As_2	.5	+ 7
SnAs	.12	+ 2.5
$Sn_4As_2Te_2$	.4	+ 20
Sn_4AsTe_3	1.0	+ 25
	Fluorite	
CuZnSb	4.9	+25
CuZnAs	8.6	+12
CuSnAs	1.2	+ 7
	Zinc Blende	
$ZnSnAs_2$	800	+ 177
$Zn_{.501}Sn_{.499}As_2$	62	+ 110
$CuAsSe_2$	3.5	+ 1
Cu_3AsSe_4	36	+ 311

It appeared as if the tin-arsenic system gave compounds exhibiting metallic conduction. The fluorides examined also appeared to be metallic.

Thermoelectric properties of a $Zn_{.9992}Ag_{.0008}Sb_{.999}Sn_{.001}$ composition are given in Figure 2. In preparing the sample an optimum doping concentration of silver in ZnSb was considered to be 0.08%. Tin was added as a result of enhanced mobilities observed for ZnSb with small additions. Properties of ZnSb are shown in Figure 3.

In order to obtain optimumally doped PbTe for use in temperature range 450-1000°K, six samples of varying doping concentration had been prepared. Their electrical and thermal properties are shown in Figures 4-9. Thermal conductivity measurements had not been completed on the .04, .07 and .10% Bi samples, so calculated values have been shown. The thermal conduction of the heavily doped samples was extrapolated to ~ 700° from the highest temperature at which measurements were made ~500°C.

A sample of composition $(CeS)_{1.39}(SrS)_{.07}$ in which 30% of the Ce vacancies have been filled with Sr atoms had been prepared. Its electrical and thermal properties are shown in Figure 10 together with data for a $CeS_{1.38}$ sample. The mobility was increased at low temperatures but there was no improvement in the useful temperature range above 900°K. Addition of Sr S appeared to increase the thermal conductivity; however the difference might have been due to experimental error. $CeS_{1.38}$ appeared to be near optimum doping. The data on $CeS_{1.37}$ is shown in Figure 11. In all of the measurements on the Ce-S system considerable difficulty has been experienced with decomposition of the samples.

Investigation was made of the effect of decreased Se concentration on the solubility of Li in $Li_xMn_{1-x}Te_{.85}Se_{.15}$ system since it appeared that optimum was obtained at x = 0.04. $Li_xMn_{1-x}Te_{.95}Se_{.05}$ and $Li_xMn_{1-x}Te_{.97}Se_{.03}$ series of compounds were made. The value of x was varied from 0.01 to 0.05 in the 3% Se series and from .01 to 08 in the 5% Se series. Room temperature resistivities and Seebeck coefficients for these compounds are given in Tables V and VI which follow.

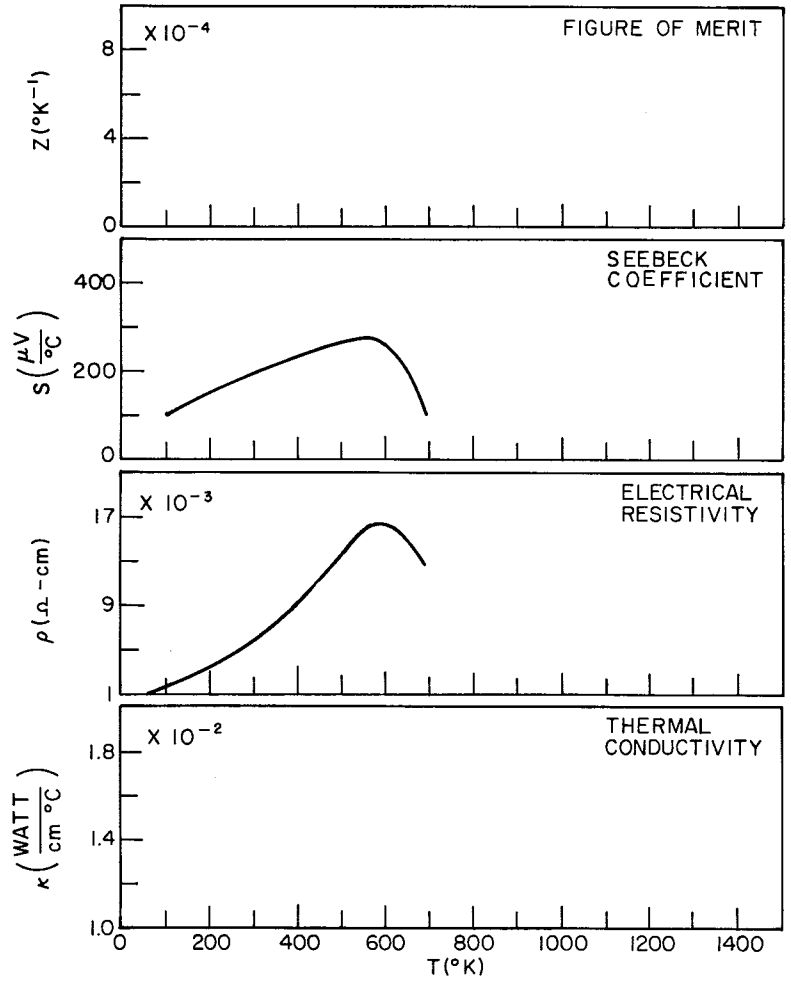

Fig. 1 - $TiS_{1.98}$ (n type)

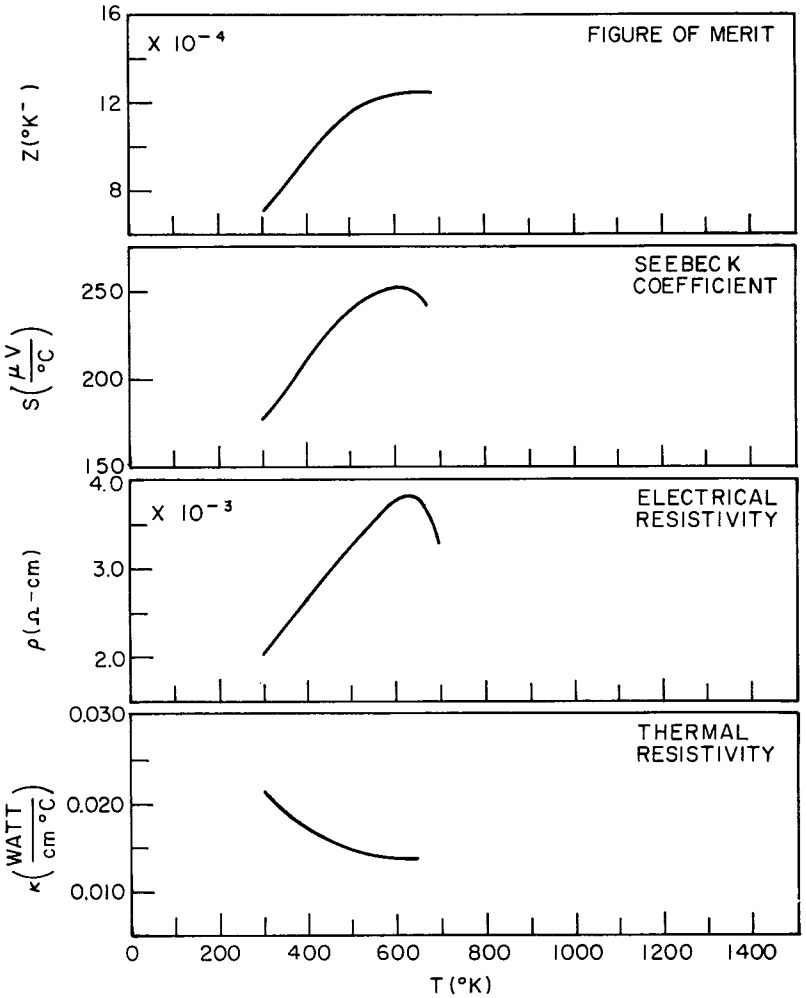

Fig. 2 - $Zn_{.9992}$ $Ag_{.0008}$ $Sb_{.999}$ $Sn_{.001}$ (p type)

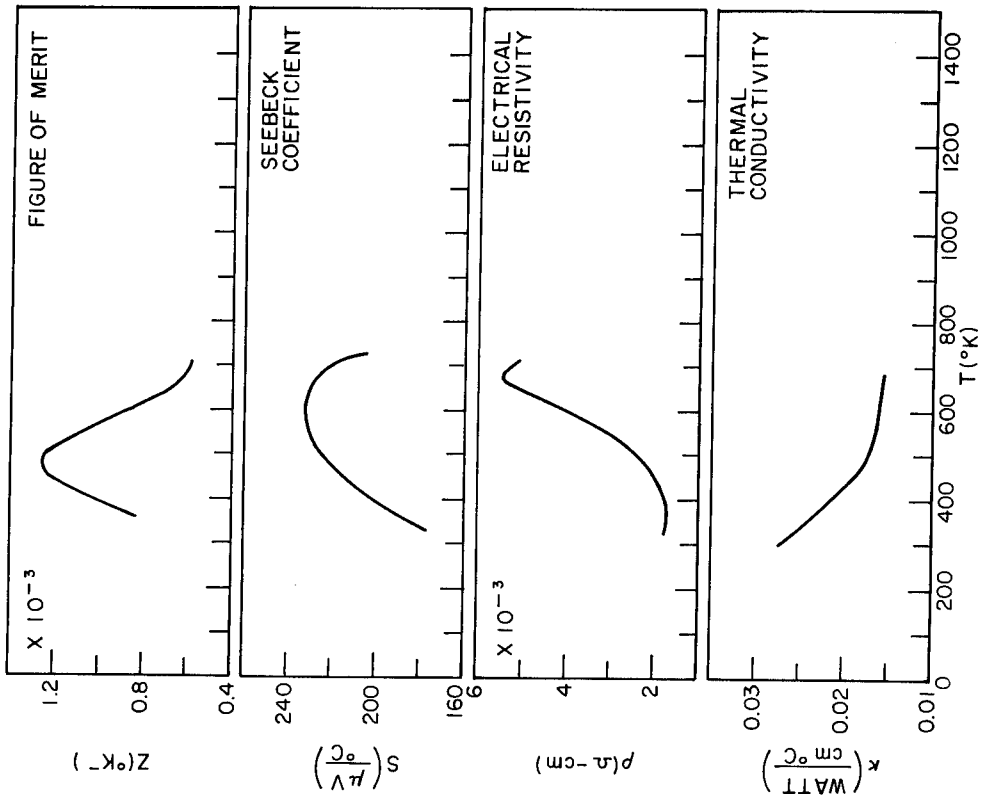

Fig. 3 - ZnSb (p type)

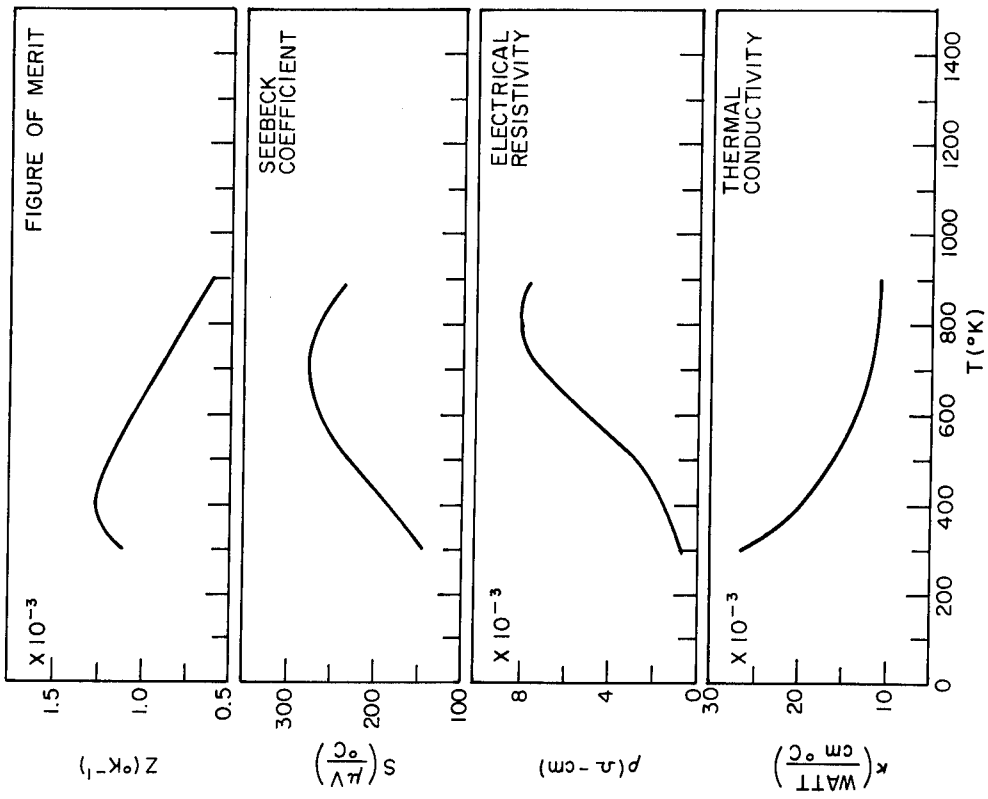

Fig. 4 - PbTe + 0.04% Bi (n type)

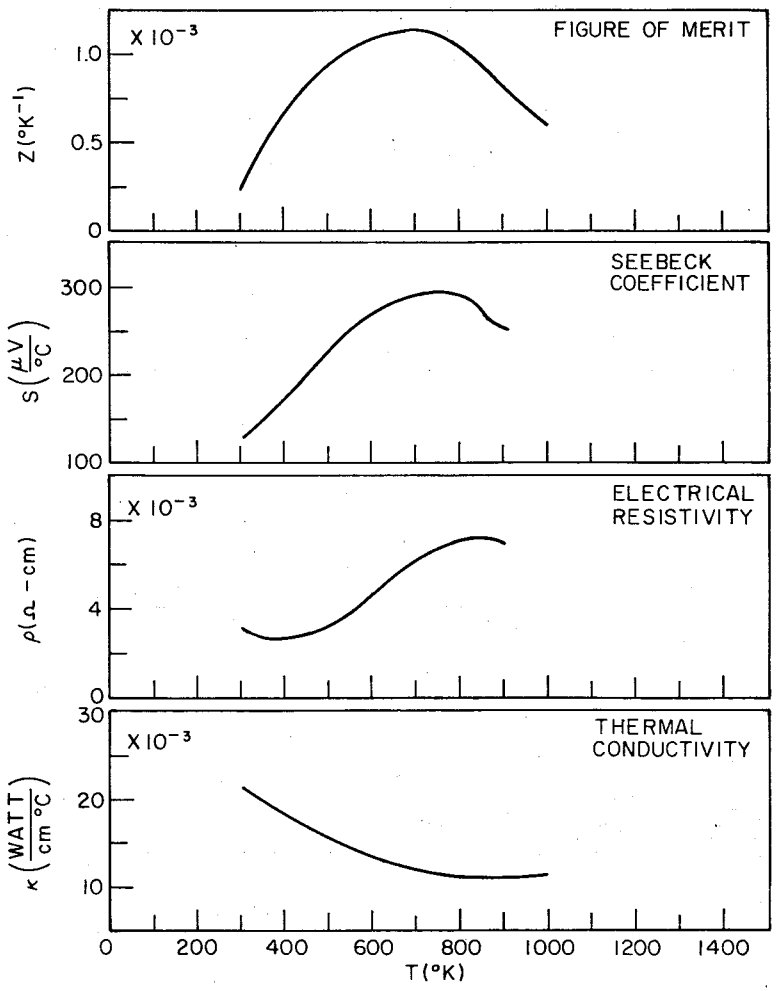

Fig. 5 - PbTe + 0.7% Bi (n type)

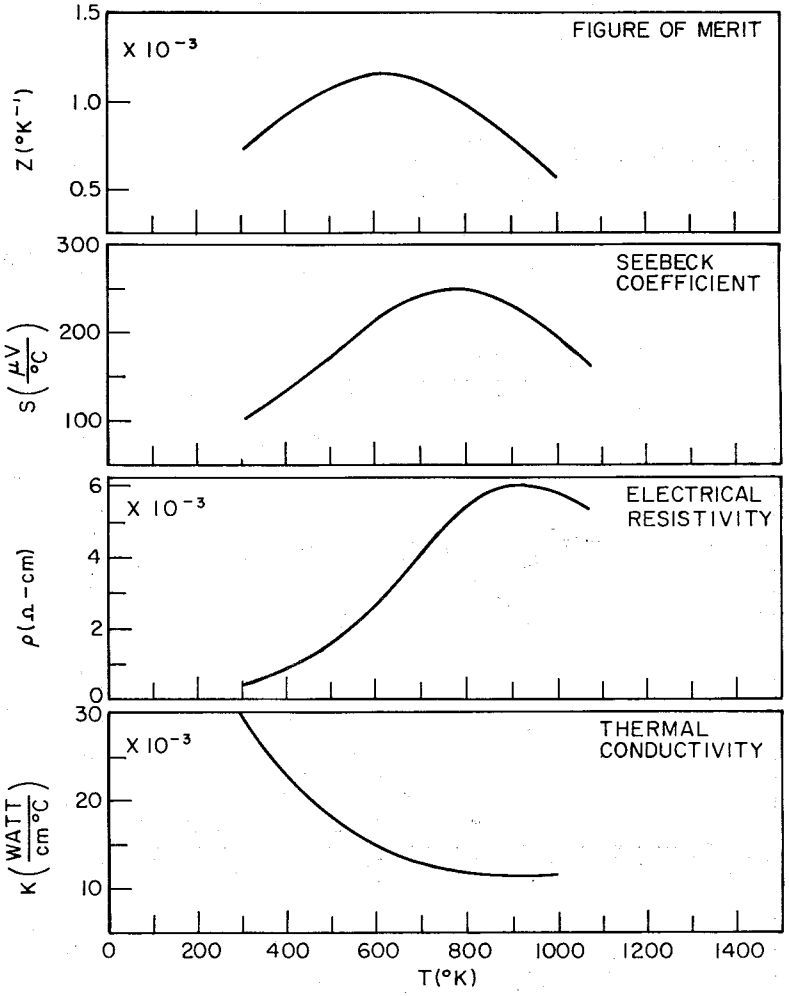

Fig. 6 - PbTe + 0.10% Bi (n type)

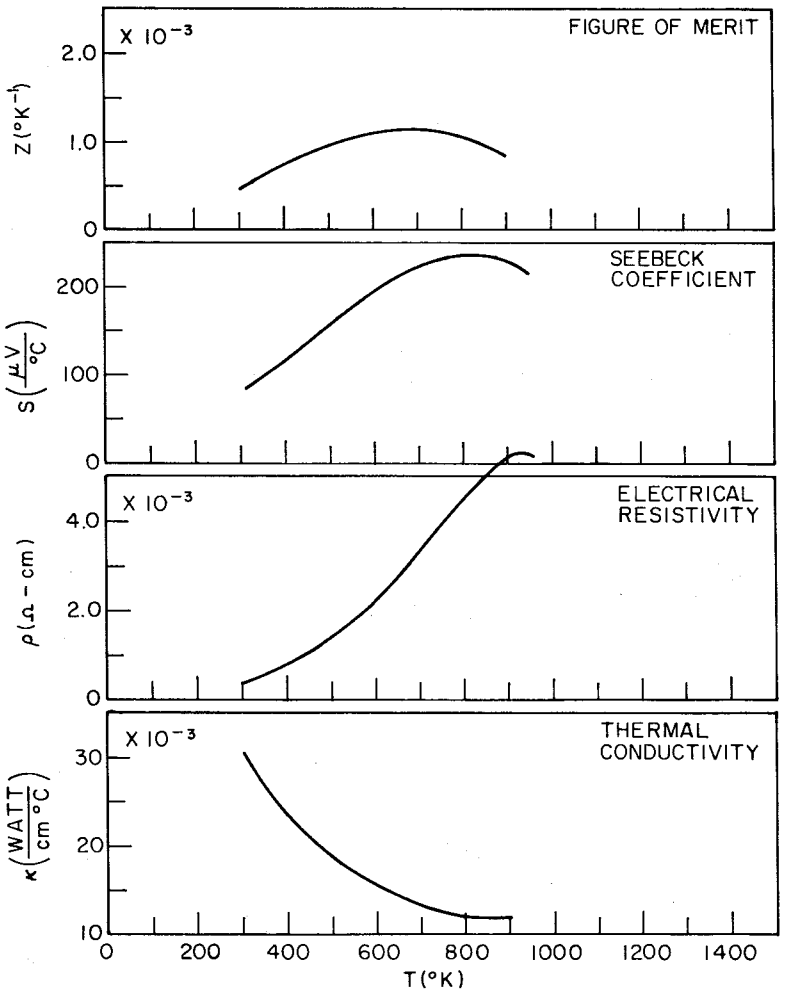

Fig. 7 - PbTe + 0.15% Bi (n type)

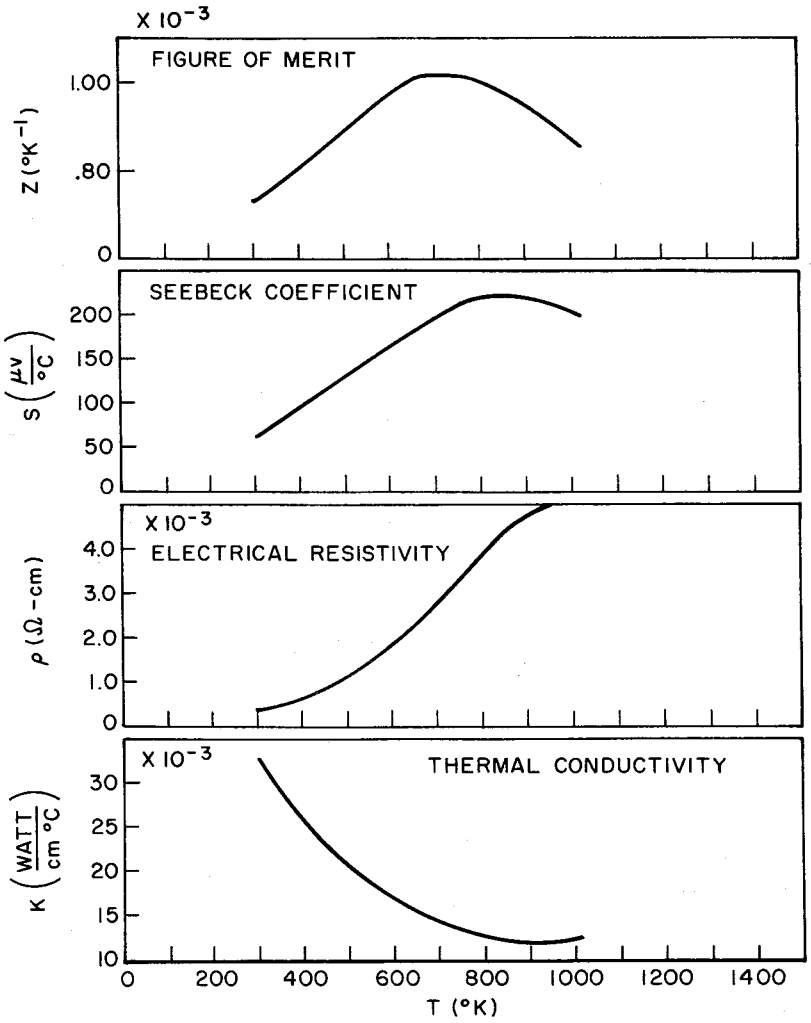

Fig. 8 - PbTe + 0.25% Bi (n type)

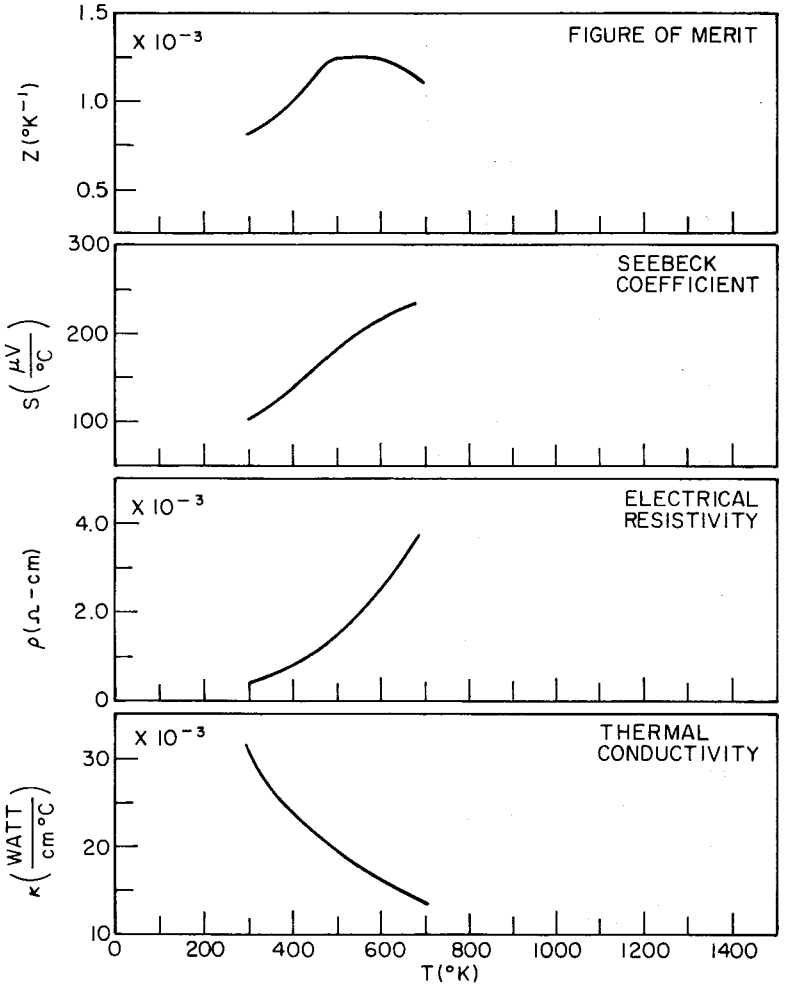

Fig. 9 - PbTe + 0.5% Pb + 0.2% Bi (p type)

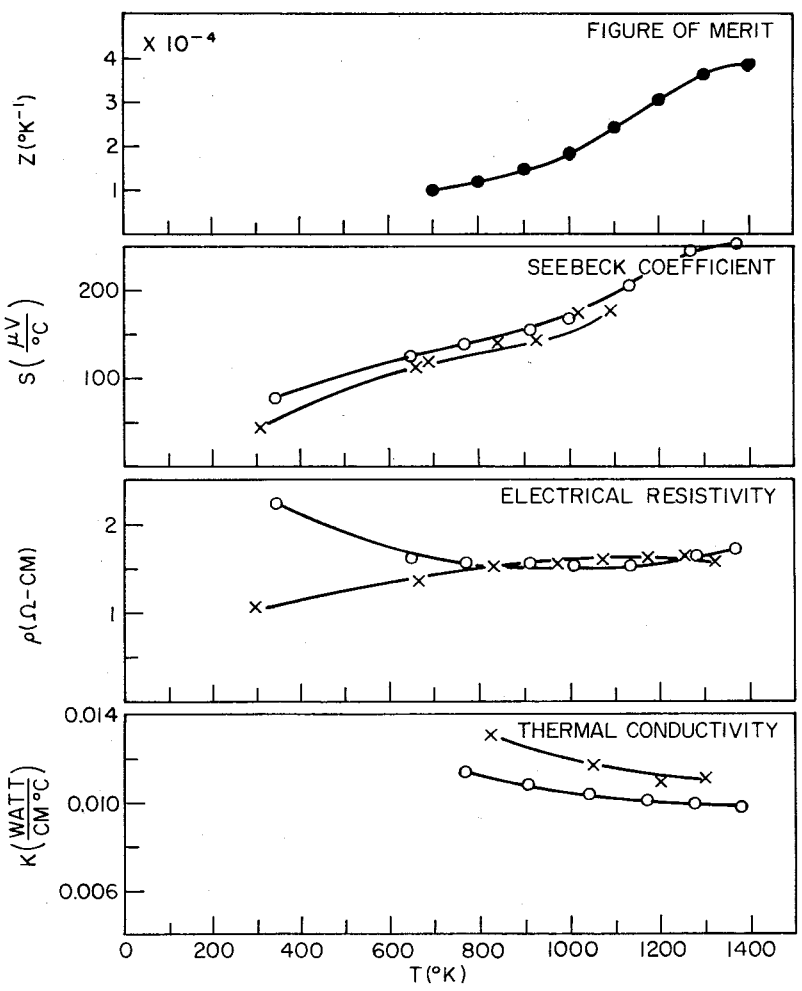

Fig. 10 - o-$CeS_{1.38}$ (p type)

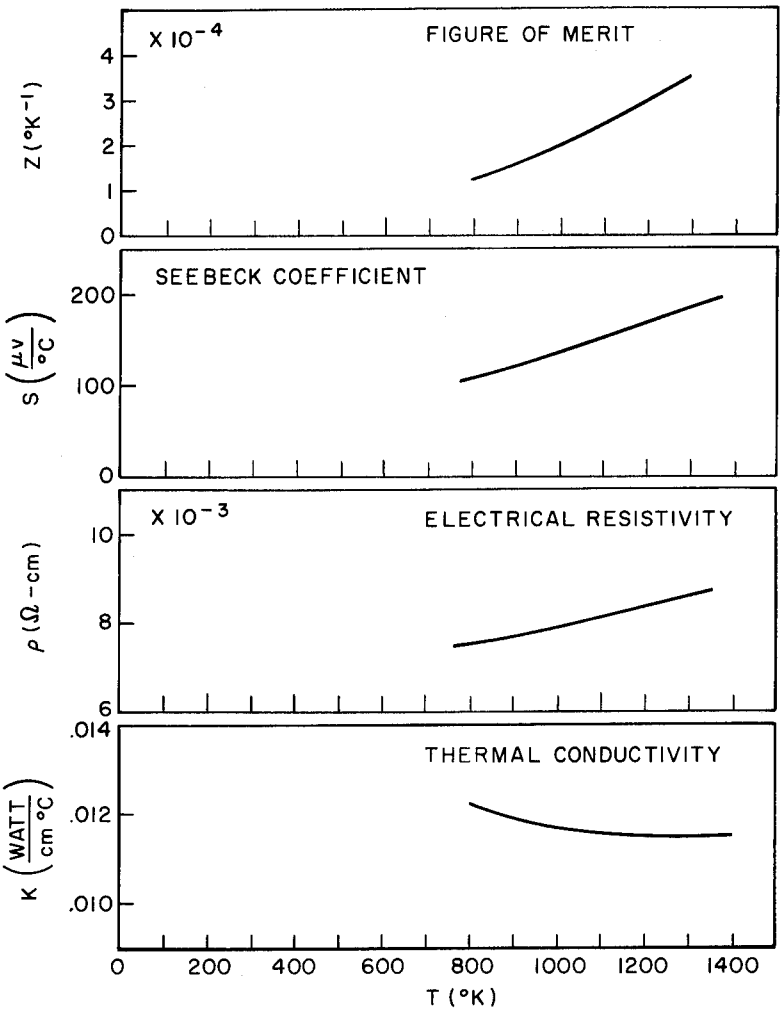

Fig. 11 - $CeS_{1.37}$ (p type)

TABLE V

$Li_xM_{1-x}Te_{.95}Se_{.05}$

x	Before Distillation S (μV/°C)	Before Distillation ρ (ohm-cm x 10^3)	After Distillation S (μV/°C)	After Distillation ρ (ohm-cm x 10^3)
.01	199	11.0	199	9.83
.02	136	5.04	139	4.71
.04	80.4	3.51	88.4	2.83
.06	56.4	2.57	60.5	3.13
.08	49.1	2.55	50.4	3.25

TABLE VI

$Li_xMn_{1-x}Te_{.97}Se_{.03}$

x	Before Distillation S (μV/°C)	Before Distillation (ohm-cm x 10^3)	After Distillation S (μV/°C)	After Distillation (ohm-cm x 10^3)
.01	199	9.19	-	--
.02	149	5.26	156	5.29
.03	114	3.41	123	3.47
.04	91.7	2.95	102	2.92
.05	75.2	3.18	94.4	2.83

Figure 12 shows the room temperature Seebeck coefficient as a function of Li composition. The solubility of Li does not appear to be affected by change in Se content and it appears that the Li solubility is about 6%.

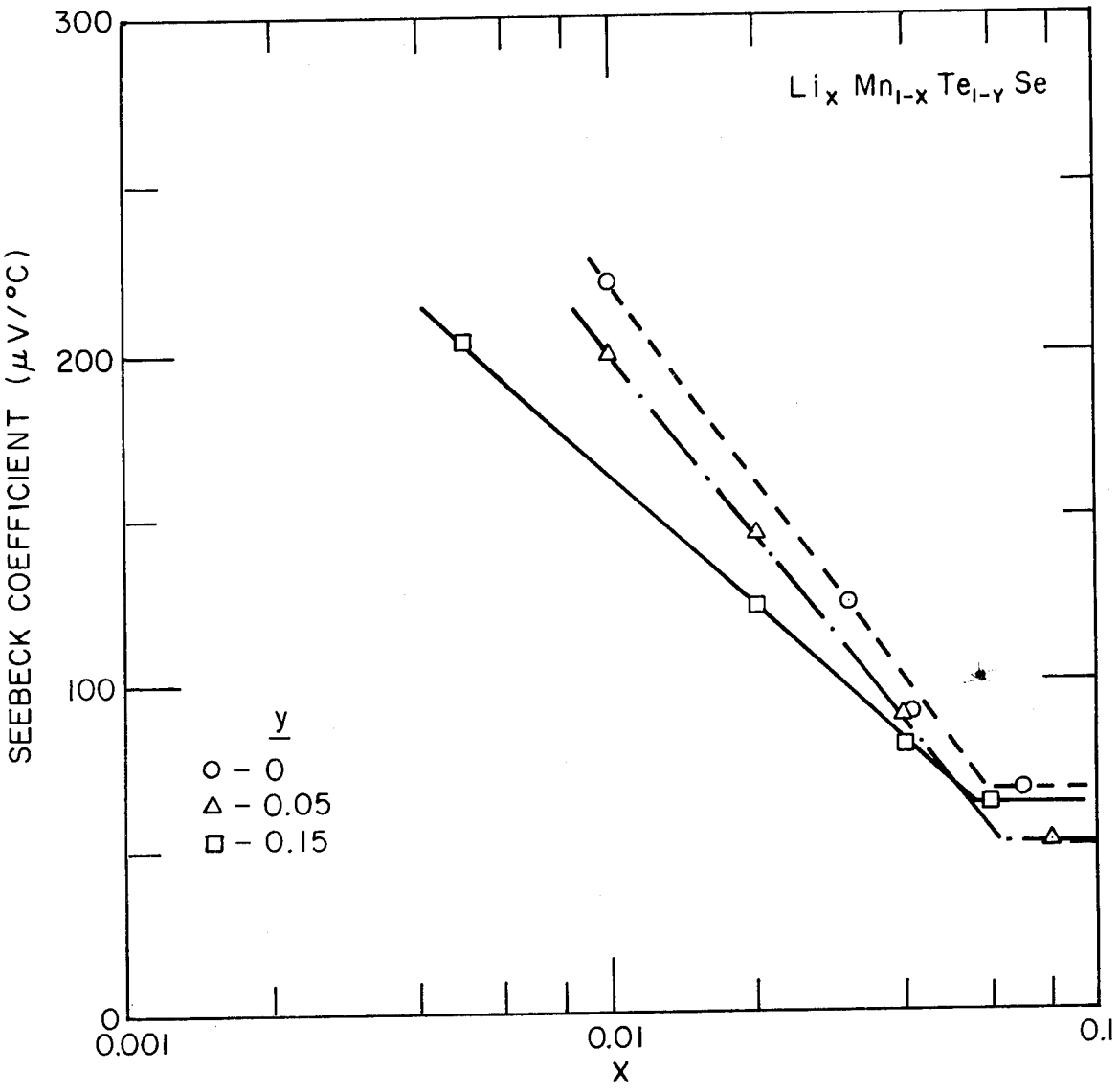

Fig. 12 - $Li_x Mn_{1-x} Te_{1-y} Se_y$ (p type)

Figure 13 shows the thermoelectric properties of a $Li_{.04}Mn_{.96}Te_{.95}Se_{.05}$ composition. Its high temperature figure of merit is greater than that of $Na_{.01}Mn_{.99}Te$ which had been the best high temperature p-type material available, Figure 14.

Investigation was made of the solubility of Li in MnTe. Table VII shows the room temperature Seebeck coefficients and resistivities with x varying from .0012 to .10 in the series $Li_xMn_{1-x}Te$.

TABLE VII

$Li_xMn_{1-x}Te$

	Before Distillation		After Distillation		Prepa-
x	S (μV/°C)	(ρ ohm-cm x 10^3)	S (μV/°C)	(ρ ohm-cm x 10^3)	ration
.0012			347	95	
.01	223	11.5	221	10.3	Li_2Te
.01	191	8.04	202	9.65	Li_2O
.03	116	3.85	126	3.50	Li_2Te
.03	112	4.49	119	4.27	Li_2O
.04	85.5	3.27	89.2	2.66	Li_2Te
*.04	80.9	3.40	88.6	2.49	Li_2O + MnO
.07	53.8	4.04	65.0	2.94	Li_2Te
.10	52.1	3.05	-	-	Li_2Te

*$Li_{.04}Mn_{.96}Te_{.90}O_{.10}$

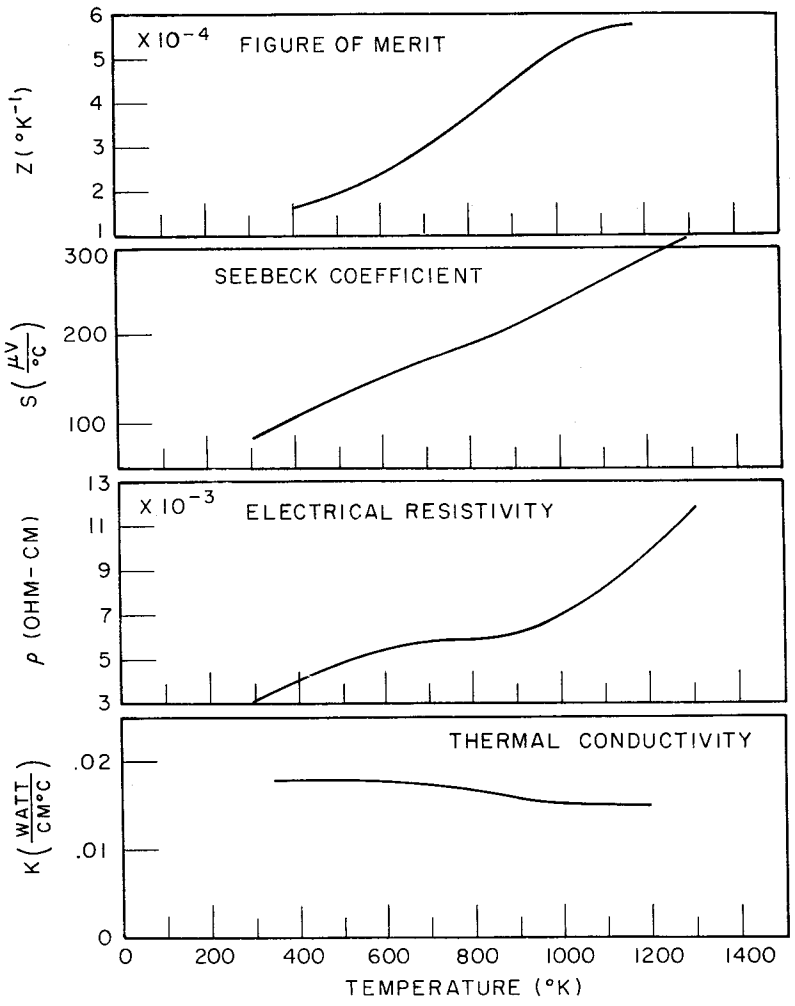

Fig. 13 - $Li_{.04}$ $Mn_{.96}$ $Te_{.95}$ $Se_{.05}$ (p type)

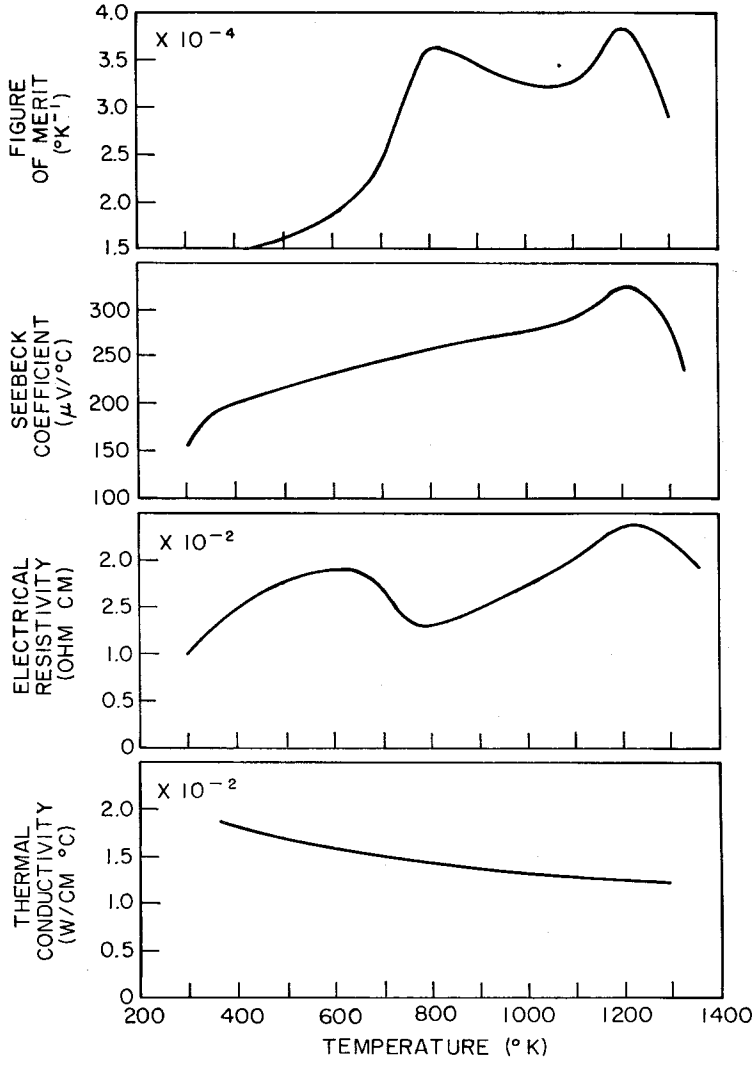

Fig. 14 - $Na_{.01}$ $Mn_{.99}$ Te (p type)

The thermoelectric properties of $Li_{.04}Mn_{.96}Te$ composition are given in Figure 15. Seebeck coefficients (at room temperature) as a function of Li content are given in Figure 16. The plot shows that the Li solubility limit is between 6 and 7%.

Large quantities of oxygen in the composition $Li_xMn_{1-x}Te$ composition do not appear to affect the electrical properties.

Composition $Li_{.05}Ni\ O$ has its thermoelectric properties given in Figure 17.

The Westinghouse Electric Company* is developing thermoelectric materials and surveying compounds having cubic or near cubic structures. Te doped $CoSb_3$ has nearly as high a differential efficiency as PbTe and also appears to have better mechanical properties and a lower vapor pressure. However, it has a lower figure of merit. Results of the study of a sample containing 5% Te, near optimum doping, are shown in Figure 18. The maximum Z occurring at 650°K is 0.85×10^{-3} as compared to roughly 1.25×10^{-3} for optimum doped PbTe at the same temperature.

$RhSb_3$ has the same structure as $CoSb_3$. At room temperature the Seebeck coefficient is +60 μV/°C and the resistivity is 1.0×10^{-3} ohm cm.

The more promising of a number of group seven and eight transition metal compounds were measured for electrical properties. With the exception of MnTe, the thermal conductivities of $OsTe_{1.9}Sb_{.1}$, PtP_2, FeS_2, and $FeAs_2$ were high. This with the low mobility indicated that none of these materials held promise as a thermoelement.

$PtAs_2$ changed from p to n-type at elevated temperatures suggesting that higher mobilities might be achieved in n-type samples. Selenium additions gave n-type samples but elevated firings resulted in a decrease

*Department of the Navy contract No. NObs 78365. Westinghouse Electric Company Quarterly Progress Report No. 4

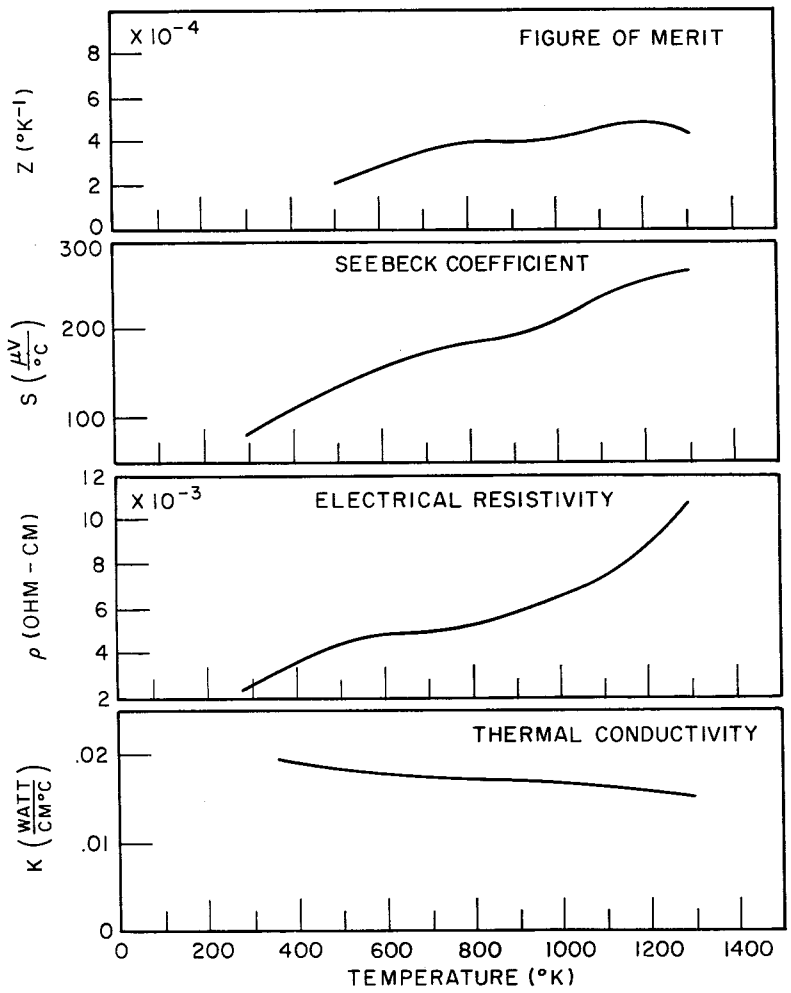

Fig. 15 - $Li_{.04}$ $Mn_{.96}$ Te (p type)

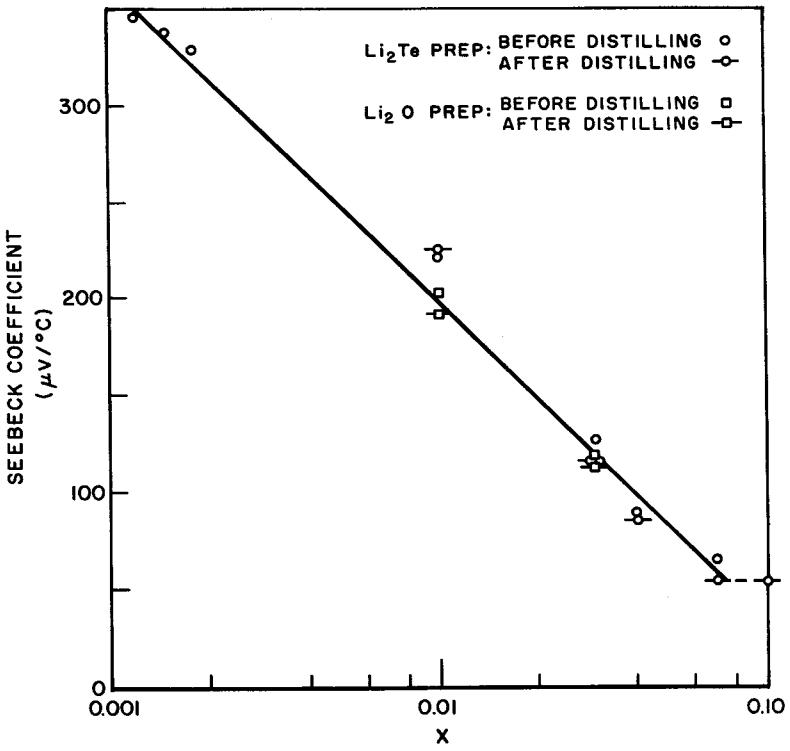

Fig. 16 - Li_x Mn_{1-x} Te (p type)
S vs log x (room temp)

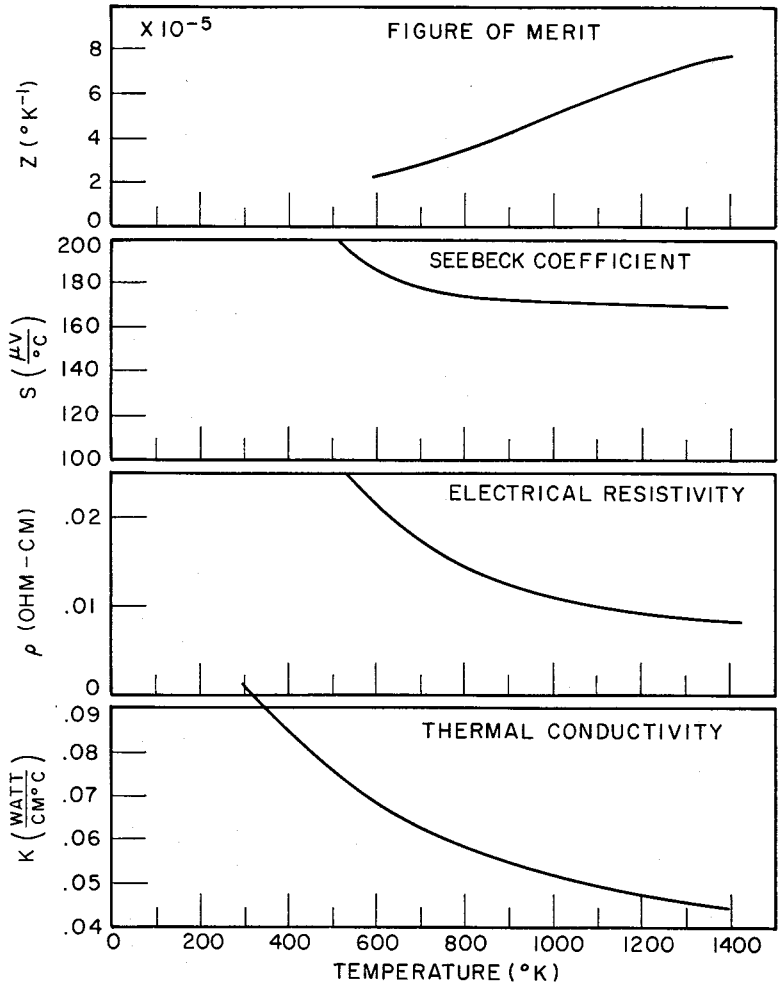

Fig. 17 - $Li_{.05}$ NiO (p type)

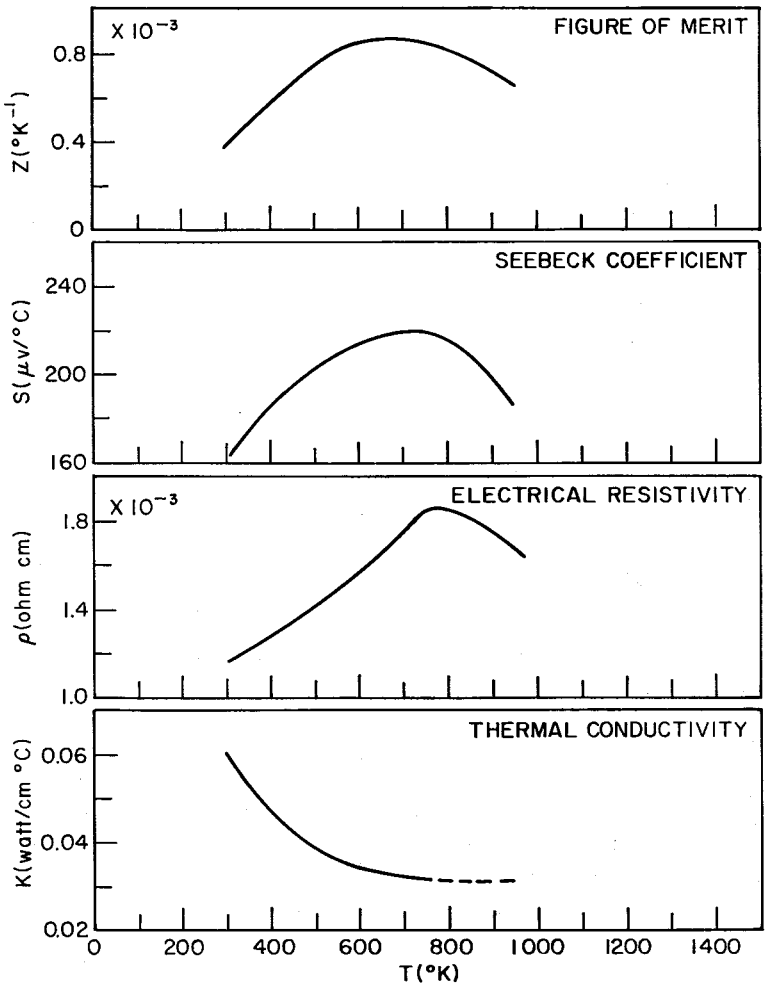

Fig. 18 - $CoSb_{2.95}$ $Te_{.05}$

in the Seebeck coefficient probably due to the loss of arsenic or selenium.

Samples of a quaternary BiSbTeSe alloy have been prepared with Z values in excess of 3×10^{-3}.

The presence of tin in ZnSb seems to result in increased mobility.

Pressed and sintered PbTe properly doped is more efficient than In-As-P over the range 800-950°K.

Thermoelectric measurements of SnSe over the range 80 -400°K indicate a poor figure of merit.

Cubic compounds of the form $CuM^{II}As$ or $CuM^{II}Sb$ where M^{II} = Zn, Sn had low Seebeck coefficient at room temperature and likelihood of being metals.

The SnAs system appeared metallic. The $SnAs_{1-x}Te_x$ system was metallic; Cu_3SbSe_4 held some promise though high efficiencies seemed unlikely. At room temperature $\rho = 3.5 \times 10^{-2}$ ohm cm, S = +370 μV/°C and K = .024 watt/cm°C.

The room temperature parameters of some rock salt-type compounds are given in Table VIII below:

TABLE VIII

Compound	Seebeck coefficient S (μV/°C)	Resistivity ρ (ohm cm)x10^3	Thermal Conductivity K (watt/cm°C)
$AuBiTe_2$	-87	1.43	0.025
$AuSbTe_2$	+49	0.18	-
TlSbTe	+75	0.91	0.015

In the range 80°K to 420°K, the Seebeck coefficient of $AuBiTe_2$ maximized around 200°K being about - 110 μV/°C. The Seebeck coefficient of $AuSbTe_2$

did not show a peak up to 670°K. The results on some materials of the nominal composition $AuSb_{1-x}Bi_xTe_2$ are given below along with the approximate temperature at which the material goes intrinsic:

TABLE IX

Compound	Seebeck coefficient S (μV/°C)	Resistivity ρ (ohm) cm) x 10^{-3}	Temperature (intrinsic) °K
$AuSbTe_2$	+ 49	0.18	610
$AuSb_{.75}Bi_{1.25}Te_2$	+ 84	0.32	500
$AuSb_{.5}Bi_{.5}Te_2$	+108	0.75	350
$AuBiTe_2$	- 87	1.43	200

$TlSbTe_2$ had large increases in Seebeck coefficient and resistivity with increase of temperature, both maximizing around 650° K with S = +222, approximately, and ρ = .0056 ohm cm, approximately.

A pseudo-binary section was present in the Ag-Sb-Te ternary system. A number of alloys having molar ratios of Sb_2Te_3:Ag_2Te in the continuous range 2.0 : 1 to 1.1 : 1 were investigated. The electrical and thermal data indicated that the better thermoelectric properties occurred with ratios in the range of 1.5 : 1 to 1.3 : 1. The average Seebeck coefficient and resistivity for cold and hot junctions of 150°C and 400°C, respectively are given in Table X below:

TABLE X

Molar Ratio Sb_2Te_3:Ag_2Te	Avg. Seebeck Coefficient S (μV/°C)	Avg. Resistivity ρ (ohm cm) x10^3
1.5 : 1	272	6.3
1.3 : 1	289	7.6
1.1 : 1	296	10.9

A sample of $AuTe_2$ was prepared. The resulting ingot fractured easily. The Seebeck coefficient was constant at +40 V/°C from 400° to 600°K. The resistivity and Seebeck coefficient data obtained indicated an undesirable high carrier concentration but that the compound might be promising if it could be undoped. At temperatures below about 225°K, the Hall coefficient was constant and corresponded to a calculated carrier concentration of about 2.5×10^{21} per cm^3. A calculated energy gap was of the order of 0.2 ev.

A series of cast specimens containing various elements were checked to determine if a significant change in the Seebeck coefficient could be produced. None of the elements used, Ni, As, Sn, Hg, Pb, I, or Na, seemed to be sufficiently soluble in $AuTe_2$ to affect the Seebeck coefficient appreciably.

Below 650°K cast PbTe was superior to the pressed and sintered. The significant difference was that the resistivity of the pressed and sintered was higher than in the cast material. However, above 650°K the sintered PbTe was as good or better than the cast. In this high temperature region the cast material could not be properly doped because of the limited solubility of excess Pb in PbTe.

THERMOELECTRIC MATERIALS FOR POWER CONVERSION

The Radio Corporation of America, RCA Laboratories,* describes exploratory materials research on ternary compound semiconductors and their alloys and transition metal silicides together with high temperature thermal diffusivity measurements on $AgSbTe_2$, Ge and Si.

AgSbTe has been prepared using the zone-leveling technique. Examination showed the presence of a minor phase distributed throughout the major phase to the extent of about 2% by volume. It is probably Ag_2Te. Zone-refining reduces the amount of the second phase.

Materials represented by $(Cu, Ag, Au)_2$ Te have been examined and a single-phase solid Ag_3CuTe_2 has been prepared. It is an n-type semiconductor which is unusual in ternary compositions. The resistivity was 1×10^{-3} ohm cm and Seebeck coefficient -40 $\mu V/°C$. Multiphase mixtures were obtained from other preparations of the three systems $(Cu, Ag)_2Te$, $(Ag, Au)_2$ Te and $(An\ Cu_2)$ Te. Further examination of transition metal silicides indicates little possibility of obtaining useful materials for high temperature thermoelectric applications. Only cobalt monosilicide is of potential use as a thermoelectric power-generating material and in the range 0°C to 700°C.

The Seebeck coefficient versus the temperature for chromium and manganese disilicides are given in Figure 19. The electrical conductivity for manganese disilicide is also shown. The thermal conductivity of chromium disilicide was 0.06 watts/cm°C and the calculated figure of merit of 0.4×10^{-3}/°C at 500°C.

Preliminary results indicated a thermal conductivity of manganese disilicide around 0.03 watt/cm°C and a maximum figure of merit of 0.4×10^{-3}/°C at 700°C. For both disilicides the Seebeck coefficient falls at temperatures above the 400°C and causes a sharp decrease in the figure of merit at high temperatures.

*Dept. of the Navy Contract NObs 77057. Quarterly Progress Report No. 6 covering the period 1 May to 31 July 1960.

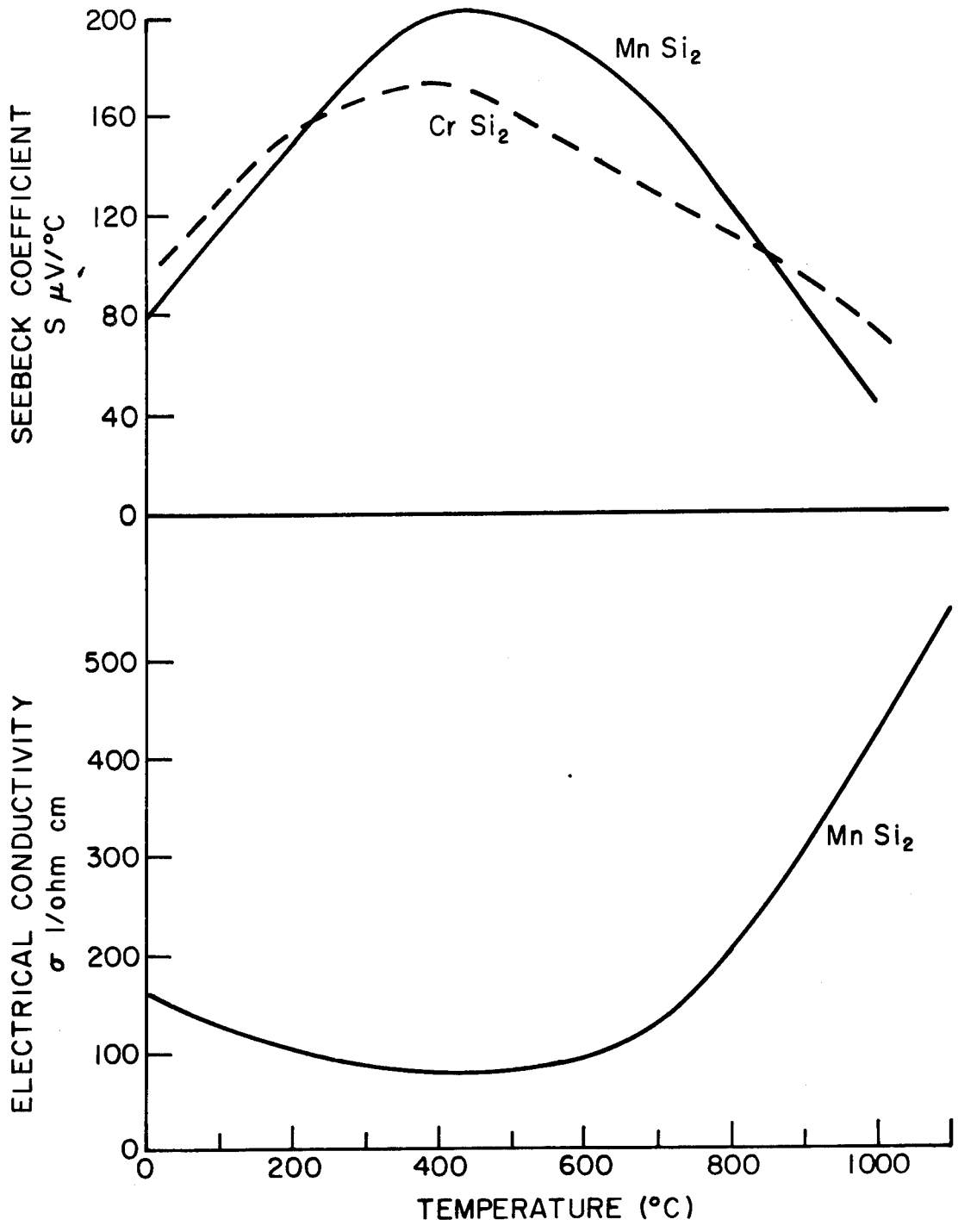

Fig. 19 - Seebeck Coefficient and Electrical Conductivity vs Temperature for $MnSi_2$ and $CrSi_2$

The Seebeck coefficient and electrical conductivity versus temperature are given for manganese monosilicide in Figure 20. The thermal conductivity at room temperature was 0.08 watt/cm°C. The maximum figure of merit was 0.3×10^{-3}/°C.

Figure 21 gives the Seebeck coefficient and electrical conductivity versus temperature for cobalt monosilicide. Thermal conductivity measurements on three samples gave 0.08 to 0.10 watt/cm°C.

The electronic contribution to the thermal conductivity of a cobalt monosilicide sample is given in Figure 22. The relationship to the electrical conductivity was obtained using the formula $K_{el} = A(\frac{k}{e})^2 T$ where K_{el} = electronic contribution to the thermal conductivity,

k = Boltzman constant,

e = electron charge,

T = absolute temperature,

σ = electrical conductivity and A is a constant which depends on the scattering mechanism. Considering cobalt monosilicide as a degenerate semiconductor a value of 2.6 was used for A. The values for K_{el} shown in Figure 22 were calculated from the above equation and the measured electrical conductivity of the sample.

The value for K_{el} at room temperature was subtracted from the measured total thermal conductivity to give the remaining lattice or phonon contribution, which was then assumed to follow an inverse proportionality to temperature. This curve, K_{phonon}, added to curve K_{el}, gives, neglecting any ambipolar contribution, the total thermal conductivity, K total over the temperature range. K total is fairly constant with temperature at about 0.08 watt/cm°C. Using this value the calculated maximum figure of merit is 0.4×10^{-3}/°C at 200°C. Above this temperature it decreases slowly but steadily.

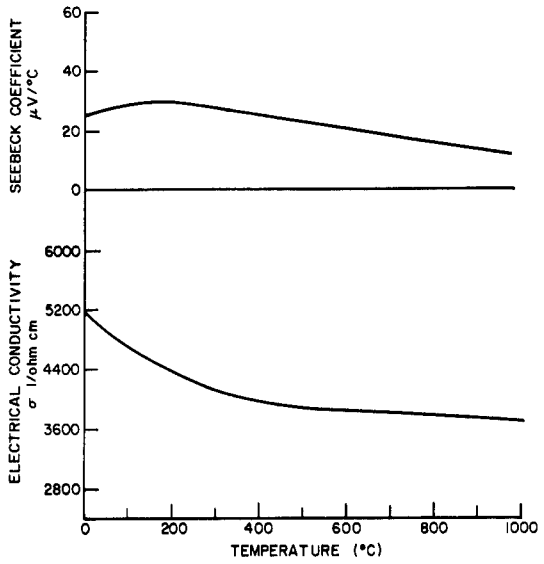

Fig. 20 - Seebeck Coefficient and Electrical Conductivity vs Temperature for MnSi

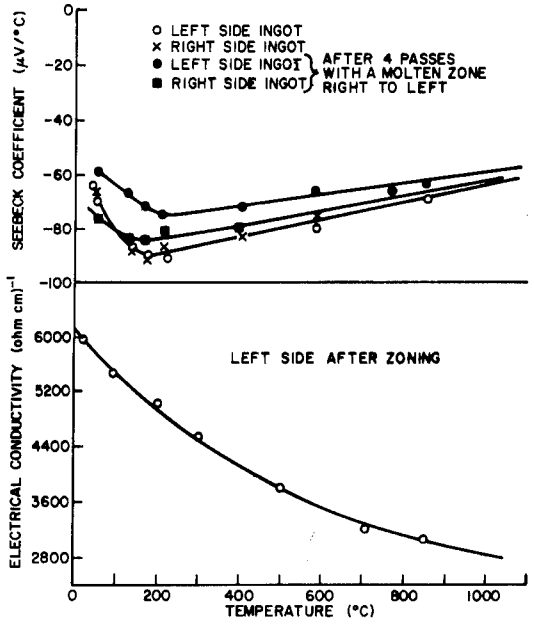

Fig. 21 - Seebeck Coefficient and Electrical Conductivity vs Temperature for CoSi

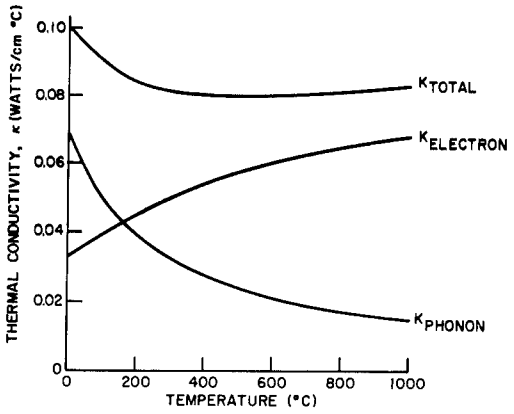

Fig. 22 - Extimated Temperature Dependence of the Thermal Conductivity of CoSi

Unless unusual increases in ratio of Seebeck coefficient to electrical resistivity are found in the materials, the maximum possible figure of merit appears to be about $0.8 \times 10^{-3}/°C$ and this is in the region below 700°C where superior materials are already known. Although these materials possess high thermal stability in the high temperature region, their poor performance at high temperatures does not indicate thermoelectric promise.

Radio Corporation of America* is conducting a materials research on ternary compounds, metal silicides and rare-earth sulfides. Two phases are obtained when an $AgSbTe_2$ stoichiometric composition is cooled from a liquid. The nature of the minor phase indicates that it forms directly from the melt and therefore the major phase is not stoichiometric $AgSbTe_2$. The material present as the minor phase has been identified as Ag_2Te. The proportion of the Ag_2Te phase decreases with decreasing Ag_2Te in the melt.

The minor phase which appears when $AgSbTe_2$ is grown from Sb_2Te_3-rich melts has not been conclusively identified.

The examination of the properties of metal silicides has been extended to include trisilicides. Only two metals, iridium and uranium, are known to form trisilicides. They are p-type semiconductors. The temperature dependence of the Seebeck coefficient and the resistivity on temperature for $IrSi_3$ are shown in Figure 23 for both the unannealed metastable high temperature form and the annealed stable low temperature form. The unannealed specimen was not heated to a high enough temperature for

* Department of the Navy Contract No. NObs 77057. RCA Quarterly Progress Report No. 7 covering period 1 August to 31 October 1960 dated 15 November 1960.

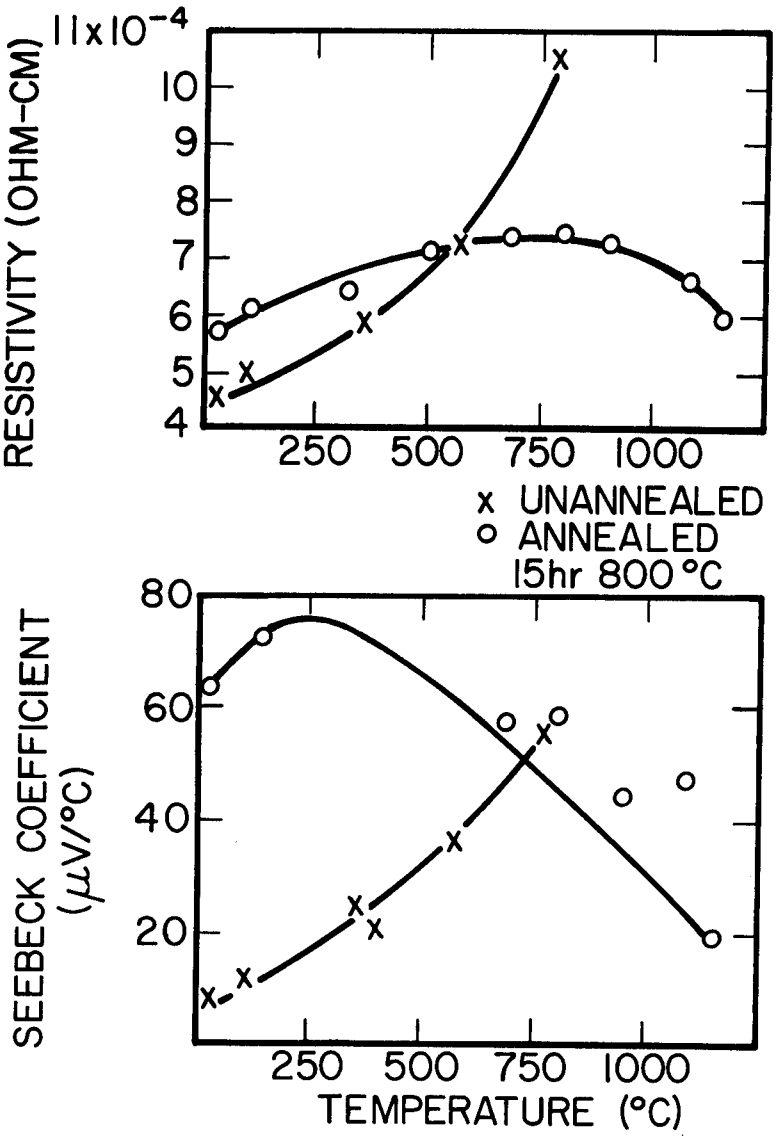

Fig. 23 - The Temperature Dependence of the Electrical Properties of $IrSi_3$

a sufficient time such that conversion to the stable annealed form could take place. $IrSi_3$ and p-type silicides $MnSi_2$ and $CrSi_2$ have a maximum Seebeck coefficient, S_1 between 250° and 500°C. At higher temperatures S decreases rapidly. In the high temperature region $IrSi_3$ appears to be superior to $MnSi_2$.

Rare-earth sulfides Ce_2S_3 and Nd_2S_3 have been prepared and electrically conducting phases obtained by decreasing the sulfur content of these materials below that present in the Ce_2S_3 phase. LnS (NaCl structure) and Ln_2S_3-Ln_3S_4 may be useful thermoelectric materials. CeS has too low a Seebeck coefficient to be a useful material. Rare-earth sulfides with the Th_3P_4 structure seemed promising and are being investigated.

The thermal diffusivity (thermal conductivity divided by specific heat) of InSb has been measured on two undoped single crystals at temperatures up to 700°K and this has been used to obtain the temperature dependence of the thermal conductivity. Results of measurement of electrical conductivity versus temperature indicated band gaps of 0.24 eV up to 600°K and 0.13 eV above 600°K. Thermal conductivity was computed from measurements of thermal diffusivity and specific heat.

HIGH TEMPERATURE PROPERTIES OF SEMICONDUCTORS

RCA Laboratories,* Princeton, N. J. have made measurements of the thermoelectric properties of the $In_xGa_{1-x}As$ system, as a function of alloy composition and of temperature. Certain alloys of this system are most promising thermoelectrically having a figure of merit as high as $1 \times 10^{-3}/°C$ for temperatures as high as 700°C. The phase diagram of this system indicates complete solid solubility over the entire compositional range. The melting point ranges from 960°C to 1242°C, the band gap from .35 to 1.35 ev and the mobility from 20×10^3 to 4×10^3 (cm^2/V-sec) on going from the InAs side to the GaAs side.

The room temperature electrical resistivity was measured using AC method in order to eliminate spurious thermoelectric EMFs. Other room temperature measurements made were thermal conductivity, Seebeck coefficient, and Hall coefficients.

High temperature measurements were made of Seebeck coefficient and electrical resistivity.

The measured values of Seebeck coefficient (S) versus the carrier concentration n at 300°K for InAs, GaAs and their alloys are plotted in Figure 24. All samples were n-type.

The maximum figure of merit for $In_{.4}Ga_{.6}As$ was $Z = 2.5 \times 10^{-4}/°C$ with resistivity, $\rho = 2.0 \times 10^{-3}$ ohm-cm. The corresponding values for InAs and GaAs were $Z = 1.0 \times 10^{-4}/°C$ with $\rho = 1.0 \times 10^{-3}$ ohm-cm and $Z = 3.0 \times 10^{-5}/°C$ with $\rho = 2.3 \times 10^{-3}$ ohm-cm, respectively. The corresponding Seebeck coefficient was 170 $\mu V/°C$ for all three materials.

---

*Department of the Air Force Contract No. AF 33(616)-6165. WADD TECHNICAL REPORT 60-266 of August 1960 covering period from 1 January 1959 to 31 March 1960.

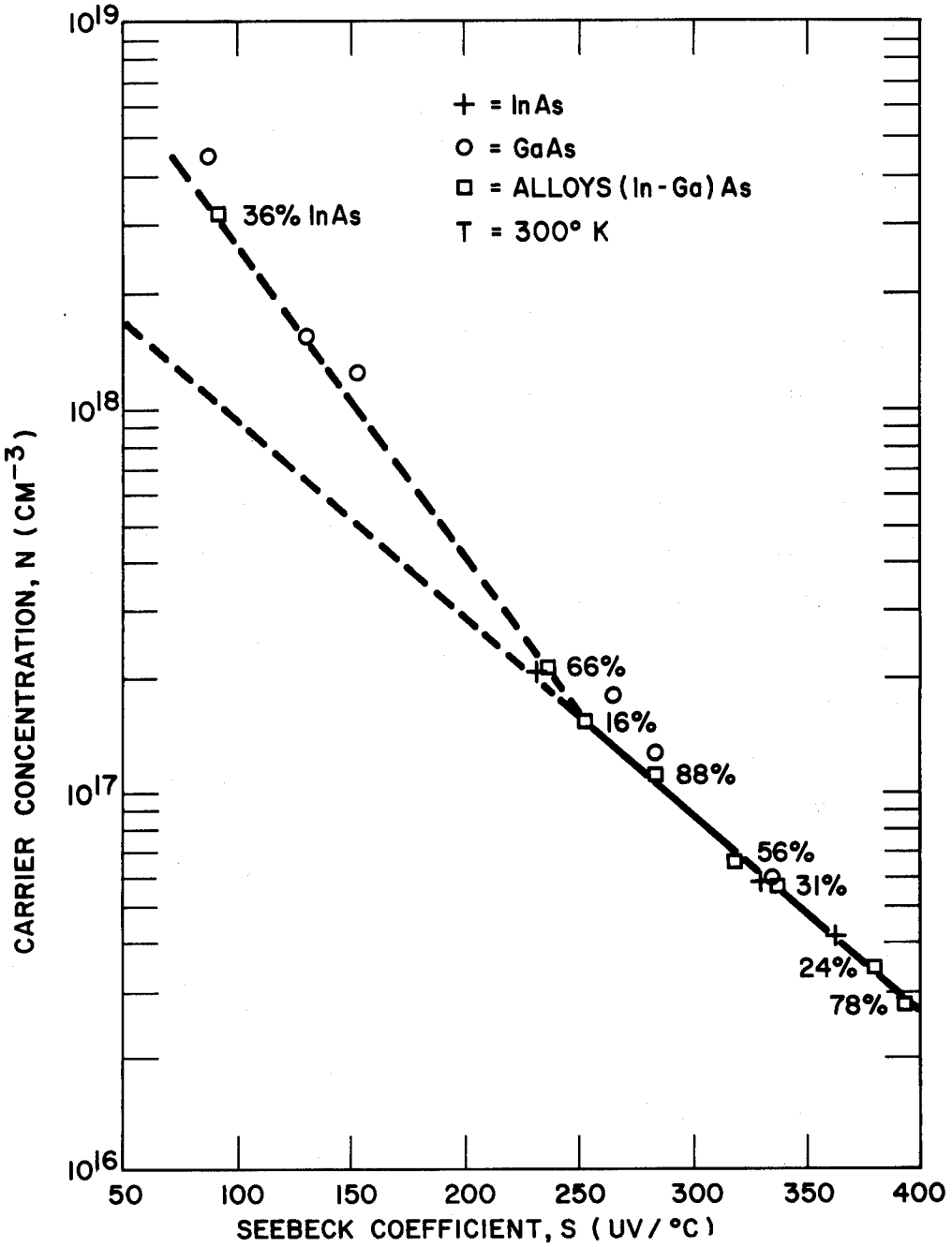

Fig. 24 - Seebeck Coefficitne of the $In_x Ga_{1-x} As$ System as a Function of the Carrier Concentration for Selected Values of x (T-300 K)

The maximum figure of merit for the alloys at room temperature were quite low compared to that of about $3.0 \times 10^{-3}/°C$ for Bi_2Te_3 - type materials.

Estimates for the figure of merit of $In_{.4}Ga_{.6}As$ alloy were $Z = 0.6 \times 10^{-3}/°C$ for T = 400°C and $Z = 1.0 \times 10^{-3}/°C$ for T = 700°C.

$In_xGa_{1-x}As$ alloys provide significant improvements in the thermoelectric properties over InAs and GaAs. For $In_{.6}Ga_{.4}As$ alloy it is indicated that the figure of merit increases as the temperature is raised and that operation up to temperatures as high as 700°C with a $Z \approx 1 \times 10^{-3}$ is quite feasible. Further, alloys closer to the indium-rich side have improved electrical properties over the $In_{.6}Ga_{.4}As$ alloys at temperatures below 400°C. $In_xGa_{1-x}As$ alloy system appears promising for thermoelectric power generation from 325° to 700°C.

The diffusivity method of measuring thermal conductivities has been developed to measure the thermal conductivity of semiconductors to an accuracy of ± 2% over the temperature range 0 - 1000°C. The apparatus has been tested on iron up to temperatures as high as 1025°C with indicated accuracy of ± 2%. Diffusivity measurements on germanium have been made up to 800°C with comparable accuracy. This method appears to be very satisfactory for determining high temperature thermal conductivities to a high accuracy independent of radiation losses.

A block diagram of the experimental set-up of apparatus for measuring thermal diffusivity of solids from room temperature up to 1000°C on samples 1-2" long with an accuracy of about 2%, is shown in Figure 25. The sample holder with sample is shown in Figure 26. The samples are in the shape of rods 2" long with .03 - 0.1 square inch cross-sectional area. Figure 27 shows the sample holder mounted in the vacuum furnace.

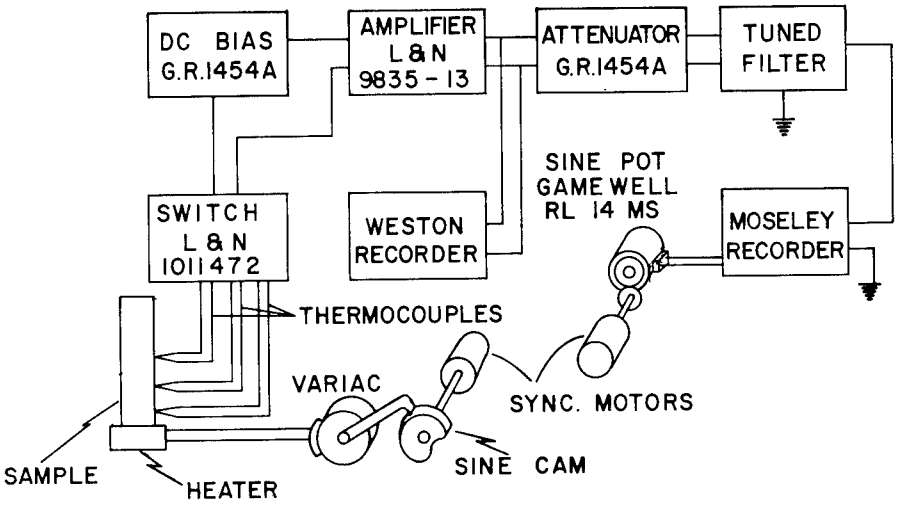

Fig. 25 - Block Diagram of Measuring Set-Up

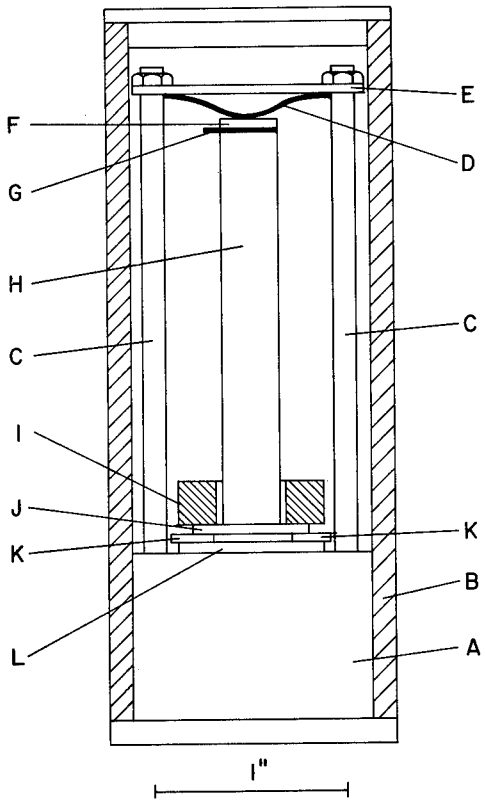

Fig. 26 - Sample Holder: A - Molydenum Sink, B - Molydenum Shielding Tube C - Stainless Steel Screws, D - Tungsten Spring, E - Molydenum Clamp, F - Ceramic Insulating Plate, G - Tungsten Current Lead to Sample, H - Sample, I - Lava Shield, J - Ceramic Heating Element, K - Nickel Current Tabs of Heating Element, L - Insulating Ceramic Plate

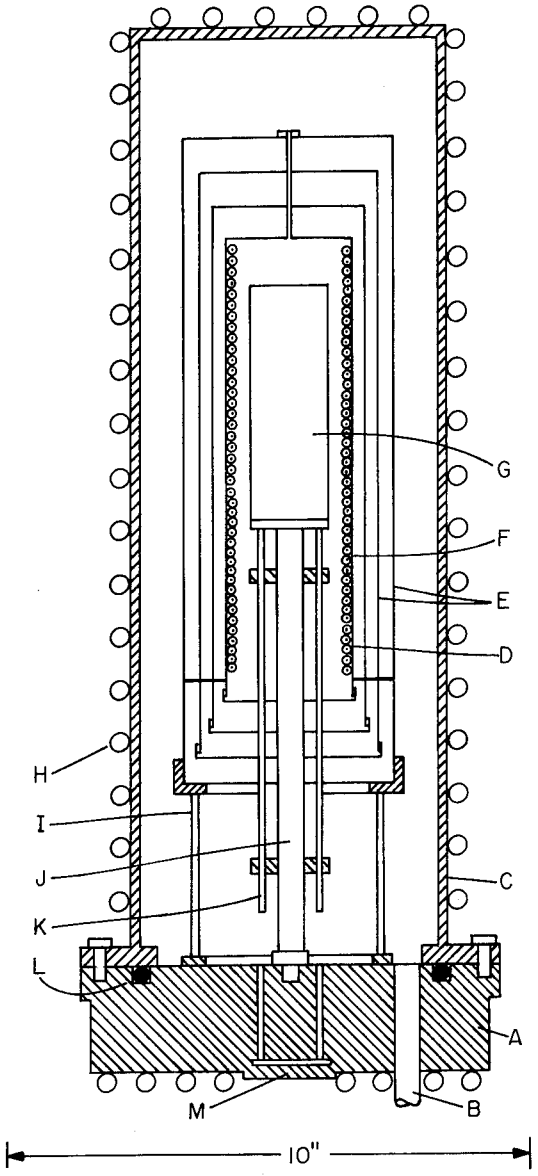

Fig. 27 - Furnace: A - Brass Base, B - Vacuum Outlet, C - Brass Bell Jar, D - Tantalum Radiation Shields, E - Nickel Radiation Shields, F - Kanthal Heater Coil with Ceramic Beads, G - Sample Holder, H - Copper Water Cooling Coil, I - Steel Stand for Heater-Shield Assembly, J - Stainless Steel Tube, K - Ceramic Tubes for Electrical Leads, L - Vacuum O-Ring, M - Vacuum Seal for Electrical Leads.

Using the differential method, the thermal EMF's are measured between three tungsten probes welded at equal intervals along the sample. A thermal wave is propagated through the solid and the thermal diffusivity is determined from the dispersion and attenuation of the wave. Use of higher frequencies reduces the effects due to radiation losses from the samples; reduces the measuring time; permits use of short samples; and obtains a better signal-to-noise ratio.

A sinusoidal heat input is provided to the sample by a heating element. Modulation is produced by a variac driven by a sine cam which in turn is driven by a synchronous motor. The furnace has its temperature regulated by a West saturable reactor controller and can be evacuated to about 10^{-6} mm Hg.

Three chromel-alumel thermocouples can be welded to the surface of the sample at equally spaced increments and used to obtain temperatures of the sample. They should be on opposite faces to the tungsten probes. Selection can be made of the thermocouple or pair of probes to be fed to the dc preamplifier. The dc part of the thermal EMF is bucked out with a dc voltage obtained from the voltage divider. The output of the dc preamplifier is fed through the attenuator and filter tuned to the signal frequency and recorded on the X axis of an X-Y recorder. For each measurement the attenuator is adjusted so as to maintain the same signal input level to the X-Y recorder.

The amplitude of the signal is determined from the deflection on the X-Y recorder and the setting of the attenuator. Phase is measured by applying to the Y input of the X-Y recorder, a reference sine voltage. This reference voltage is obtained from a sine potentiometer driven by a synchronous motor having the same RPM as the cam motor. The phase of the sine potentiometer can be adjusted with respect to the synchronous motor by means of a differential gearing mechanism.

THERMOELECTRIC MATERIALS

The Transitron Electronic Corporation* is in the process of evaluating the metal silicides with view to (1) obtaining an indication of trends for an isotypic series in relation to bond lengths as interpreted from interatomic distances and (2) adjusting the parameters in the future program by suitable substitutional additions or varying stoichiometry.

It was determined that $CoSi_2$ has, at room temperature, a Seebeck coefficient, $S = +8\ \mu V/°C$ and a resistivity, $\rho = 100$ ohm cm.

Substitution of Ge for Si in $CoSi_2$ produced N-type properties in the higher Ge content alloys. From the metallographic examination of $CoSi_2$-50.0 mole % $CoGe_2$ it appears to be either two phase or possibly three phase. There was evidence of a liquid phase being present around 700°C in the 66% alloy. The phase change occurring in these compositions interrupts the promising trend observed in the lower $CoGe_2$ content alloys.

In the $Cr_{1-x}M_xSi_2$ type compounds, with increasing Mo content the peak S decreases as does also the temperature at which it occurs. The product of $S^2\sigma$ is less than that of $CrSi_2$ in the high temperature range. Mn additions in polycrystalline arc melted material gave values of S and ρ considerably worse thermoelectrically than those of crystal grown material.

Ta substitution for Cr in $CrSi_2$ had little effect on S peak value but a large reduction of peak temperature. With increasing Ta content there was reduction of thermal conductivity, K.

Metal additions to the transition metal silicides were considered as being made by (1) keeping the stoichiometry constant or (2) altering the stoichiometric with suitable additions within the solid solubility range.

---

*Department of the Navy Contract NObs-78345. Quarterly Progress Report No. 5 covering period 4 September to 3 December 1960.

With the stoichiometry constant, Mn additions to $CrSi_2$ elevated the peak S value and decreased its temperature. Ta had little effect on peak S but a large decrease in peak temperature.

In the hexagonal $CrSi_2$-C40 series of the transition metal silicides data concerning the lattice spacing on the $(TiMo)Si_2$ alloys show a decrease in the axial ratio with increasing $TiSi_2$ content. This change appears to produce no significant effect on S and ρ.

Chromium disilicide exhibits semiconducting properties. In its crystallographic isotypic series the members becomes more metallic as the c/a ratio decreases. It becomes intrinsic about 450°C. An energy gap of 0.9 e.v. has been estimated.

The magnetic state of single crystal cobalt silicide apparently has no effect on the Seebeck coefficient but is a function of the annealing temperature.

Thermal conductivity measurements, using the heat flow method, were made on CoSi+.1% Al (single crystal), CoSi+.5% FeSi (single crystal), and pure polycrystalline CoSi. CoSi+.1%Al obeyed a 1/T law above 200°C but below this the phonon component of thermal conductivity increased. CoSi+.5% FeSi obeyed a 1/T law over the temperature range investigated.

The polycrystalline material had a lower thermal conductivity than the single crystal material from room temperature to 225°C but higher above. The thermal conductivity of the polycrystalline CoSi was nearly independent of temperature.

REFRACTORY GADOLINIUM AND HAFNIUM COMPOUNDS

Research Chemicals, a division of Nuclear Corporation of America*, have investigated gadolinium compositions with antimony, bismuth, boron, phosphorus, selenium and silicon, and hafnium compounds with boron and silicon for their potential as thermoelectric materials at elevated temperatures. Seebeck coefficients, electrical resistivities and melting points only, were determined. Several refractory systems were uncovered, with melting points as high as 3000°C. Compounds in the gadolinium-selenium systems have shown possible value as thermoelectric material.

In the gadolinium-selenium system Seebeck coefficients as high as 500 $\mu V/°C$ have been obtained, but these and resistivities have been found to vary unconventionally with treatment and mild variations in composition.

The material structure requirement leading to both high temperature stability and the production of an appreciable thermoelectric output was of specific concern. The Seebeck coefficient of a system could be predicted, but the formulae used required the knowledge of precise structural data which were lacking in many instances. Therefore, examination was required of many previously unexamined materials on a generalistic basis.

The concept that mixed valence compounds should provide valuable thermoelectric parameters was felt to be ambiguous. It was felt that a more precise concept was one based upon systems in which bonding resonated between covalent (or homopolar) and ionic characteristics. Such resonance strengthened the bond and thus increased the melting point of the system and most probably the energy gap. Because of the covalent bonding, it was expected that such materials would be semiconductors.

---

*Department of the Navy Contract NObs 77145. Final Report covering the period 18 May 1959 to 1 May 1960.

For valuable application to thermoelectricity it was necessary that semiconductors be extrinsic, since otherwise hole and electron conductance would militate against each other.

With the foregoing generalizations in mind, the value of intermetallic compounds as thermoelectric materials was considered. The semiconducting properties of intermetallics are due to the number of states and number of available electrons, such that the valence bond comprises all the bonding states, and that the conduction bond is formed by anti-bonding states. The chemical stability of the system must be higher than that of a metal phase. This stability is further increased by the covalent-ionic resonance and increase in the energy gap.

Electrical resistivity is of direct importance in determining the values of a material for thermoelectric purposes. Resistivity shows a sharp increase at compositions satisfying simple chemical valence rules. The structure of such compositions is not metallic.

One appears to be constrained to the examination of intermetallic compounds in which ionic-covalent resonance occurs in non-stoichiometric compositions, and in which conduction is electronic rather than ionic, the whole system being also an extrinsic semiconductor. Through a constitutional series, however, it was noted that resistivity will vary with the degree of order-disorder obtaining and hence low resistivities are to be expected where non-stoichiometric intermetallic compounds are formed. In the work reported only arbitrarily chosen compositions were studied.

In the rare earth series gadolinium is of specific interest because its 4f shell carries the maximum number of unpaired electrons. Lutetium has 14 4f electrons but because of its rarity, consideration was given to hafnium which also has 14 4f electrons and an additional electron in the 5d shell.

Gadolinium and hafnium with selected elements to the right of the Zintl boundary in the Periodic Table and boron compounds were examined for thermoelectric properties.

The purity of materials employed in the preparation of the refractory compositions considered was as follows:

Antimony	99.999%	Phosphorus	99.9
Bismuth	99.9	Selenium	99.999
Boron	99.9	Silicon	99.999
Gadolinium	99.7	Calcium phosphite, technical grade	
Hafnium, electron beam ingot grade		Zinc phosphide, technical grade redistilled to 99.9	

Four types of reaction procedures were employed for the preparation of compositions: (1) direct reaction, (2) vapor diffusion, (3) arc melting, and, in phosphide production, (4) metathesis. In "direct reaction" the two material components were reacted together in an inert argon atmosphere, induction heating being used to trigger the initial reaction. Once the critical reaction temperature was reached, the heat of reaction supplied the final heat required to complete the reaction. Products were inhomogeneous. Preparation of gadolinium phosphide by this procedure was not successful. The "vapor diffusion reaction" was effected in a Vycor tube, which had a constriction separating materials on either side. The constriction prevented direct, solid contact of the reactants. Heating was accomplished in a tube combustion furnace. Because of the high vapor pressure of selenium, the gadolinium-selenide compounds were prepared by this technique. The "arc melting" procedure was conducted in a furnace consisting of a water cooled vacuum chamber fitted with a water cooled copper hearth plate and tungsten electrode. The melting operation was carried out in the presence of a helium-argon mixture. Using

the "metathetical reaction" technique, a "double decomposition sintering" in the presence of argon was carried out in an induction furnace. Gadolinium phosphide was obtained through the metathetical reactions using zinc phosphide and gadolinium. A double decomposition followed by a vapor reaction was employed to increase the phosphorus content of the product. A double decomposition reaction employing distilled zinc phosphide was carried out followed by vacuum sintering of the product. In similar manner a product of slightly higher phosphorus content was obtained by using calcium phosphide.

The analytical procedures employed for determination of chemical composition of the materials prepared followed classical techniques.

The refractory hafnium and gadolinium compositions were hard and brittle making difficult the preparation of samples suitable for resistivity and Seebeck evaluations. A cut off wheel suitable for specimen preparation was developed consisting of 100 mesh silicon carbide powder bonded in a rubber base matrix.

Accuracy of Seebeck measurements was about ± 10% and that of resistivity ± 5%. Lack of physical integrity of specimens, e.g. undetected voids, cracks and other imperfections, may lead to erroneously high resistivity values. Examinations were made without the benefit of structural x-ray studies. Assumption cannot be made that each sample was monophase. Competing order-disorder transitions may present another source of error.

Gadolinium-antimony compositions were prepared at first by the direct action technique, followed by arc melting. Later only the arc melting technique was used. The Seebeck coefficient values are shown graphically in Figure 28. The relationship of room temperature resistivity and melting point to composition are shown in Figure 29. Resistivity values range between 140 and 300 microhm-cm. A complicated band structure in alloys of

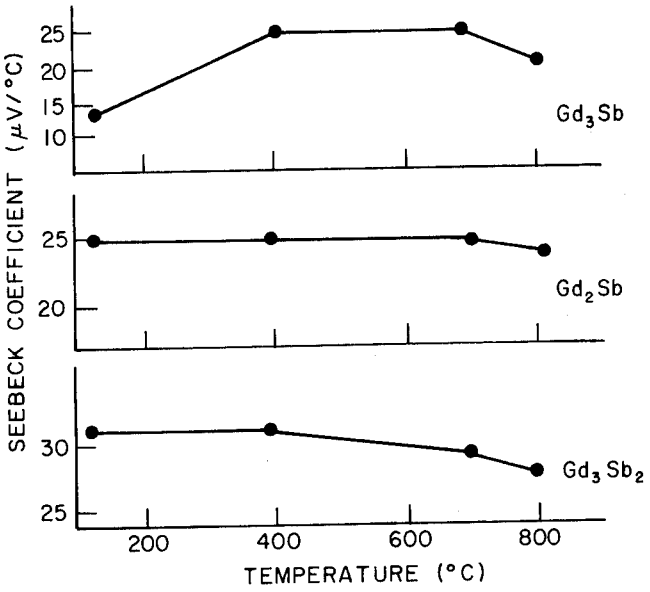

Fig. 28 - Gadolinium-Antimony System

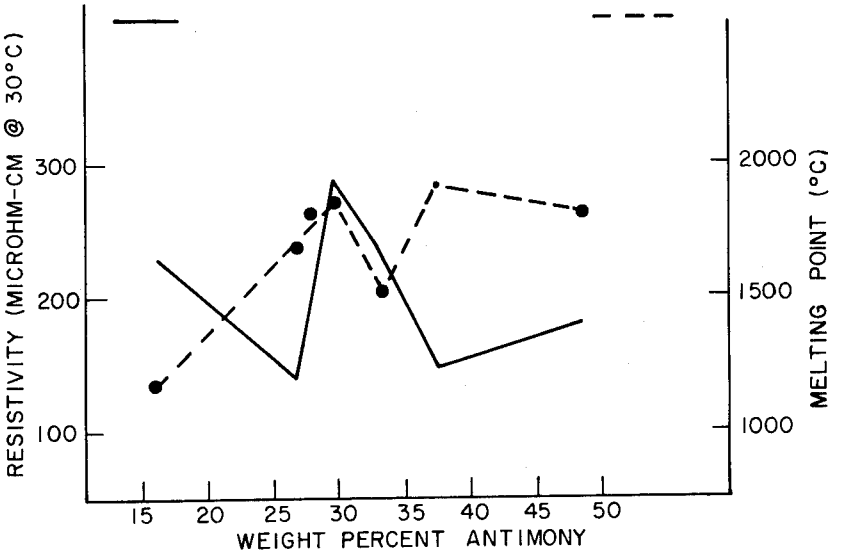

Fig. 29 - Gadolinium-Antimony System Resistivity and Melting Points

the gadolinium-antimony system is indicated in the melting point curve. Figure 30 relates resistivity to temperature and composition. The relatively low Seebeck coefficient and high electrical conductivities seem to confirm that the bonding is complex and semi-metallic.

Gadolinium-bismuth compounds were initially prepared by direct reaction followed by arc melting procedure. Later compositions were prepared by arc melting. Figures 31, 32, and 33 present the data obtained. Room temperature resistivities ranged between 150-500 microhm-cm. The general instability of compositions in this system-rapid oxidation and hydrolysis - militates against their further consideration.

Gadolinium-selenium compositions were prepared by the vapor diffusion reaction technique followed by arc melting. Figures 34 to 39 present data obtained. Examination was made on that portion of the system in the region of GdSe, Gd_2Se_3 and $GdSe_2$ intermetallic compound formation.

This system was the only one studied which presented resistivity values of any magnitude and high Seebeck coefficients. Copper "doping" between 0.1 and 1% had little or no effect upon Seebeck coefficient or resistivity. Selenium, in excess over stoichiometry during initial reaction, seemed to increase both Seebeck and resistivity values, however, in mild variations in composition from that of 2:3 compound, it tended to lower them.

GdSe melts around 1350°C. A melted material containing 67.6% gadolinium and 32.3% selenium was essentially monophase. It is probably of B 1 (NaCl) type structure, cubic O_h^5 - Fm3m, a_o 5.758A; x-ray density 8.2 gm/cm^3. Each selenium atom is surrounded by six gadolinium atoms at the vertices of a regular octahedron. Each gadolinium atom is surrounded by six selenium atoms but no contact exists between the gadolinium atoms.

Gd_2Se_3 was the most stable of the system examined. The compound melts at about 1750°C. Melted specimens containing 57.3% gadolinium and

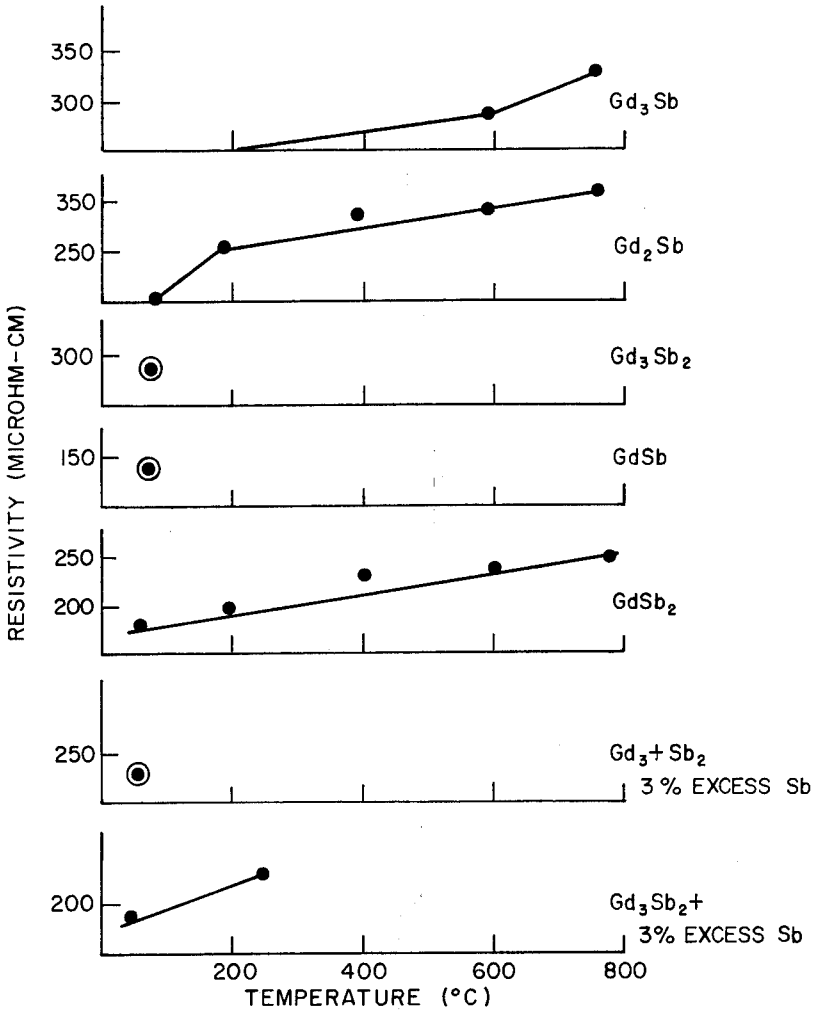

Fig. 30 Gadolinium-Antimony System

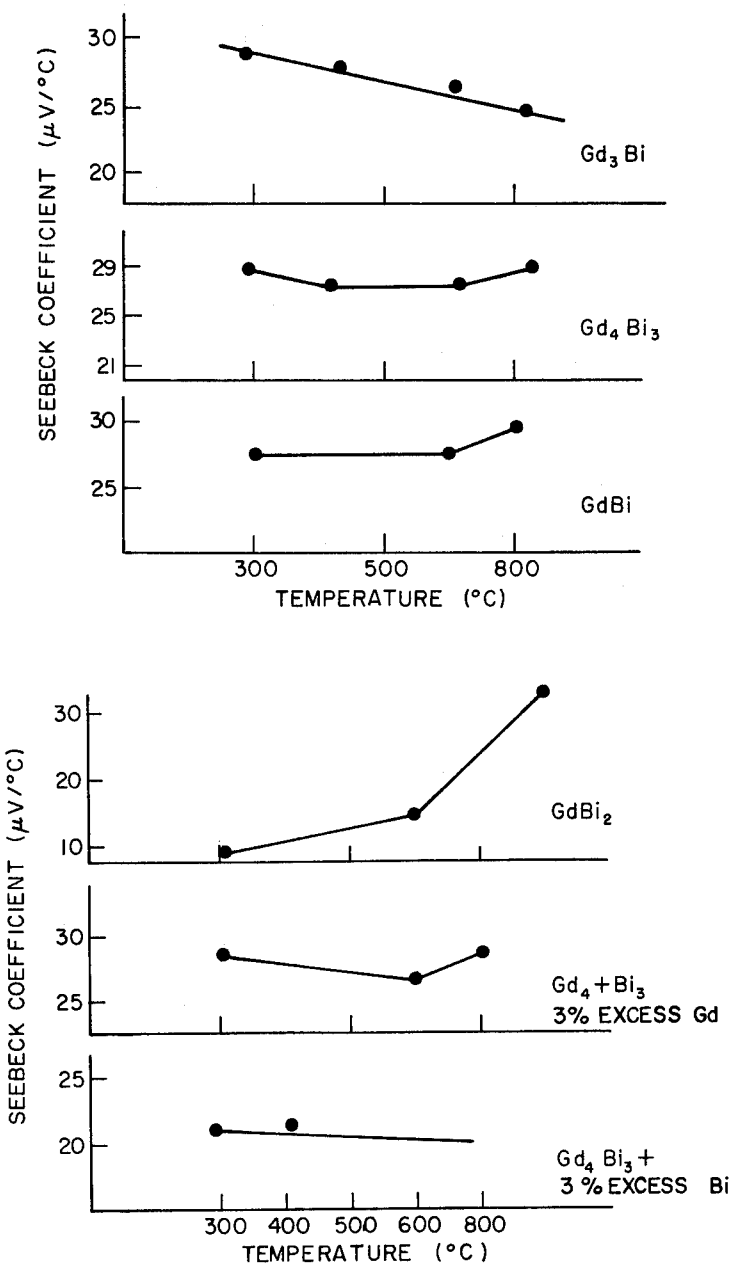

Fig. 31 - Gadolinium-Bismuth System

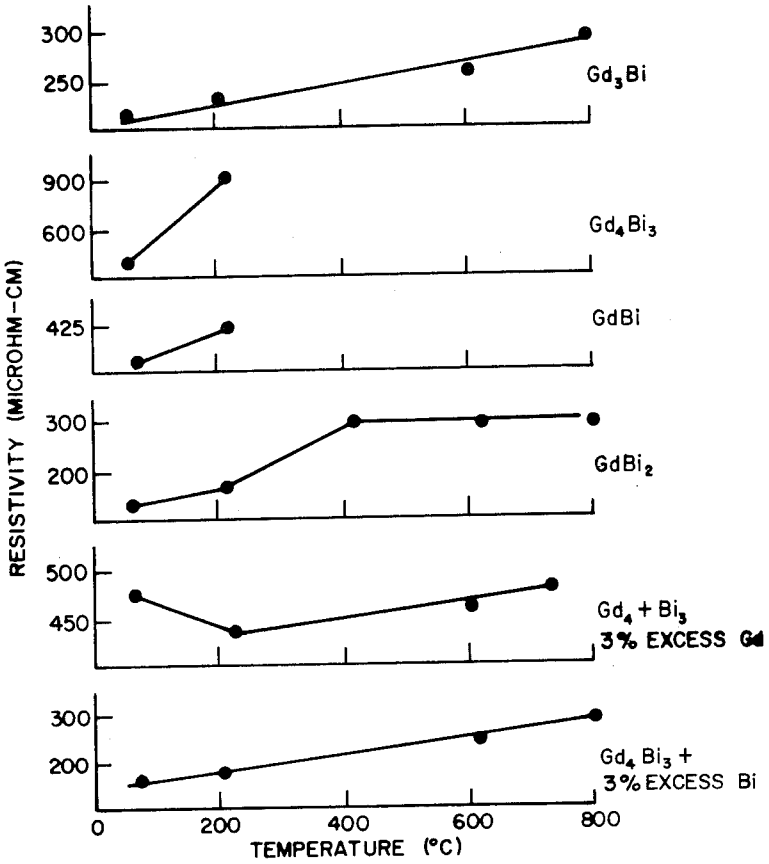

Fig. 32 - Gadolinium-Bismuth System

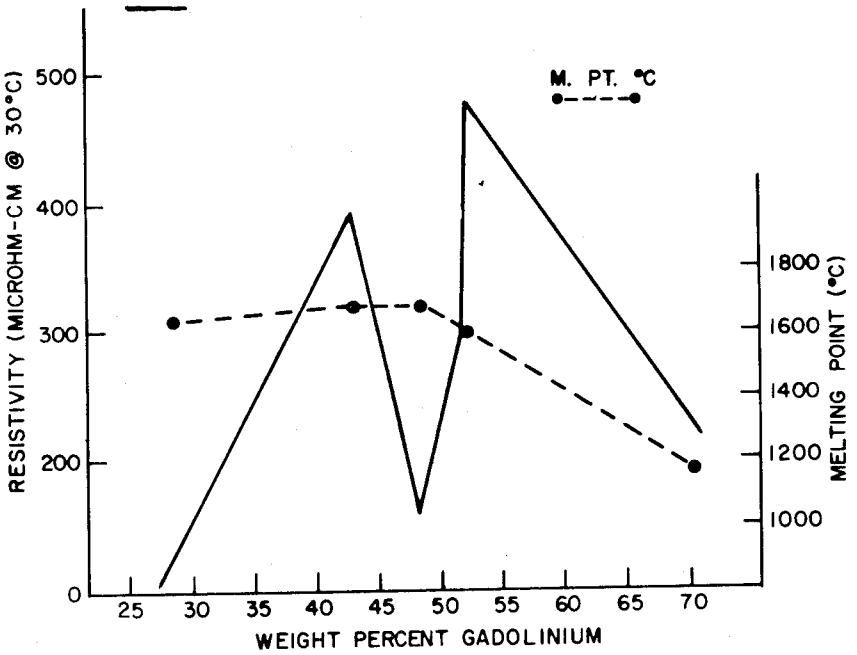

Fig. 33 - Gadolinium-Bismuth System
Resitivity and Melting Points

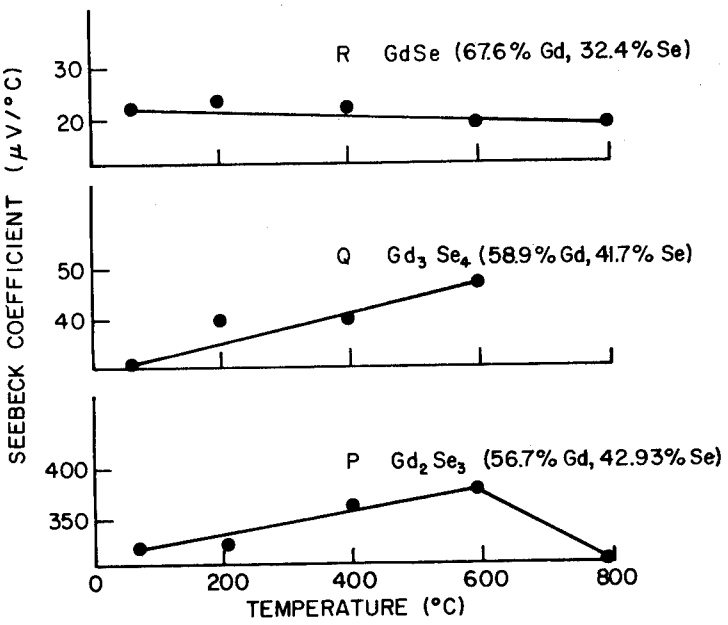

Fig. 34 - Gadolinium-Selenium System

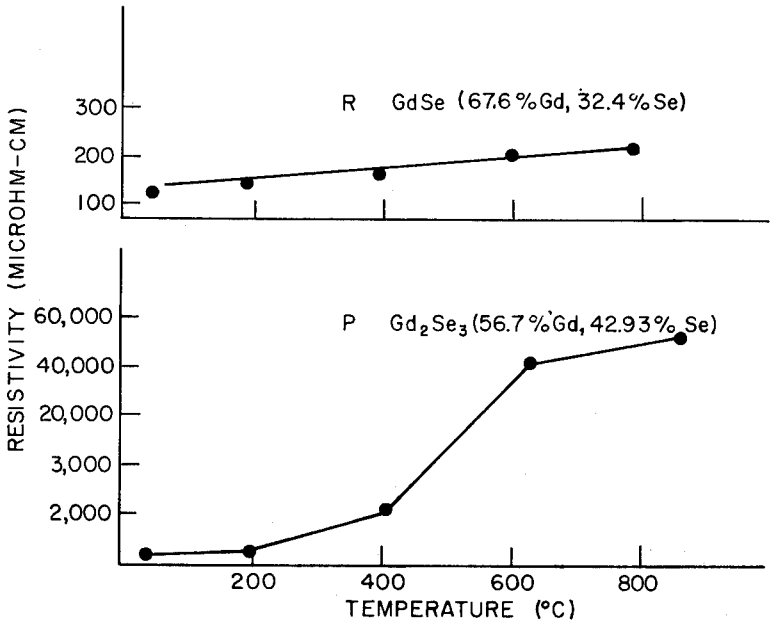

Fig. 35 - Gadolinium-Selenium System

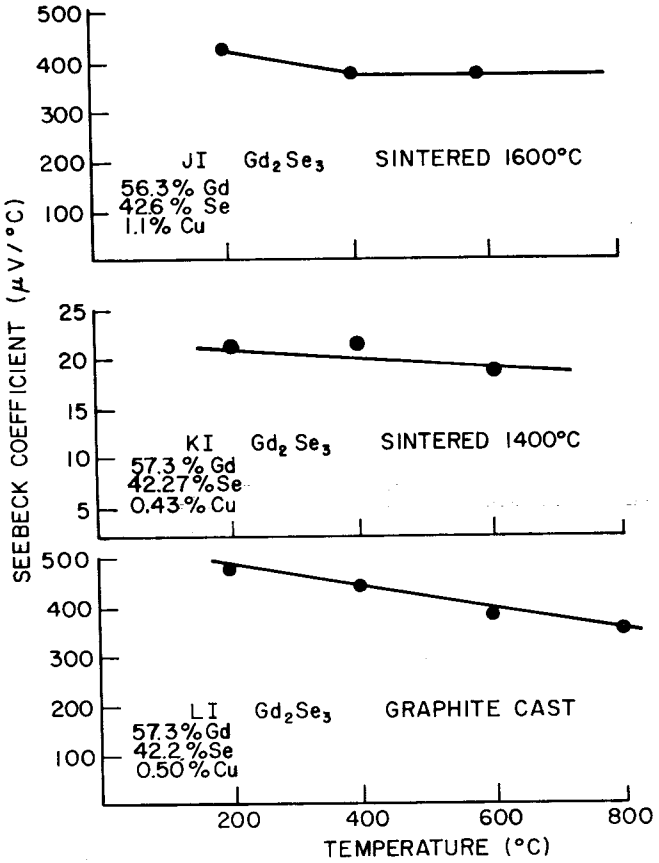

Fig. 36 - Effect of Processing Variables upon Seebeck Coefficient of $Gd_2 Se_3$

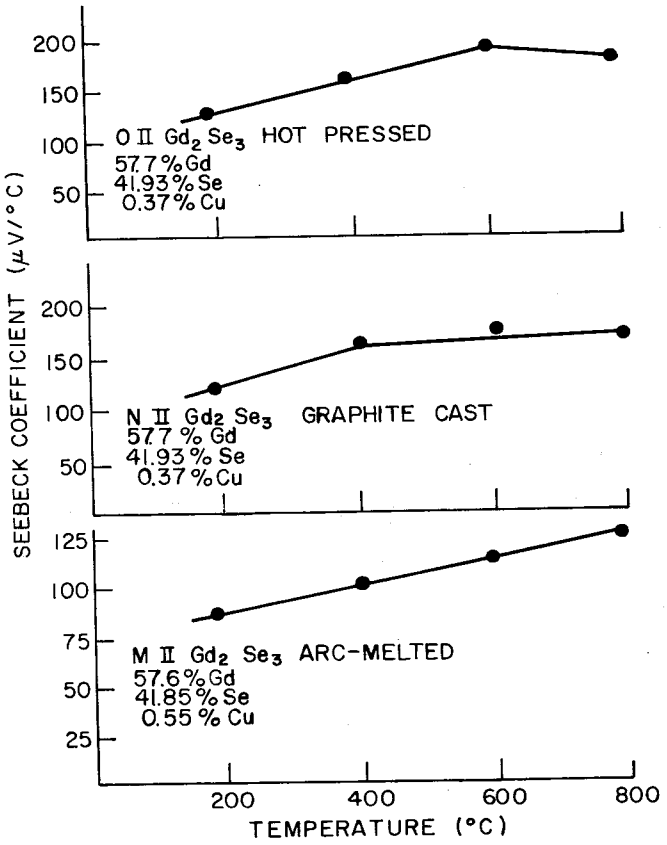

Fig. 37 - Effect of Processing Variables upon Resistivity of $Gd_2 Se_3$

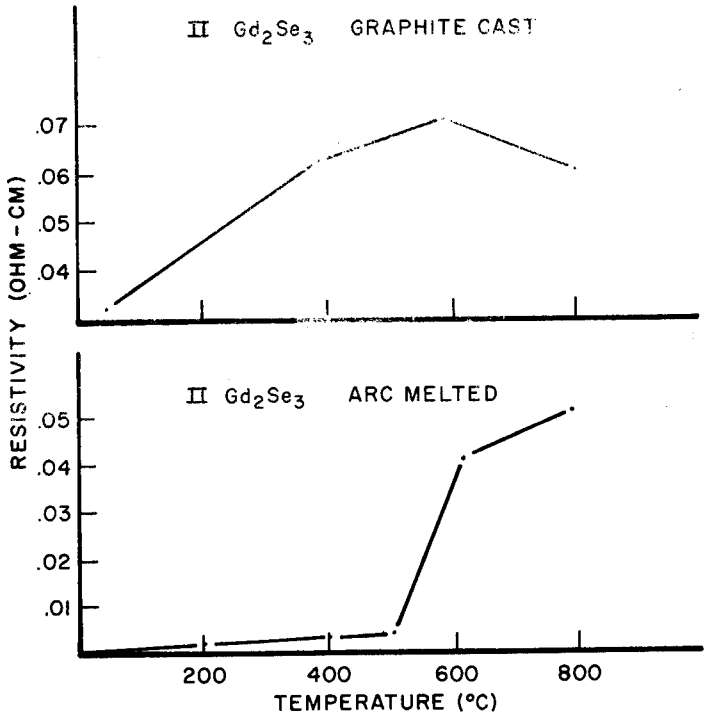

Fig. 38 - Effect of Processing Variables upon Seebeck Coefficient of $Gd_2 Se_3$

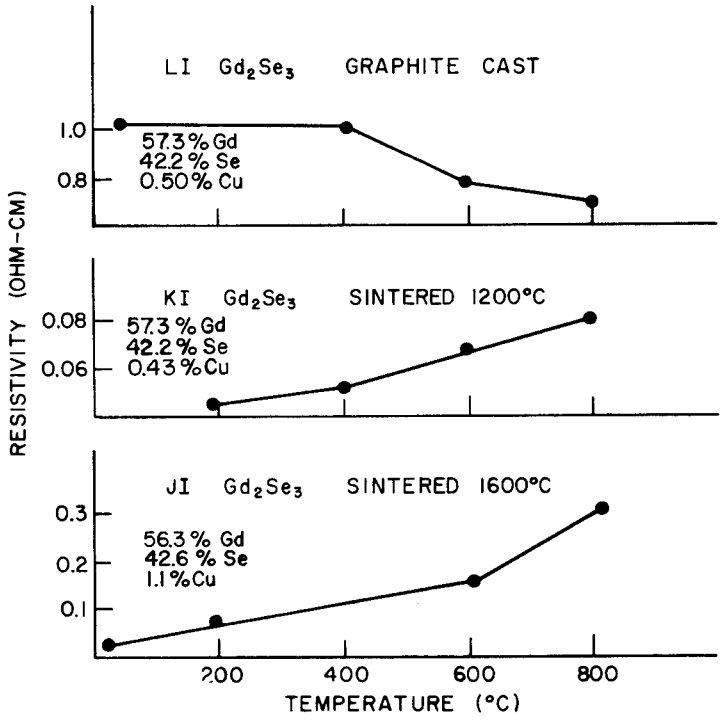

Fig. 39 - Effect of Processing Variables upon Resistivity of $Gd_2 Se_3$

42.5% selenium were largely monophase but with a trace of eutectic component. Results indicate a $D7_3$ (Th_3P_4) type structure, b.c.c. O_d^5 - 143d, a_o 8.72 ±0.005A, x-ray density 7.36 gm/cm^3. The unit cell contains 26 2/3 atoms, of which 10 2/3 gadolinium atoms randomly occupy the metal positions giving a disordered or defect structure. In the ordered assembly postulated for this compound, a degree of covalent bonding between Gd-Se atoms was again suggested. The Gd-Gd distance was 4.072A and that of Gd-Se less than the theoretical 2.96A. A tight packing of the selenium atoms indicates ionic bonding between the atoms. Research Chemicals has not been able to verify the existence of Gd_3Se_4. The presence of a high temperature eutectic at 61% weight of gadolinium is considered further evidence against the existence of a 3:4 compound in this system.

$GdSe_2$ was least stable of the compounds examined. It decomposes above 200°C and gradually loses selenium. Results suggest it to have an orthorhombic structure with a_o 7.27A, b_o 4.03A, c_o 8.30A.

Resistivity values obtained through the compositional sequence indicated a gradual increase of resistivity of 0.1×10^{-3} ohm-cm from 0% by weight of selenium to 30%, thence rapid increase to a maximum value of 1000×10^{-3} ohm-cm at about 39%, thereafter a sharp drop in the resistivity to about 0.15×10^{-3} ohm-cm at 50% selenium. Only Gd_2Se_3 possessed semi-conductor characteristics. This behaviour was in keeping with the defect structure of this compound. Extrinsic conductance will develop in such a structure. Preliminary measurements of Hall effect show p-type conductivity. The resistivity of 1000×10^{-3} ohm-cm is nearly constant from room temperature to about 500° C. Thence, it drops sharply to 0.15×10^{-3} ohm-cm at 590°C and thereafter gradually decreases to about 0.12×10^{-3} ohm-cm at 800°C. The exceptionally high room temperature resistivities of Gd_2Se_3 and low resistivities of the other compounds

in this series, indicate that only in the 2:3 compound does bonding become potentially ionic.

The magnetic susceptibility of gadolinium-selenium compounds is approximately 1.70×10^{-3} at 30% by weight of selenium and decreasing linearly with increase of selenium reaching a value of approximately 1.14×10^{-3} at 50%. Present inferences are that the gadolinium-gadolinium inter-atomic distance in the gadolinium-selenium compounds is less than that in the oxide.

The semiconductor nature of Gd_2Se_3 and the rather small gadolinium-selenium distances can indicate that the selenides are not wholly ionic entities, but are probably intermetallic in nature possessing partially covalent bond characteristics. Using such an hypothesis, it is possible to establish a rationale of electronic properties resulting from lattice interpenetration of such covalentionic-covalent structures.

Suggestion was made that covalency in the compounds now studied might involve hybridization of Gd5d and 6s and Se 4p electron levels. The definitive phenomena exhibited by the compounds GdSe, Gd_2Se_3 and $GdSe_2$ may be interpreted in terms of ionic covalent resonance in the gadolinium-selenium bond.

Gadolinium-silicon compounds were prepared by direct reaction. Seebeck outputs (15 -30 microvolts/°C) are shown in Figure 40. Plots of resistivity vs composition and temperature (Figures 41 and 42) show the development of ionicity at the stoichiometric composition Gd_4Si_3. Resistivity values (900 microhm-cm at 200°C) for this composition were two or three times those of adjacent compositions and Seebeck coefficients were lower. The smooth variation in melting points (Figure 42) indicates a simple band structure.

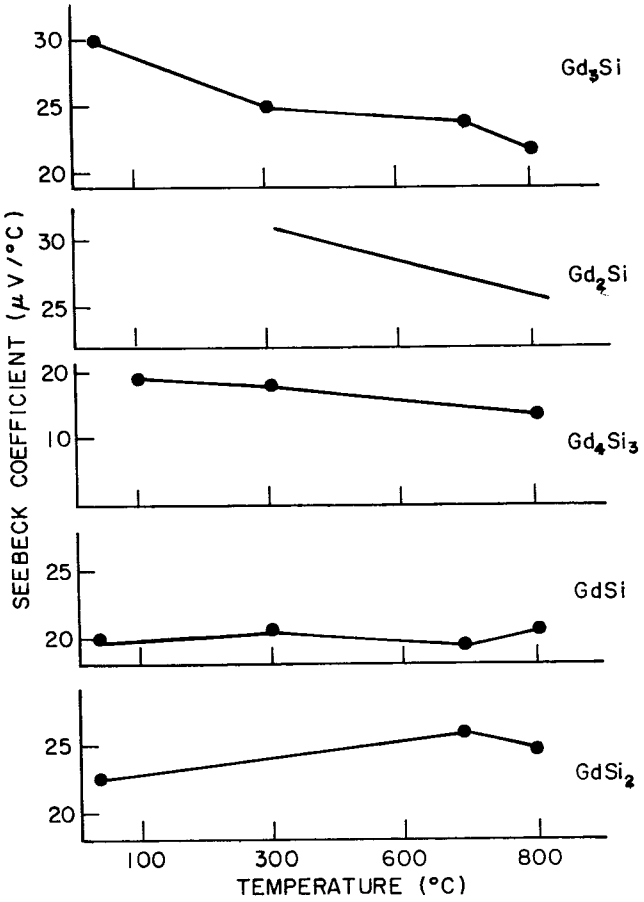

Fig. 40 - Gadolinium-Silicon System

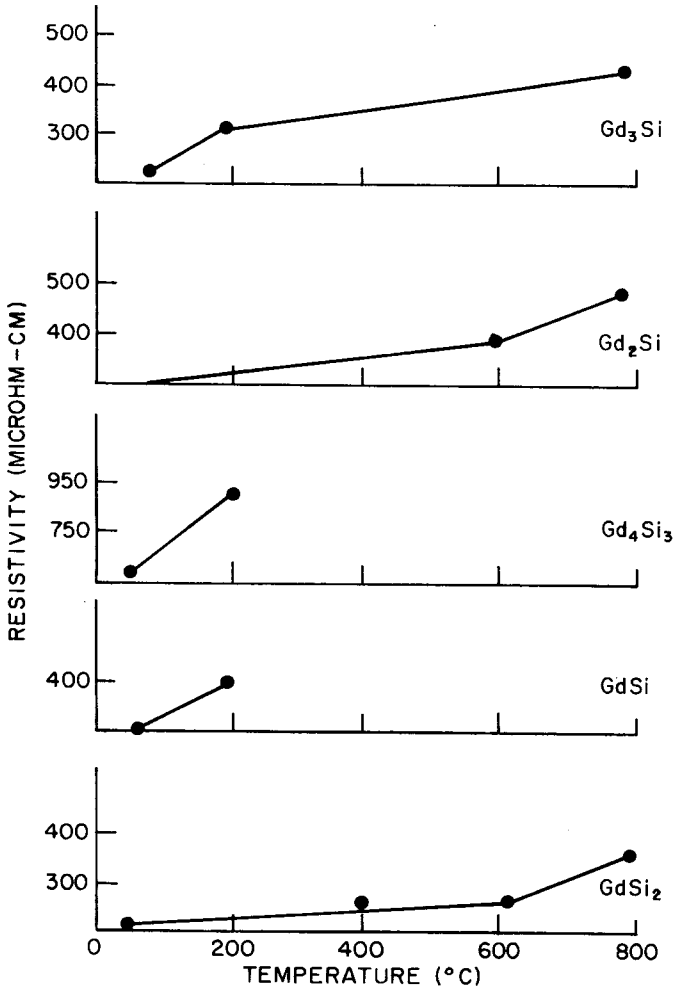

Fig. 41 - Gadolinium-Silicon System

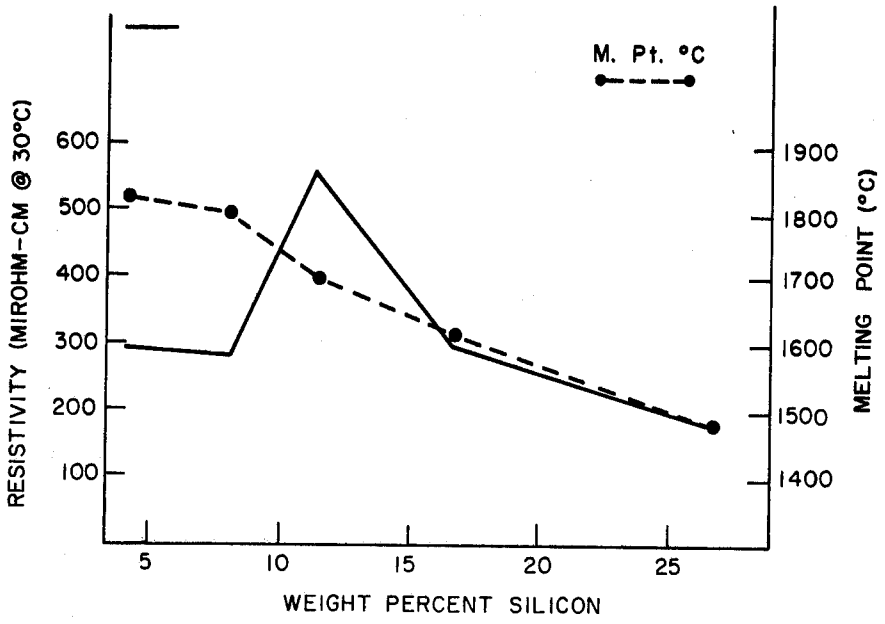

Fig. 42 - Gadolinium-Silicon System
Resistivity and Melting Points

The gadolinium-phosphorus compositions are compared in Figures 43 and 44 as to Seebeck coefficient and resistivity at various temperatures. Those low in phosphorus appeared very stable and refractory with melting points from 1900° to 2800°C.

Compounds GdB_4 and GdB_6 of the gadolinium-boron system were prepared by the arc melting procedure. Figure 45 shows that the Seebeck coefficients for each compound were almost identical. The hexaboride had a much smaller low temperature resistivity (Figure 46) than the tetraboride.

Hafnium-silicon compounds were prepared by arc melting procedure. In general increasing the silicon content had no effect upon the Seebeck coefficient (Figure 47) until the $HfSl_2$ compound was reached. Resistivities (Figure 48) decreased with increasing silicon content.

Hafnium-boron compounds were also prepared by the above procedure. Its highly refractory nature made more difficult its preparation. Consistent but low Seebeck coefficients are shown in Figure 49. Brittleness prevented determination of most resistivities.

The graphs indicated that most of the materials examined had Seebeck coefficient and electrical resistivity values in a range common for semi-metals and semi-metallic compounds. In general the Seebeck coefficient ranged from 10 to 30 $\mu V/°C$ and the resistivity 30 to 500 microhm-cm. An increase of resistivity with increase of temperature was observed in almost all cases, an exception was Gd_2Se_3. There was tendency for gadolinium selenide samples of higher resistivity to have higher Seebeck coefficients. The sample having the highest resistivity (1 ohm-cm at 200°C) had one of the highest Seebeck coefficients (500 $\mu V/°C$) at the same temperature.

A variation of about 0.5% selenium from the Gd_2Se_3 composition reduces by some 75-80% the Seebeck coefficient obtained from the 2:3 compound.

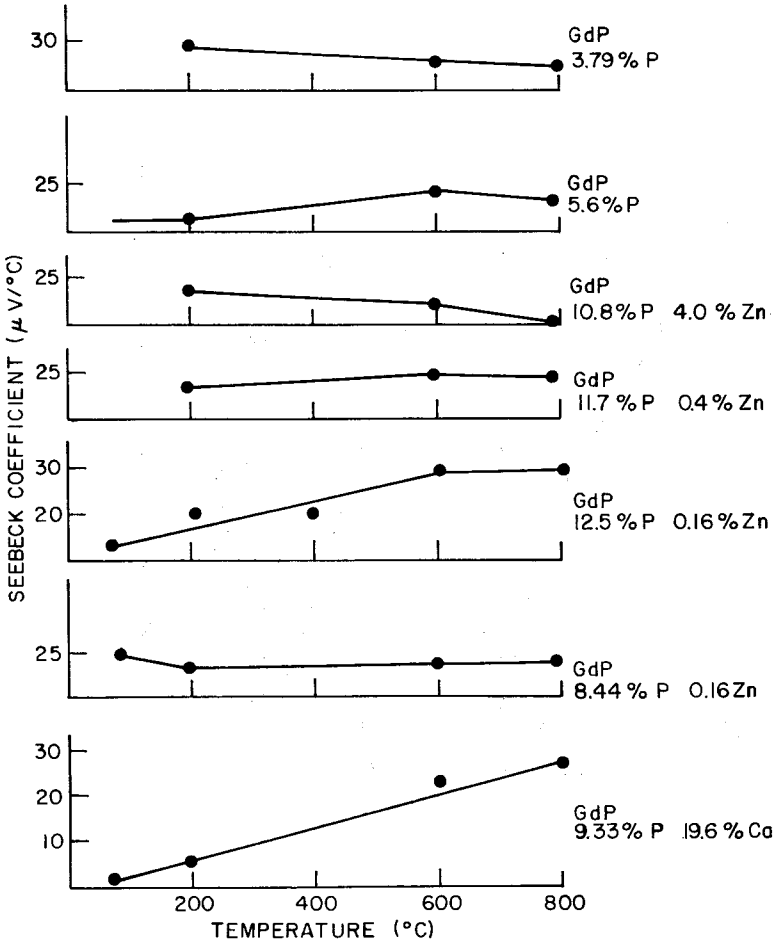

Fig. 43 - Gadolinium-Phosphorus Systems

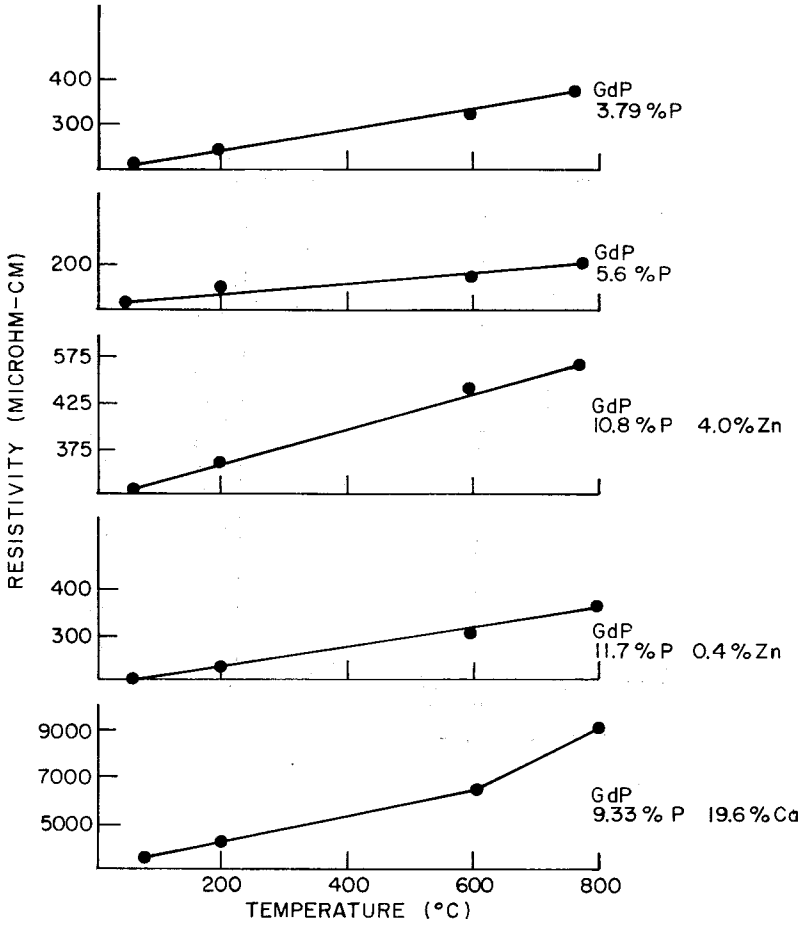

Fig. 44 - Gadolinium-Phosphorous System

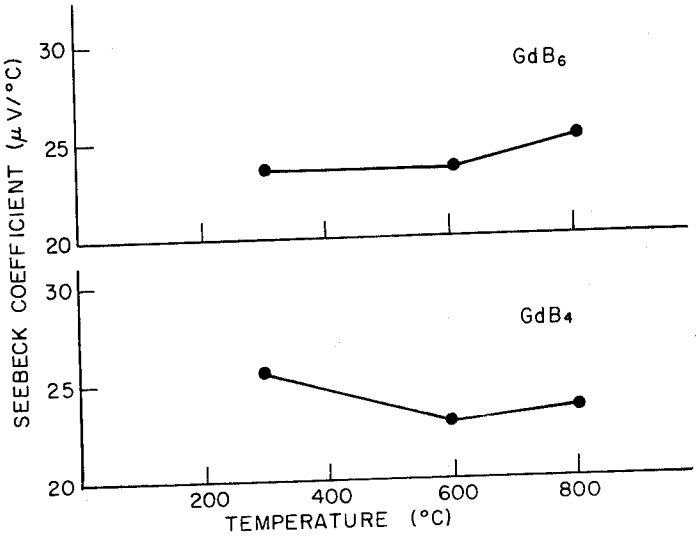

Fig. 45 - Gadolinium-Boron System

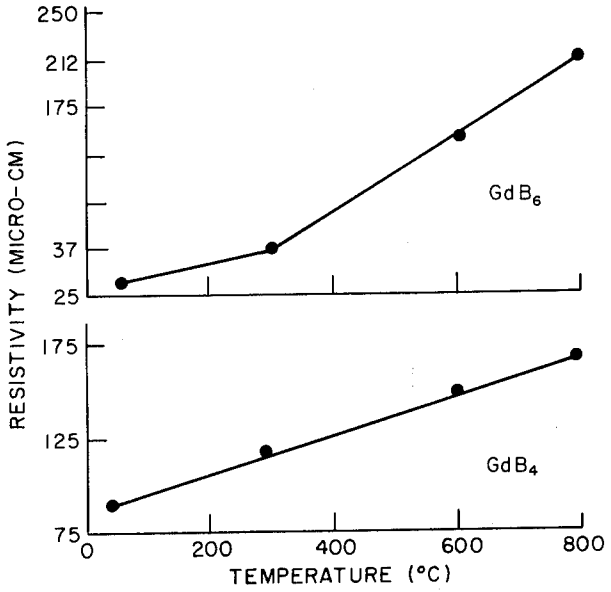

Fig. 46 - Gadolinium-Boron System

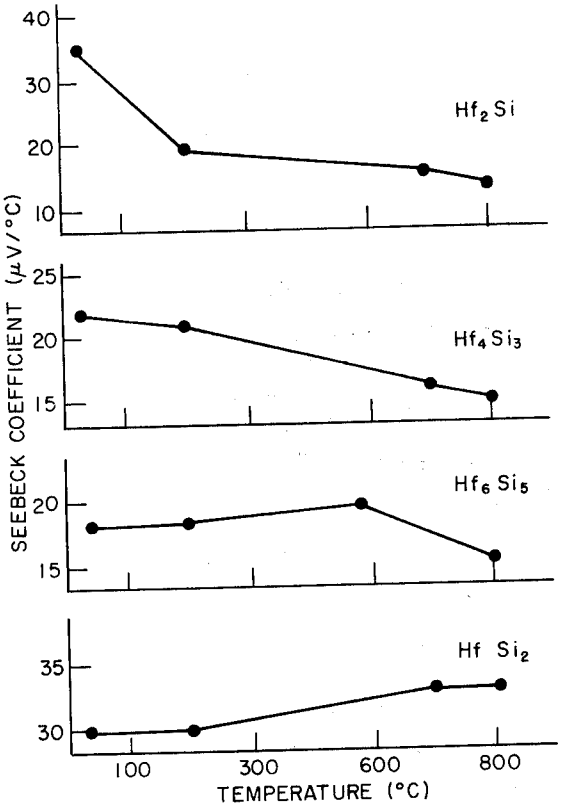

Fig. 47 - Hafnium-Silicon System

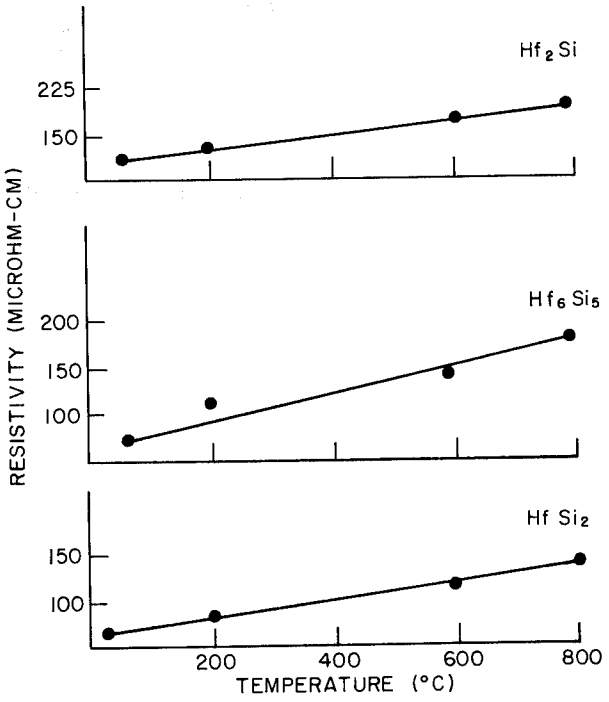

Fig. 48 - Hafnium-Silicon System

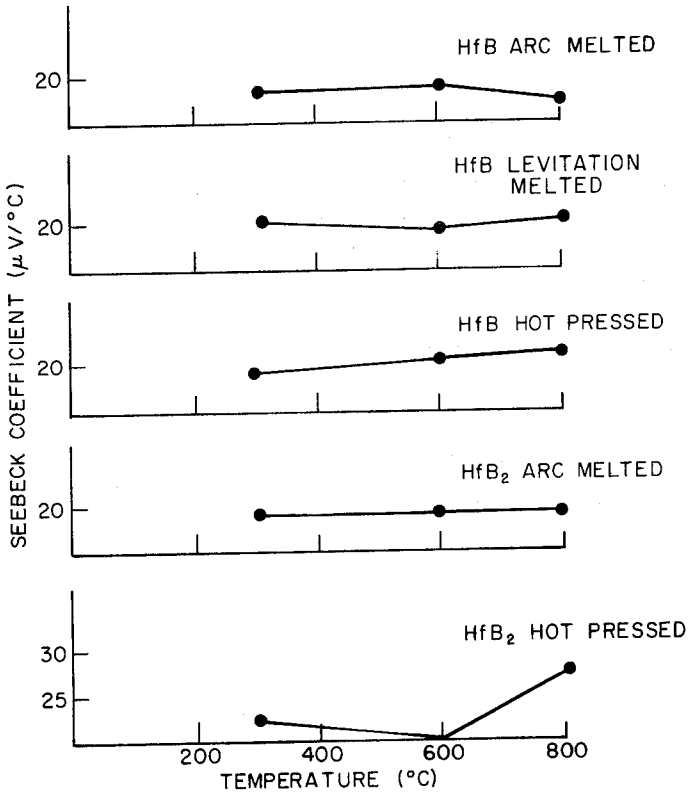

Fig. 49 - Hafnium-Boron System

The relationship between the gadolinium mono-and diselenides appears to develop as follows. The cubic GdSe lattice can accept selenium atoms interstitially forming, in part $GdSe_2$. However, not until a composition equivalent to Gd_3Se_4 is reached, does the cubic lattice become strained to the orthorhombic conformance required for $GdSe_2$. The proximity of this lattice change point to the Gd_3Se_4 composition may account for previous assumptions of the existence of such a compound having a "lacunary" structure. The existence of a high temperature eutectic at the 3:4 composition is further evidence against the existence of a Gd_3Se_4 entity.

X-ray and metallographic examinations indicated that, in low temperature preparations, compositions equivalent to Gd_2Se_3 are composed of GdSe with $GdSe_2$ or Se.

Magnetic data and the results of electrical measurements would seem to indicate a degree of covalent bonding in the compounds formed.

The higher resistivities found for Gd_2Se_3 and $GdSe_2$ would suggest a tendency towards ionic characteristics, but the magnetic moments found do not confirm a purely ionic state. The high thermal stability of Gd_2Se_3, combined with the foregoing considerations, may be interpreted in terms of resonance between the covalent and ionic contributions to the bond.

RARE EARTH CHALCOGENIDES

Research Chemicals*, division of Nuclear Corporation of America, is continuing the examination of the thermoelectric properties of rare earth compounds with sulfur, tellurium and selenium at elevated temperatures. Forty-five chalcogenide compounds have been prepared. Included are a number of gadolinium selenide compositions prepared under varying conditions; selenide compounds of lanthanum, yttrium, samarium, ytterbium, erbium and paraseodymium; telluride compounds of gadolinium and yttrium, and sulfides of gadolinium and yttrium. Yttrium-gadolinium selenide has been synthesized. The starting material has been a vapor-reacted product which was melted in the arc furnace, induction furnace under variable pressure, and/or the travelling zone furnace under varying number of passes and passage speed.

Examination of the apparent effect of processing variables upon thermoelectric parameters of GdSe indicates that the major contribution lies in developing the optimum composition by adjustment of heat treatment parameters.

The effect of these parameters is yet to be determined. Zone melting does detract from thermoelectric power of gadolinium selenide. Ytterbium selenide shows an anomalous Seebeck coefficient. Lanthanum and samarium selenides are isostructural with the gadolinium compound. Gadolinium selenide appeared to have more promise than gadolinium telluride or sulphide. See Table VIII.

---

*Department of the Navy Contract No. NObs 78503. Progress Report No. 3 for period 1 October to 30 November 1960.

TABLE VIII

Thermoelectric Properties of Some Chalcogenide Compounds

Selenides	Seebeck Coefficient (μV/C)		Resistivity (milliohm-cm)	
	100°C	800°C	30°C	800°C
Yttrium	0	-97	4440	75 (700°C)
Lanthanum	-84	-208	4.7	15
Praseodymium	-62	-168	5.7	23.4
Samarium	-65	-79	2.0 (200°C)	2.1 (600°C)
Gadolinium	-136	-506	1.1	4.5
Erbium	-108	-164	49.5	68.7
Ytterbium	230	298	---	---
Tellurides				
Yttrium	0	-127	.25	.47
Gadolinium	0	-31	13	14
Sulphide				
Gadolinium	-250	-452	38,000	4100

RESEARCH PROGRAM ON SEMICONDUCTING COMPOUNDS FOR THERMOELECTRIC POWER GENERATION AT HIGH TEMPERATURES

Chrysler Corporation* is investigating semiconducting combinations of the heavy refractory metals with high atomic weight elements of groups IV B, V B, and VI B of the periodic table, and of less metallic variations of the refractory superlattice intermetallic compounds, as possible materials for high temperature thermoelectric elements. All combinations of the heavy refractory metals to be included in this survey have been studied for compound formation with the exception of materials containing arsenic. Figure 50 shows the status of materials which have been studied as to compound preparation.

The existence of 14 intermetallic compounds has been confirmed. With the possible exception of arsenic, tungsten formed only two inter-metallic compounds. Tantalum formed compounds with selenium, tellurium, germanium and antimony. Hafnium formed compounds with selenium, germanium, and antimony. The hafnium and tellurium reaction product gave no X-ray diffraction pattern and that for hafnium-bismuth gave only lines due to bismuth. Rhenium formed compounds with selenium, tellurium and germanium.

Property measurement (S, ρ , and K) have been made on samples of NiAl, TaSb, WTe_2, TaTe, $TaGe_2$, $TaGe_2 + Ta_2Ge + Ta$, TaSb, $ReSe_2$. The data does not extend beyond 550°C. Only WSe_2, Figure 51, appeared to have promise and that for medium temperature application if it could be alloyed to decrease the resistivity without too great a decrease in Seebeck coefficient.

*Department of the Navy Contract NObs-78664, Chrysler Corporation Bimonthly Progress Report No 3 covering period of 15 September through 14 November 1960 and No. 4 covering period of 15 November 1960 through 14 January 1961.

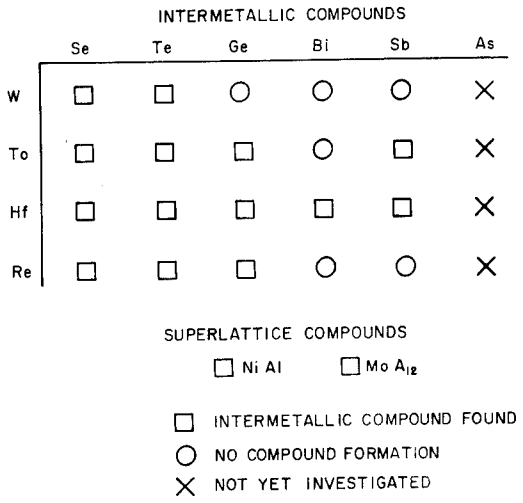

Fig. 50 - Status of Compound Preparation

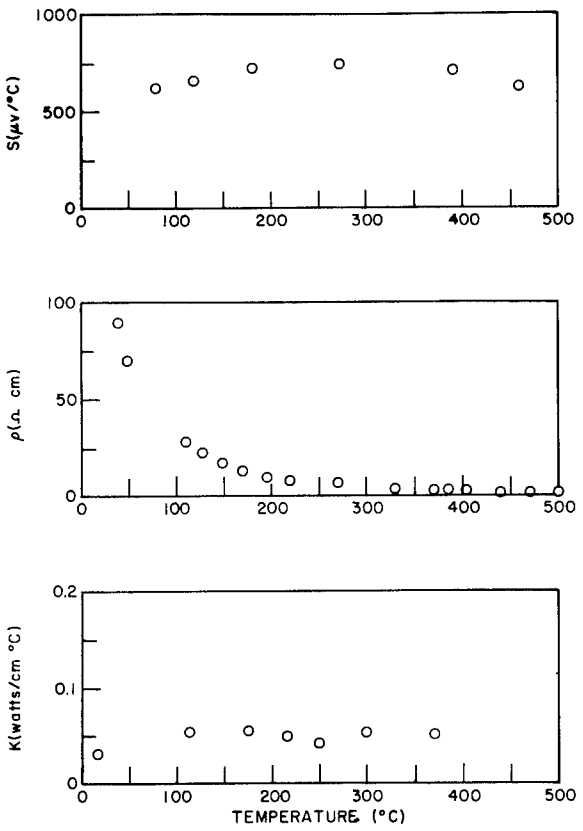

Fig. 51 - WSe_2

STRUCTURAL INVESTIGATIONS IN THERMOELECTRIC MATERIALS

Merck, Sharp & Dohme Research Laboratories*, division of Merck & Company, Inc., has conducted further studies of alloy system $Bi_{24}Sb_{60+x}Se_6Te_{150-x}$ in the range $+5 \leqslant x \leqslant +10$. Alloy 68, $Bi_{24}Sb_{68}Se_6Te_{142}$, obtained by setting x = 8, was the composition representing the optimal thermoelectric system. The purity of the antimony used in Alloy 68 preparation had some bearing on the thermoelectric properties of the ingot. The greatest changes occurred in the thermal conductivity. All ingots were zone-levelled. The results are listed in Table IX below.

TABLE IX

x	Seebeck Coefficient S(μV/°K)	Resistivity ρ (ohm cm) x 10^4	Thermal Conductivity K (watt/cm°K)	Figure of Merit Z(deg.$^{-1}$) x 10^3
6	+210	10.2 ± 0.3	0.0155	2.8
7	+205	10.0 ± 0.3	0.0138	3.1
8	+225	10.1 ± 0.4	0.0145	3.5

Alloy 68 has a Seebeck coefficient of +225 μV/°K, resistivity 10.1 ± 0.4 x 10^4 ohm cm, thermal conductivity of 0.0145 watt/cm°C, and Figure of Merit of 3.5 x 10^{-3}/°C.

Results of doping Alloy 68 with copper and mercury indicated that both agents tended to render the alloy degenerate. The results with copper were

* Department of the Navy Contract No. NObs 78503. Progress Report No. 3 for period 1 October to 30 November 1960.

highly erratic, whereas those with mercury were quite consistent. The trend to more metallic behavior with increasing mercury content was obvious. The Seebeck coefficient, resistivity, thermal conductivity and figure of merit of Alloy 68 as a function of weight % of mercury are shown in Figures 52 and 53, respectively. Electrical conductivity versus thermal conductivity of Alloy 68 doped with mercury is shown in Figure 54 for the purpose of determining phonon thermal conductivity, (Kph). Line 1 represents the Wiedemann-Franz law for non-degenerate semiconductors. Line 2 represents the law for degenerate semiconductors. The points shown on Lines 3 and 4 are taken from the curves in Figures 52 and 53. The lower four points, in the compositional range of 0-0.4% Hg., fall on a line (line 3) which parallels the non-degenerate semiconductor line. The highest of these four points, plus the next two points, fall on a line (line 4) paralleling that for degenerate semiconductors. This is the compositional range 0.4 - 0.75% Hg. Thus, Alloy 68, remained a non-degenerate semiconductor up to 0.4% Hg. beyond which degenerate behavior occurred. The carrier concentration of undoped material was $2 \times 10^{19}/cm^3$, whereas the threshold for degenerate behavior was estimated to occur at about $2.5 \times 10^{19}/cm^3$. From Figure 54 it can be determined that Kph for Alloy 68 is 0.007 watts/cm°K, and 0.0025 watts/cm°K for degenerate material.

The results on "stoichiometric" material, $Bi_{24}Sb_{68}Se_6Te_{132}$ and materials prepared in which 10 atoms excess of TeSe, Bi, and Sb were added, are listed in Table X which follows:

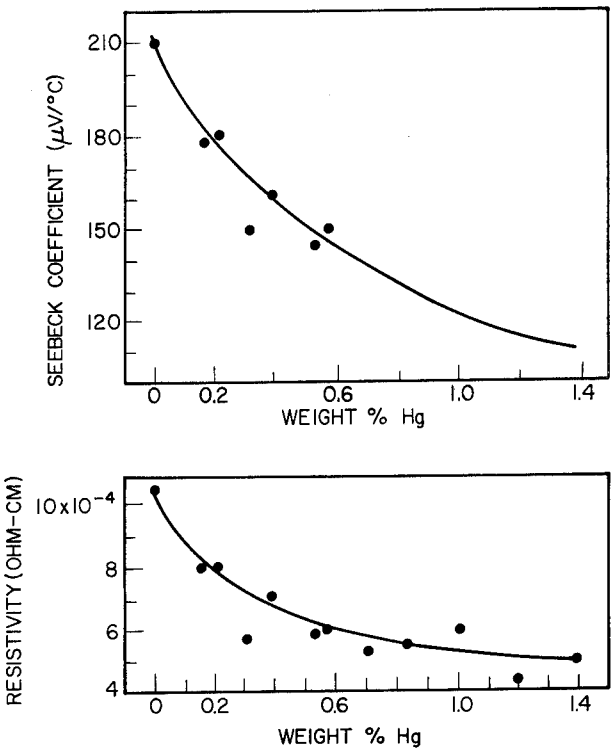

Fig. 52 - Seebeck Coefficient and Resistivity of Alloy 68 as a Function of Weight % of Mercury

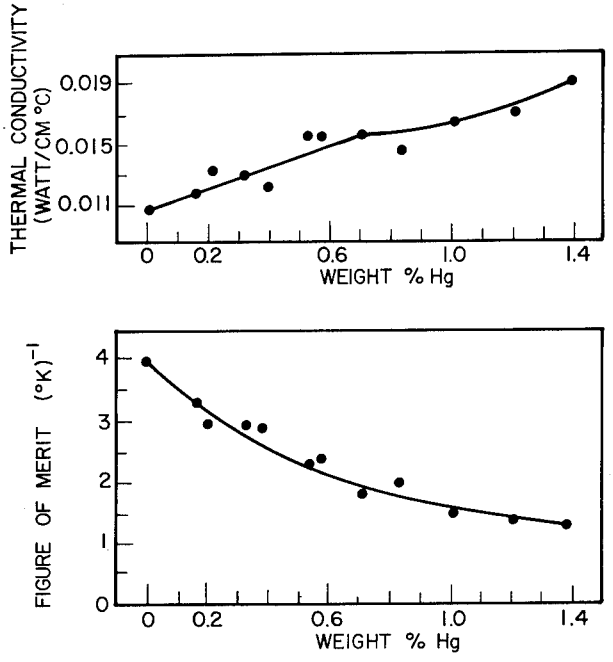

Fig. 53 - Thermal Conductivity and Figure of Merit of Alloy 68 as a Function or Weight % of Mercury

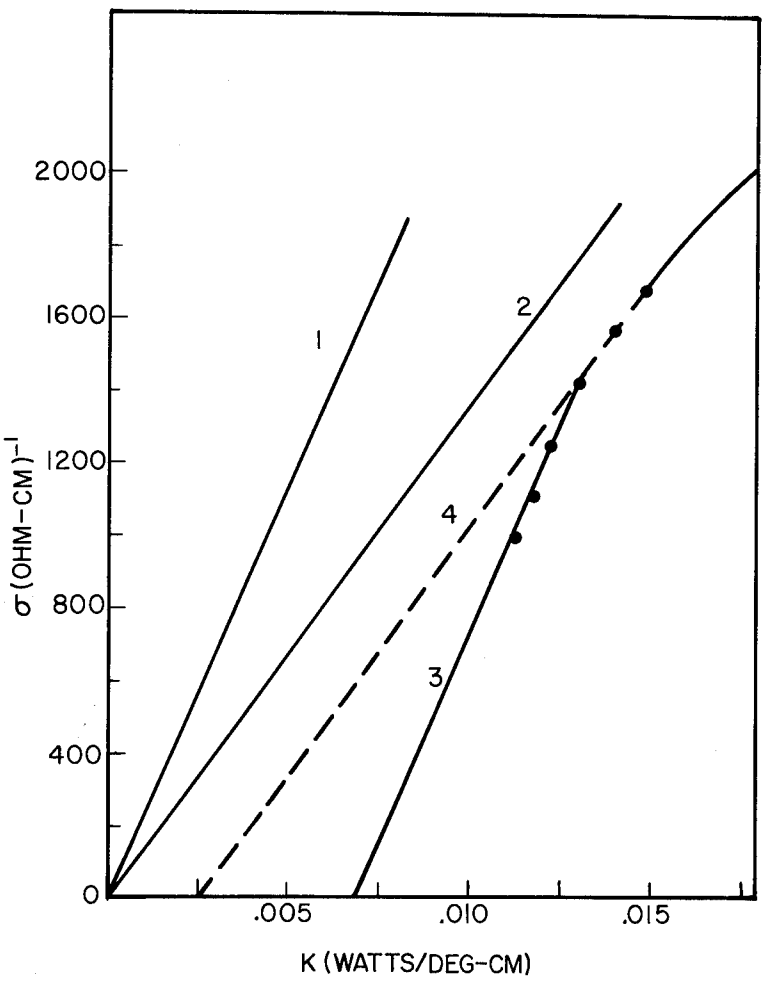

Fig. 54 - Electrical vs Thermal Conductivity of Alloy 68 Doped with Mercury: Curve 1 - Widermann-Franz Law for non-degenerate semi-conductors; Curve 2 - Widermann-Franz Law for degenerate semi-conductors; Curve 3 - Shows that low mercury content gives rise to non-degenerate semi-conductor behavior; Curve 4 - Shows that higher mercury content gives rise to degenerate semi-conductor behavior.

TABLE X

Material	Seebeck Coefficient $S(\mu V/°C)$	Resistivity ρ (ohm c m) x 10^4	Thermal Conductivity K(watts/cm°C)	Figure of merit $Z(deg^{-1}) \times 10^3$
Stoichiometric $Bi_{24}Sb_{68}Se_6Te_{132}$	+169	8.1	0.0204	1.7
Stoich. + 10 Te (Alloy 68) $Bi_{24}Sb_{68}Se_6Te_{142}$	+210	10.5	0.0110	4.0
Stoich. + 10 Se $Bi_{24}Sb_{68}Se_{16}Te_{132}$	+235	21.7	0.0204	1.2
Stoich. + 10 Bi $Bi_{34}Sb_{68}Se_6Te_{132}$	+102	7.2	0.0286	0.5
Stoich. + 10 Sb $Bi_{24}Sb_{78}Se_6Te_{132}$	+ 83	5.3	0.0284	0.5

Results from stoichiometric material $Bi_{24}Sb_{68}Se_6Te_{132}$ + 10 Te, (Alloy 68), were S = +210 $\mu V/°C$, $\rho = 10.5 \times 10^{-4}$ ohm cm $K = 0.0110$ watts/cm°C, and $Z = 4.0 \times 10^{-3}/°C$. Alloy 68 had low thermal conductivity caused by excess tellurium. Better Seebeck coefficients and resistivities were found among four other compositions but none of them approached Alloy 68 in thermal conductivity or figure of merit.

The effect of oxygen on Alloy 68 was to lower the thermal conductivity and increase the electrical resistivity. Oxygen was introduced into the lattice of Alloy 68 by addition of Sb_2O_4. The resulting ingots were zone-leveled. The actual amount of oxygen in the material is unknown. Results of measurements are given in Table XI which follows:

TABLE XI

Wt. % Sb_2O_4	Coefficient S(μV/°C)	Resistivity ρ(ohm cm) x 10^4	Thermal Conductivity κ(watt/cm°C)	Figure of Merit Z(deg.$^{-1}$) x 10^3
0.05	+209	10.2	.0123	3.5
0.10	+212	10.6	.0127	3.3
0.50	+211	11.0	.0114	3.6

In an initial search for n-type systems displaying poising properties, $BiSeTe_2$ and $AsBiTe_3$ were considered possible points of departure, with $AsBiTe_3$ derivatives more attractive. Both compositions had Seebeck coefficients of about -200 μV/°K but their resistivities were rather high ($\sim 30 \times 10^{-4}$ ohm cm).

Merck, Sharp & Dohme Research Laboratories*, have continued their studies of the BiSbTe system by selecting for manipulation compositions $Bi_2Te_3 \cdot 2Sb_2Te_3$ and $Bi_2Te_3 \cdot 7Sb_2Te_3$ containing a lesser and a greater proportion of antimony than series $Bi_2Te_3 \cdot 3Sb_2Te_3$ (of which alloy 68 is a member). The sets $Bi_{28}Sb_{48+x}Te_{134-x}$ and $Bi_{12}Sb_{70+x}Te_{158-x}$ were investigated. Measurement data is given in Tables XII and XIII which follow:

TABLE XII

The System $Bi_{28}Sb_{48+x}Te_{134-x}$

	Seebeck Coefficient S (μV/°K)	Resistivity ρ (ohm cm) x 10^4
-8	-10	19.0
-4	+62	18.5
0	+148	19.0
+2	+172	16.0
+4	+183	14.0
+6	+175	9.0
+8	+150	5.0

*Department of the Navy Contract NObs 78503. Progress Report No. 4 for period 1 December 1960 to 31 January 1961.

TABLE XIII

The System $Bi_{12}Sb_{70+x}Te_{158-x}$

X	Seebeck Coefficient S(μV/°K)	Resistivity ρ(ohm cm) x 10^4	Thermal Conductivity K(watt/cm°K)	Figure of Merit Z x 10^3
-10	+135	5.5	-	-
- 6	+129	6.2	-	-
- 2	+155	5.1	0.0224	2.1
0	+137	4.8	-	-
+ 2	+145	4.9	0.0203	2.1
+10	+137	4.3	0.0220	2.0

No thermal conductivities were measured for system $Bi_{28}Sb_{48+x}Te_{134-x}$ because of its poor characteristics. A few were obtained for $Bi_{12}Sb_{70+x}Te_{158-x}$. Neither had an alloy of outstanding properties. Referring to Table XII, the Seebeck coefficient changes rapidly with composition, eventually becoming negative. The resistivity becomes invariant with composition below x = 0. Table XIII indicates slight change in either Seebeck coefficient or resistivity. These systems which bracket the Alloy 68 series, indicate greater resistance to compositional change with greater concentration of antimony content.

Substitution of selenium for tellurium in the alloys x = -2 and -6 leads to an over-all degradation of the figure of merit as indicated in Table XIV which follows.

TABLE XIV

Alloy	Seebeck Coefficient S(μV/°K)	Resistivity ρ(ohm cm) x 10^4	Thermal Conductivity K(watt/cm°K)	Figure of Merit Z x 10^3
$Bi_{12}Sb_{68}Se_{12}Te_{148}$	+140	10.2	0.0190	1.0
$Bi_{12}Sb_{68}Se_{24}Te_{136}$	+137	12.7	0.0165	0.9
$Bi_{12}Sb_{64}Se_{12}Te_{152}$	+147	7.5	-	-
$Bi_{12}Sb_{64}Se_{24}Te_{140}$	+130	11.6	-	-

Investigations were continued in the analogous vanadium alloy system of Alloy 68. Compositions $V_{24}Sb_{60}Se_6Te_{150}$ and $V_{60}Sb_{24}Se_6Te_{150}$, see Table XV, turned out to be nearly degenerate and further work was discontinued.

TABLE XV

Alloy	Seebeck Coefficient S(μV/°K)	Resistivity ρ(ohm cm) x 10^4	Thermal Conductivity K(watt/cm°K)	Figure of Merit Z x 10^3
$V_{24}Sb_{60}Se_6Te_{150}$	+70	8.0	0.0196	0.31
$V_{60}Sb_{24}Se_6Te_{150}$	+40	7.0	0.0206	0.11

Determination was made on whether vanadium containing n-type alloys could be produced based on the system $Bi_2Se_xTe_{3-x}$ where x ranged from 1 to 1.5. An n-type composition Bi_2SeTe_2 was obtained and abandoned because of its extremely erratic behavior and evident intractability.

The arsenic-containing series $(Bi, Sb)_x As_{2-x}Te_3$ were investigated for an n-type alloy and experimented difficulties precluded reasonable results. The system $Sb_xAs_{2-x}Te_3$ was found to be all p-type with low Seebeck coefficients as shown in Table XVI which follows.

TABLE XVI

Alloy	Seebeck Coefficient S(μV/°K)	Resistivity ρ (ohm cm) x 10^4	Thermal Conductivity K(watt/cm°K)
$Sb_{0.5}As_{1.5}Te_3$	+35	-	-
$Sb_{1.0}As_{1.0}$	+73	15.5	0.0150
$Sb_{1.5}As_{0.5}Te_3$	+65	6.6	-

As_2Te_3 and Sb_2Te_3 were p-type

Several compositions in the $Bi_xAs_{2-x}Te_3$ system were studied. The samples were n-type in the range of 20% to about 80% as_2Te_3. The somewhat erratic results are shown in Table XVII which follows:

TABLE XVII

Alloy	Seebeck Coefficient S(μV/°K)	Resistivity ρ (ohm cm) x 10^4	Thermal Conductivity K(watt/cm°K)
$Bi_{1.9}As_{0.1}Te_3$	+177	29	-
$Bi_{1.8}As_{0.2}Te_3$	+150	16	0.0200
$Bi_{1.7}As_{0.3}Te_3$	+ 85	24	0.0157
$Bi_{1.6}As_{0.4}Te_3$	+ 35	32	0.0163
$Bi_{1.5}As_{0.5}Te_3$	-158	15	0.0148
$Bi_{1.5}As_{0.5}Te_3$	- 50	34	0.193
$Bi_{1.2}As_{0.8}Te_3$	-180	56	0.0092
$Bi_{1.0}As_{1.0}Te_3$	-128	26	-
$Bi_{1.0}As_{1.0}Te_3$	-180	72	0.0086
$Bi_{1.0}As_{1.0}Te_3$	-180	25	-
$Bi_{0.5}As_{1.5}Te_3$	- 45	12	0.0148

An attempt was made to lower the resistivity of $AsBiTe_3$ by substituting HgTe (n-type) for 20% of the Bi_2Te_3 and, in turn, the As_2Te_3. The resulting materials were p-type, however high resistivities, and are unpromising. $Bi_{1.0}As_{0.8}Hg_{0.2}Te_{2.9}$ had S = +160 $\mu V/°K$ and ρ = 40×10^{-4} ohm cm. $Bi_{0.8}As_{1.0}Hg_{0.2}Te_{2.9}$ had S = +130 $\mu V/°K$ and ρ = 70×10^{-4} ohm cm.

Further investigations, not directly covered by the contract, were carried out on alloy system $Bi_{24}Sb_{68}Se_6Te_{142}$ (Alloy 68). Alloy 68 compositions are, as a rule, not single-phase. Homogeneous single-phase samples had been prepared but their exact composition had not been determined. In the single-phase material, no evidence for a superstructure had been uncovered. Previous claims for a superstructure on Alloy 68 were in error. The superstructure lines were due to a second phase rich in tellurium. The thermal conductivity measurements were found in error necessitating a correction factor (multiple) of at least 1.1. This reduced the figure of merit, the best for Alloy 68 compositions, being around $3.5 \times 10^{-3}/°K$. Due to recent developments, a re-examination of previous results on Alloy 68 compositions is being made to remove any uncertainties as to their thermoelectric performance.

SEMICONDUCTING MATERIALS

State University of New York College of Ceramics* at Alfred University Alfred, New York, have tested for thermoelectric properties single-crystal and hot-pressed polycrystalline samples of Cd Te, Bi_2Te_3 and Bi_2Se_3 and a high-density hot-pressed sample of boron phosphide. The boron phosphide sample was prepared by rapidly hot-pressing cubic boron phosphide at between 1800° and 2000°C under a pressure of 5000 psi. Above 1550° the compound decomposed, so the pressed compact is deficient in phosphorus. The final specimen was extremely hard and was very resistant to oxidation. The sample appeared to be a p-type conductor.

Both single-crystal and hot-pressed Bi_2Se_3 samples were n-type. Bi_2Te_3 samples varied.

All thermoelectric measurements were conducted from room temperature to 350°C in a helium atmosphere. Direct current measurement techniques were used. Activation energy values were determined to be about 0.09 ev for single-crystal bismuth selenide, 0.11 for single-crystal bismuth telluride, and 0.11 and 0.14 for the respective hot-pressed samples. It was about 0.12 ev for the hot-pressed boron phosphide sample. Other thermoelectric properties of the samples are given in Table XVIII. These measurements should be considered as tentative results. The Seebeck coefficients, S, and figure of merit, Z, are exceptionally high, particularly those of boron phosphide with its high thermal conductivity and low electrical conductivity. The top operating temperature of boron phosphide is possibly in excess of 1500°C. Z for boron phosphide and bismuth selenide decreases with increase in temperature. The polycrystalline samples generally exhibit higher values of Z than do the single crystals.

TABLE XVIII

RESULTS OF THERMOELECTRIC MEASUREMENTS

Sample	Temp. °C	k-w/°cm	ρ -ohm^{-1}cm^{-1}	S -volts/°C	Z-deg^{-1}
Boron Phosphide #7	76	8.0×10^{-3}	57	2.73×10^{-3}	5.2×10^{-2}
	162	8.6×10^{-3}	105	2.0×10^{-3}	4.9×10^{-2}
	352	6.7×10^{-3}	220	3.8×10^{-4}	4.8×10^{-3}
Bi_2Se_3 (Single Crystal)	51	7.7×10^{-3}	1700	2.2×10^{-4}	10.9×10^{-3}
	140	5.2×10^{-3}	1260	1.7×10^{-4}	7.0×10^{-3}
	238	3.9×10^{-3}	1020	1.30×10^{-4}	4.8×10^{-3}
Bi_2Te_3 (Single Crystal)	244	3.36×10^{-3}	780	2.1×10^{-4}	10.3×10^{-3}
Bi_2Se_3 * HP #4	155	4.7×10^{-3}	780	2.4×10^{-4}	9.3×10^{-3}
HP #7	172	6.0×10^{-3}	1200	2.0×10^{-4}	8.2×10^{-3}
Bi_2Te_3 HP #3	155	4.0×10^{-3}	500	4.9×10^{-4}	2.9×10^{-2}

* HP - Hot-Pressed

MATERIALS DEVELOPMENT

Battelle Memorial Institute* has made high-temperature electrical measurements on selected specimens of III-V compounds, specifically Ga As - Al As alloy of various compositions.

The "solute buildup technique" was used in preparing an ingot of Ga As. It has been demonstrated that the technique is applicable for preparation of sound, directionally grown ingots of intermetallics at temperatures far below their melting points and under conditions of relatively low activity of solute.

A plot of energy gap values for Ga As - Al As in the mole percent of Al As composition, shown in Figure 55, indicates that the energy gap of the alloy varies linearly with Al As content. This implies that the band structures of Ga As and Al As are similar. By extrapolation to 100% Al As as an energy gap of 2.3 ev is obtained.

A plot of resistivity versus reciprocal temperature for a Ga As - Al As specimen is shown in Figure 56. The initial decrease in the resistivity as temperature was increased was probably associated with the grain boundaries since the material was high poly-crystalline. Above about 400°C the grain-boundary effect is apparently overcome by the normal decrease in mobility with increasing temperature. Around 730°C the resistivity levels off due probably to the onset of intrinsic condition.

Hall coefficient data for the above Ga As - Al As specimen are shown in Figure 57. The plot is similar to those observed for n-type Ga As and other n-type Ga As-Al As alloys. The increasing Hall coefficient at

*Department of the Navy contract NObs 77034. Tenth Bimonthly Report covering period 7 July through 7 September 1960.

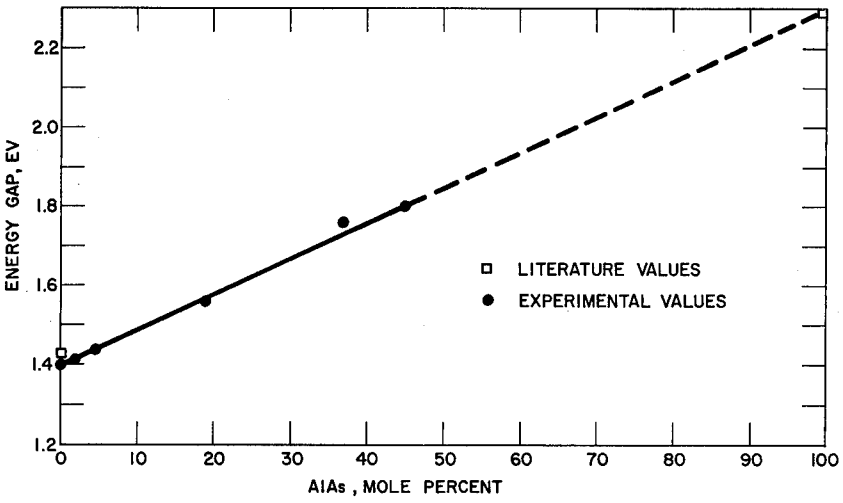

Fig. 55 - Optical Energy Gap vs Composition GaAs-AlAs

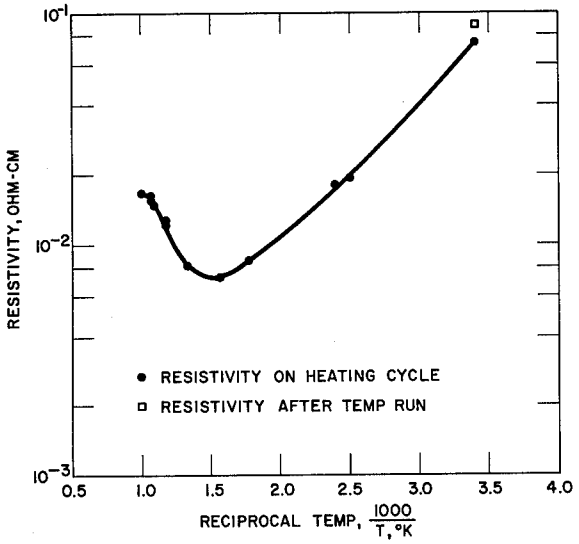

Fig. 56 - GaAs-22.3 Mole percent AlAs (n type)

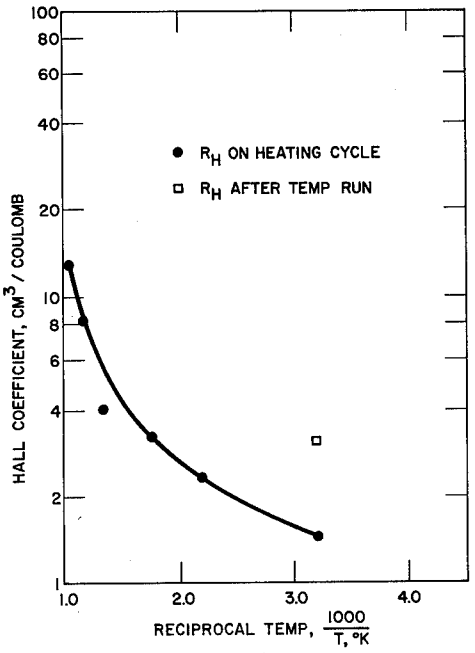

Fig. 57 - GaAs-22.3 Mole percent AlAs (n type)

elevated temperatures has been explained in terms of a second minimum in the conduction band; this may also hold for the n-type alloy. The initial room-temperature Hall coefficient was not reproduced after the temperature run; its increase was unexplained.

The Seebeck coefficient for the GaAs - AlAs specimen is shown in Figure 58. The value at 730°C was in question. Additional measurements are necessary to determine if a maximum is reached around 700°C. The plot is similar to that which was observed for an n-type gallium arsenide.

Qualitative consideration of available data indicates that Z as great as 10^{-3}/°C may be difficult to achieve in GaAs - 22% AlAs alloys at any temperature.

Detailed experimental investigations of the adiabatic and isothermal Hall coefficients, R^a and R^i respectively, were carried out in PbTe from 77 to 300°K.

R^a and R^i measurements versus reciprocal temperature are shown in Figure 59. The differences between R^a and R^i at lower temperatures is small. The temperature dependence of ratio $\frac{\Delta R}{R} = \frac{R^a - R^i}{R^i}$ is shown in Figure 60. The calculated values were made with the assumption that the charge-carrier scattering mechanism could be described in terms of an energy-independent relaxation time and that the carrier mobility varies as T^{-2}. The lattice contribution to the thermal conductivity was taken to be a simple inverse function of the temperature. With such assumptions made in the calculation, the quantitative agreement between the theoretical and experimental values of $\frac{\Delta R}{R}$ should not be taken too seriously. The sharp rise in $\frac{\Delta R}{R}$ at the higher temperatures is not presently understood. If intrinsic conduction was beginning to be significant, it would have been expected that the figure-of-merit would decrease, although the quantity $\frac{\Delta R}{RZT}$ should not change markedly.

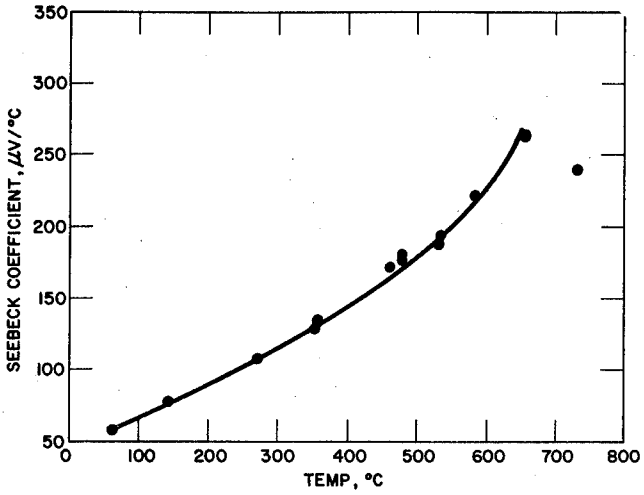

Fig. 58 - GaAs-22.3 Mole percent AlAs (n type)

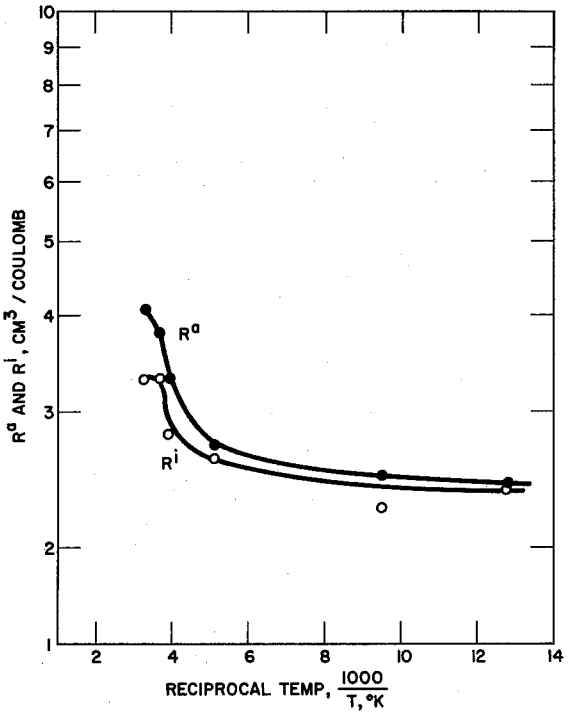

Fig. 59 - R^a and R^i versus 10^3/ T at 14000 Gauss for PbTe

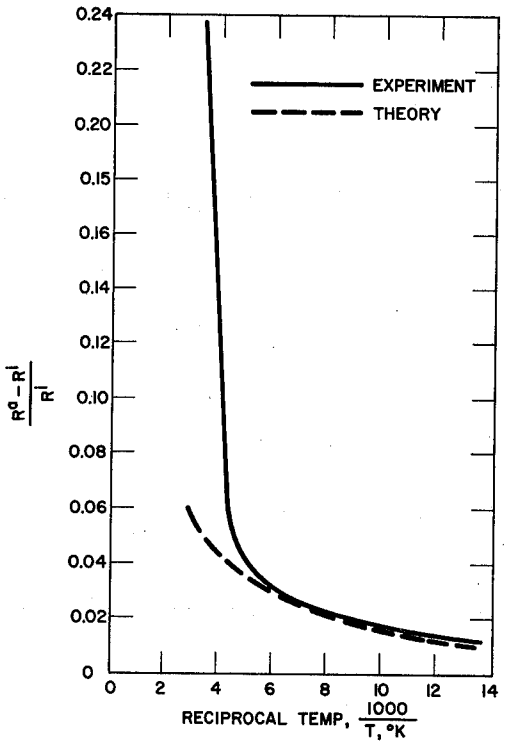

Fig. 60 - Comparison of Measured and Calculated values of R^a - R^i/R for PbTe

Battelle Memorial Institute* have made high-temperature electrical measurements on selected gallium arsenide-aluminum arsenide specimens of various compositions.

Determination was made of the effect of a boron nitride versus a quartz melt container on the purity of the resulting ingot of GaAs prepared by the solute build-up technique. In view of probable contamination of the melt by silicon, it was considered that quartz was not a suitable material for the melt container if long reaction times were required.

High-temperature measurements were made on n-type GaAs-AlAs alloy samples containing 3.8, 7.8 and 22.3 mole percent AlAs, under maintained arsenic pressure, to approximately 730°C. There was an initial decrease in resistivity as temperature was increased. The higher alloy, n-type had increasing Hall coefficient at elevated temperatures. The low alloy had a small p-type Hall coefficient, which was unexplained. The sample was n-type according to thermoelectric probe.

The Hall mobility for GaAs-AlAs alloys at room temperature is extremely low. At temperatures where the alloys would be considered as thermoelectric materials (700°C) it is high and still increasing at the highest temperature reached in the measurements.

The Seebeck coefficient increases with temperature, Figure 61. The data suggest that the Seebeck coefficient of the GaAs-AlAs alloys(having roughly equivalent carrier concentrations) increases with AlAs concentration. Behaviour of the 3.8 mole percent AlAs sample was not understood. The Seebeck coefficient increased slowly with increasing temperature to 57.2 μV/°C and after heating for approximately 2-1/2 hours it increased to 185.8 μV/°C and continued to increase to 201.5 μV/°C at 726°C. The original curve was not reproduced on cooling to 400°C.

*Department of the Navy Contract NObs-77034. Battelle Memorial Institute Eleventh Bi-monthly Report covering period 7 September through 7 November 1960 dated 18 January 1961.

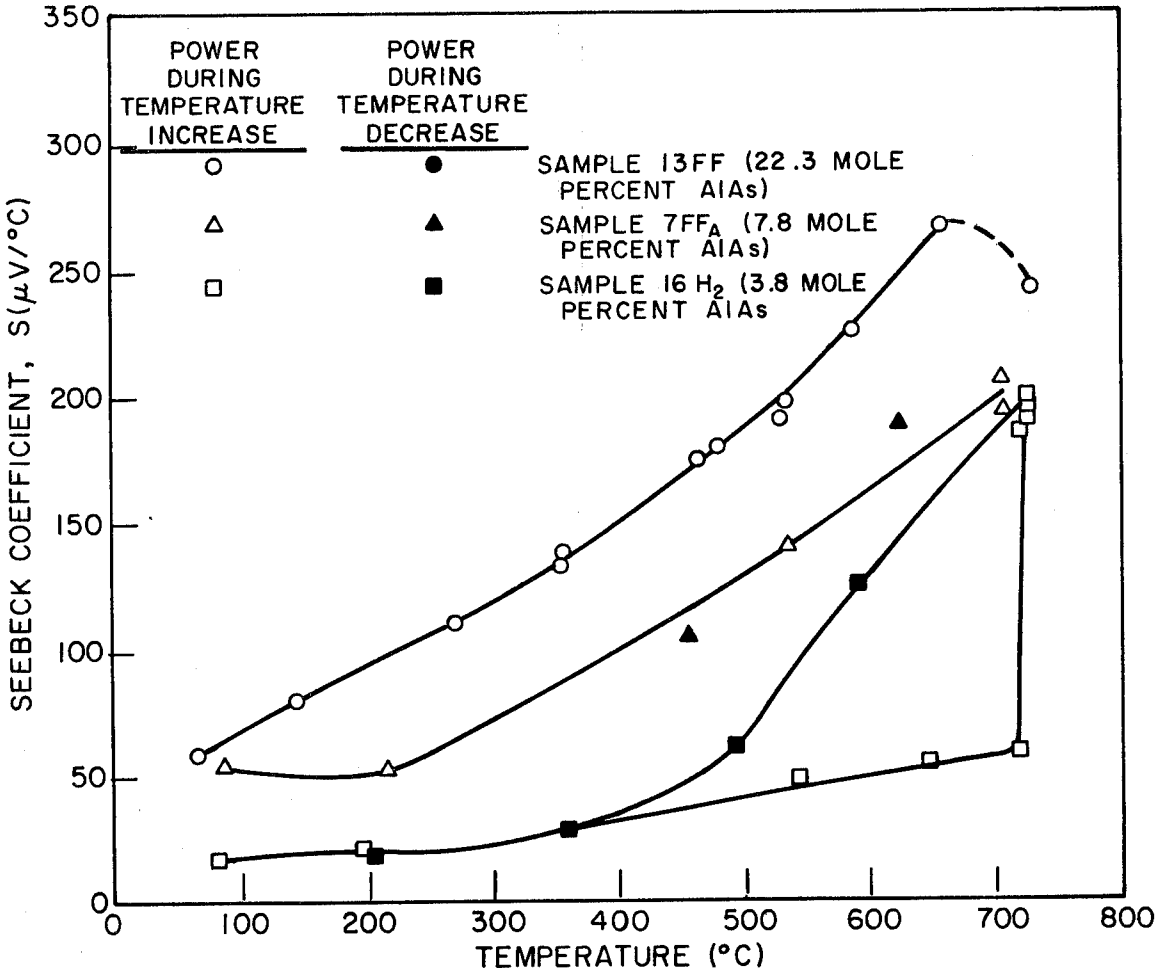

Fig. 61 - GaAs-AlAs Alloys

MATERIALS FOR THERMOELECTRIC POWER GENERATION

General Electric Company* reported on their study of the effects of Tellurium loss from $CuGaTe_2$. Results of room temperature measurements of the semiconducting properties were as follows:

	Before Heat Treatment	After First Evaporation	After Second Evaporation
Resistivity, ρ (ohm-cm)	4.06×10^{-3}	4.13×10^{-3}	$\sim 5 \times 10^{-3}$
Thermal conductivity, K (watts/cm°C)	2.4×10^{-2}	2.7×10^{-2}	1.9×10^{-2}
Seebeck coefficient, S ($\mu V/°C$)	+ 101	+90.4	+180
Figure of merit, Z ($°K^{-1}$)	0.104×10^{-3}	0.07×10^{-3}	0.34×10^{-3}

First evaporation was the heating of the sample to evaporate about 0.1% of its weight. Due to experimental difficulties the amount of Tellurium volatilized may have been as much as 1.8%. Second evaporation was heating to evaporate an additional 1% of Tellurium. This data is preliminary and more detailed work is planned. X-ray diffraction analysis of a stoichiometric $CuGaTe_2$ sample indicates a single phase. Optical metallography of a sample indicated the presence of two phases. This apparent discrepancy is to be clarified.

*Department of the Army Contract DA-44-177-TC-639. Progress Report No. 2 for period 27 June through 24 July, 1960.

The General Electric Company* has measured the resistivity and Seebeck coefficient at room temperature on a sample of copper gallium telluride ($CuGaTe_2$) quenched from the melt. The resistivity values along the samples were obtained by measuring the spreading resistance of a tungsten cat-whisker contact operated at a constant value of current. In this single probe method the voltage between sample and whisker is a direct measurement of the local sample resistivity and may be applied to samples of any shape. The profile method in effect measures local resistivity averaged over the cross-section of the sample. Resistivity and Seebeck coefficient of parts of a sample were:

	Resistivity	Seebeck Coefficient
Top part	6.9×10^{-2} ohm cm ± 18%	190 - 222 μV/°C
Middle part	8.0×10^{-2} ± 6.4%	226 - 247 μV/°C
Bottom part	7.9×10^{-2} ± 35%	257 -274 μV/°C

The resistivity shown is about 6 times higher than that of slowly cooled samples (1.3×10^{-2} ohm cm). The large deviations for the top and bottom parts indicate that they are less homogeneous than the middle part.

*Army Transportation Research Command, Transportation Corps, Fort Eustis, Virginia, Contract No. DA-44-177-TC-639. Progress Report No. 5 of 18 November 1960 covering period from 26 September through 23 October 1960.

The General Electric Company* has prepared slow cooled samples of copper gallum telluride ($CuGaTe_2$) and have obtained their resistivity profiles and Seebeck coefficients at room temperature. The furnace cooling rate was 18°C per minute at the melting point. The samples were removed from the furnace at various temperatures. There was apparently no correlation between property variations and different cooling schedules. Values of ρ varied from 2.3 to 38 x 10^{-3} ohm cm. Resistivity profiles were relatively unfiorm except for some samples having major imperfections. S varied from 20 to 280 μV/°C. Values of S^2/ρ were from 1.8 x 10^{-6} to 4.4 x 10^{-6} w/cm°C^2, excluding questionable samples. They vary less than the individual quantities S and ρ. Such quantities as S^2/ρ, or of the Hall mobility, might be more useful in assessing the properties of thermoelectric samples than either of the qualities S and ρ.

*Army Transportation Research Command, Transportation Corps, Fort Eustis, Virginia, Contract No. DA-144-177-TC-639. Progress Report No. 6 of 16 December 1960 covering period from 24 October through 27 November 1960.

The General Electric Company* have examined prepared samples which include stoichiometric Cu $GaTe_2$ as well as those of Cu $GaTe_2$ with both deficient and excess tellurium. Data obtained are shown in Table XIX. Results indicate that furnace cooling to about 700°C produces samples with much lower resistivity than obtained when furnace cooling to room temperature. A comparable increase in resistivity is shown by samples containing an excess tellurim.

Figure 62 gives the Seebeck coefficient and resistivity vs. temperature up to 600°C for the Cu $GaTe_2$ sample which was furnace cooled to 680°C. After the first run measurements, which were made in vacuum over an 8 hour period, the room temperature values of Seebeck coefficient and resistivity increased appreciably. This may have been due partly to a phase transformation and partly to tellurium evaporation. In view of this the second and third runs for high temperature measurements were made in argon at atmospheric pressure. Two successive runs in argon showed an irreversible change in the sample properties. Results indicate that the energy gap derived from resistivity measurements is of the order of 1 ev, rather than 1/2 ev obtained from previous measurements. This agrees with the value of about 1 ev obtained by reflectance measurements. From results on both room temperature and high temperature measurements it appears that a phase transformation together with some chemical change is taking place in the Cu GaTe samples at relatively low temperatures.

By prolonged annealing of samples it is hoped that stable properties may be obtained over their optimum temperature range for thermoelectric conversion.

---

*Department of the Army Contract Da-44-177-TC-639. General Electric Company, Progress Report No. 7 covering period 27 Novermber 1960 through 1 January 1961 dated 27 January 1961.

TABLE XIX

ROOM TEMPERATURE DATA ON QUENCHED AND SLOW-COOLED $CuGaTe_2$ SAMPLES

SAMPLE	COMPOSITION	PREPARATION	ρ M OHM-CM (****)	S V/°C	S^2/ρ W/CM°C^2 IN UNITS OF 10^{-6}	NOTES
10ct	$CuGaTe_2$	Quenched	80 ± 6%	230(*)	.66	Brittle. Broke in Handling
12ct-2	"	FC to 720°C(**)	6.4 ± 4%	85	1.13	Nonuniform at end.
-3	"	FC to 680°C	4.4 ± 2%	180	7.4	Nonuniform at end.
-4	"	FC to 580°C	2.5 ± 2%	115	5.3	Crack in the middle.
-5	"	FC to 730°C	3.1 ± 5%	155	7.8	Crack at one end.
-6	"	FC to 760°C	2.3 ± 4%	160	11.1	Crack at one end.
13ct-1	"	FC to R.T.(***)	109 ± 1%	305	.85	Nonuniform at one end.
-2	"	" " "	120 ± 2%			Uniform.
-3	"	" " "	161 ± 4%	305	.58	Nonuniform at end.
14ct E-1	$CuGaTe_{2.04}$	FC to 700°C	3.2 ± 3%	120	4.5	Uniform.
-3	"	FC to 700°C	3.6 ± 3%	150	6.2	Uniform.
15ct D-1	$CuGaTe_{1.96}$	FC to 560°C	181 ± 2%	245	3.3	Nonuniform at end.
-2	"	FC to 720°C	165 ± 5%	125	.95	Nonuniform at end.
-3	"	FC to 720°C	220 ± 10%	160	1.16	Nonuniform at end.

(*) The uncertainty in all of these measurements is of the order of 10 to 20% for measurements taken at different points on the sample.
(**) Furnace cooled. Initial rate of cooling: 18°C/min. Sample removed at temperature as indicated.
(***) Room temperature.
(****) The resistivity is obtained from the slope of a straight line drawn through the experimental points of the resistance profile. The percentage values indicate the maximum relative deviation of the experimental points from the straight line and represent a measure of the sample homogeneity.

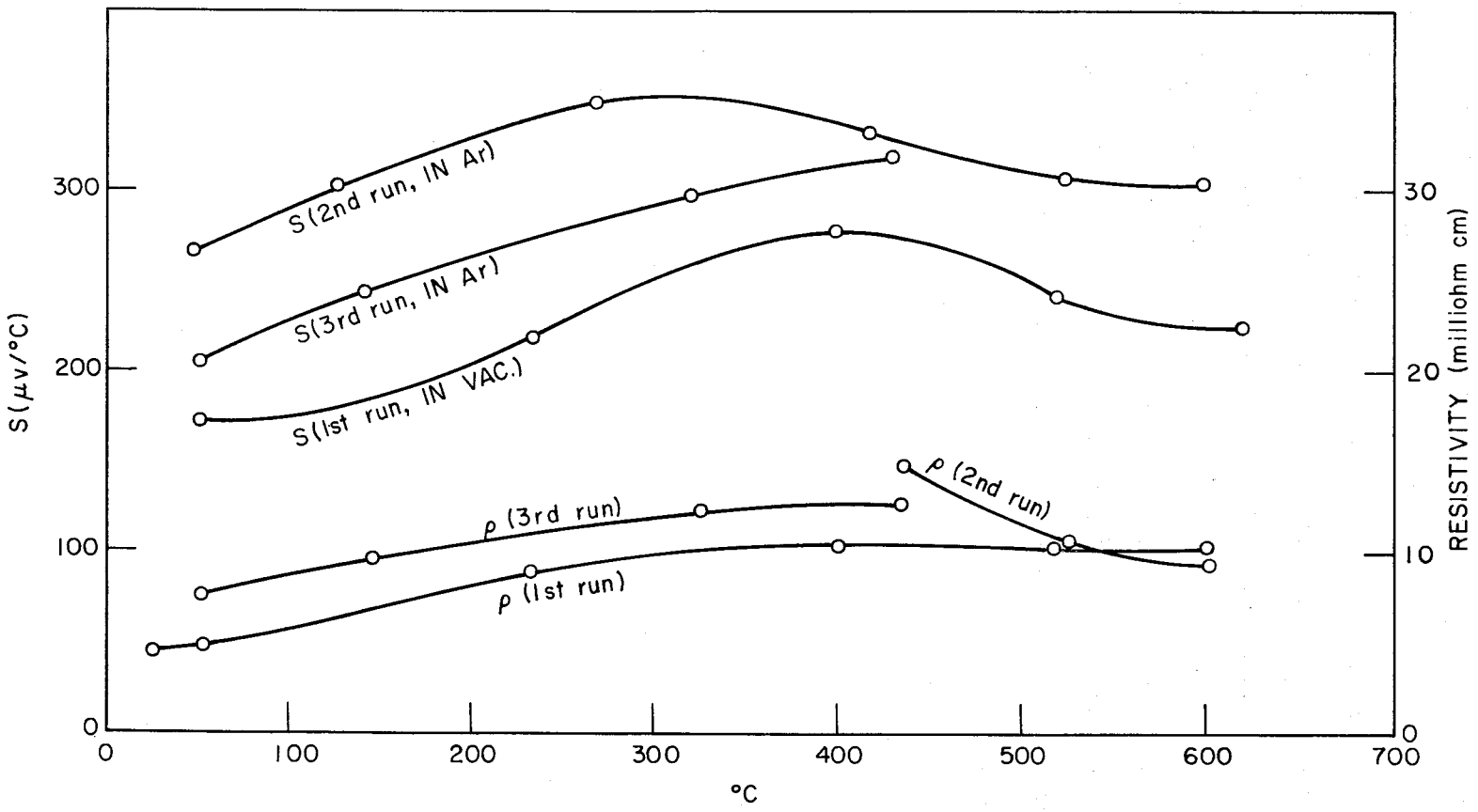

Fig. 62 - $S_2\rho$ vs Temp. $CuGaTe_2$

Experimentation is in progress to obtain easier and faster measurements of thermal conductivity by a comparative method in which a sample of known thermal conductivity is placed in series with a sample to be measured and heat is applied at each of the free ends. Three thermocouples are placed at equal intervals along each sample. From the temperature and voltage readings both K and S can be deduced. By means of four thermocuples on the unknown sample and by injecting a small current through the outer ones, ρ can be measured. If a sample, whose thermal conductivity is known as a function of temperature, is used, this method can be extended to high temperatures.

A STUDY OF A CLASS OF INTERMETALLIC COMPOUNDS, THE CHALCOPYRITES

New York University* has investigated three compositions of the class of polyatomic semiconductors of the chalcopyrite structure $A^{I}B^{III}C^{VI}$. $CuInTe_2$ and $AgInTe_2$ were found to be intermetallic semiconductors. $AuInTe_2$ showed the metallic character of a two phase alloy $Au_{.25}In_{.25}Te_{.50}$.

Typical values determined for $CuInTe_2$, $AgInTe_2$ and $Au_{.25}In_{.25}Te_{.50}$ were as follows:

	Melting Point	Hardness VHN(kg/mm^2)	Electrical Resistivity (Room Temp.)	Seebeck Coefficient (Room Temp.)
$CuInTe_2$	778 ± 3°C	218 ± 20	10^{-2} ohm cm	+200 μV/°C
$AgInTe_2$	678 ± 2°C	180 ± 10	5 ohm cm	-110 μV/°C
$Au_{.25}In_{.25}Te_{.50}$	617 ± 3°C (start of solidification) 420 ± 3°C (end of solidification)	165 ± 10 (dark matrix peritetic region) 114 ± 10 (white region)	10^{-4} ohm cm	- 28 μV/°C

The Seebeck coefficient of $CuInTe_2$, $AgInTe_2$ and $Au_{.25}In_{.25}Te_{.50}$ at selected temperatures are given in Table XX. Those of various alloys

*Aeronautical Research Laboratory, Air Force Research Division, Air Research and Development Command, U.S. Air Force, Wright-Patterson Air Force Base, Ohio, Contract No. Af 33 (616)-3959. ARL Technical Report 60-316 of October 1960 covering period from February 1957 to August 1960.

TABLE XX

Seebeck Coefficient of $CuInTe_2$, $AgInTe_2$ and $Au_{.25}In_{.25}Te_{.50}$ at Selected Temperatures.

Substance	Seebeck Coefficient, V/°C							
	-150°C	-50°C	Room temp. +20°C	+100°C	+200°C	+300°C	+400°C	+500°C
$CuInTe_2$(C-8T)	+138	+251	+304	+335	+357	+374	+380	+348
$CuInTe_2$(C-8B)	+209	+335	+346	+340	+330	+322	+312	--
$CuInTe_2$(C-5)	+ 44	+ 94	+130	+168	+218	+265	+312	+376
$CuInTe_2$(C-10)	+ 68	+123	+160	+192	+223	+249	+270	+287
$AgInTe_2$(S-8B)	-112	-114	-101	- 50	+146	+189	+408	+520
$AgInTe_2$(S-8B) annealed	--	--	- 52	- 15	+205	+550	+518	+487
$AgInTe_2$(S-9)	-110	-108	- 98	- 39	+172	+240	+307	+421
$Au_{.25}In_{.25}Te_{.50}$ (H3-2)	- 13	- 23	- 28	- 28	- 27	- 23	- 20	--

$AgInTe_2$ - $CuInTe_2$ given in Table XXI were taken from the curves of Figure 63. The Seebeck coefficient of $CuInTe_2$ was positive over the entire range tested. It increased from about +25 μV/°C at -190°C, to +130 - 346 μV/°C at room temperature, and up to +280 - 380 μV/°C at about 400 - 500°C, the intrinsic region. $AgInTe_2$ had an approximately constant negative Seebeck coefficient of -110 μV/°C from -160°C up to room temperature. At higher temperatures its value became positive and increased rapidly to +500 μV/°C, reaching its intrinsic region above 500°C. $Au_{.25}In_{.25}Te_{.50}$ had a Seebeck coefficient of about -28 μV/°C at room temperature, in the metallic range.

Substitution of Cu into $AgInTe_2$ resulted in a continuous transition in the room temperature Seebeck coefficient from the negative ($AgInTe_2$) to the positive ($CuInTe_2$). A zero coefficient was obtained at about $Cu_{.55}Ag_{.45}InTe_2$.

The resistivity of $CuInTe_2$ and $AgInTe_2$ are well in the semiconductor range, see Table XXII. That for $Au_{.25}In_{.25}Te_{.50}$ is very low as expected of a non-equilibrium metallic mixture. A criterion for the physical and chemical homogeneity of semiconductor ingots is the constancy of electrical resistivity along their length.

The pseudo-binary system AgInTe - $CuInTe_2$ retained their semiconductor character over the range of compositions. The sytem $AgInTe_2$ - $AuInTe_2$ possessed metallic character except for pure $AgInTe_2$.

The effect of annealing of $AgInTe_2$, $Ag_{.50}Cu_{.50}InTe_2$ and $CuInTe_2$ was pronounced tendency toward positive, hole conduction. The "n" type $AgInTe_2$ and $Ag_{.50}InTe_2$ were changed into "p" type semiconductors. Heating of $AgInTe_2$, $CuInTe_2$ and their solid solutions, in a vacuum irreversibly affected the Seebeck coefficient. Annealing $AgInTe_2$ for two hours at 400°C substantially increased the Seebeck coefficient measured

TABLE XXI

Seebeck Coefficient of Various Alloys
$AgInTe_2$-$CuInTe_2$ at Selected Temperatures

Alloy	At % of $CuInTe_2$	-150°C	-50°C	+20°C	+160°C	+300°C	+500°C
SC-3	2	-126*	-162	-115	+ 58	+278	+493
SC-4	5	-118	-103	- 80	+250	+372	+414
SC-5	10	-132	-127	-102	+130	+245	+440
SC-6	25	-106	-100	- 78	+142	+348	+437
SC-1	50	- 65	- 48	- 28	+300	+450	+403
SC-8	75	+103	+186	+239	+304	+427	+363
SC-15	75	+130	+198	+248	+336	+405	--
SC-9	90	+112	+180	+217	+290	+370	+344
SC-10	95	+118	+205	+258	+327	+385	+360

* Seebeck coefficient in microvolts/°C

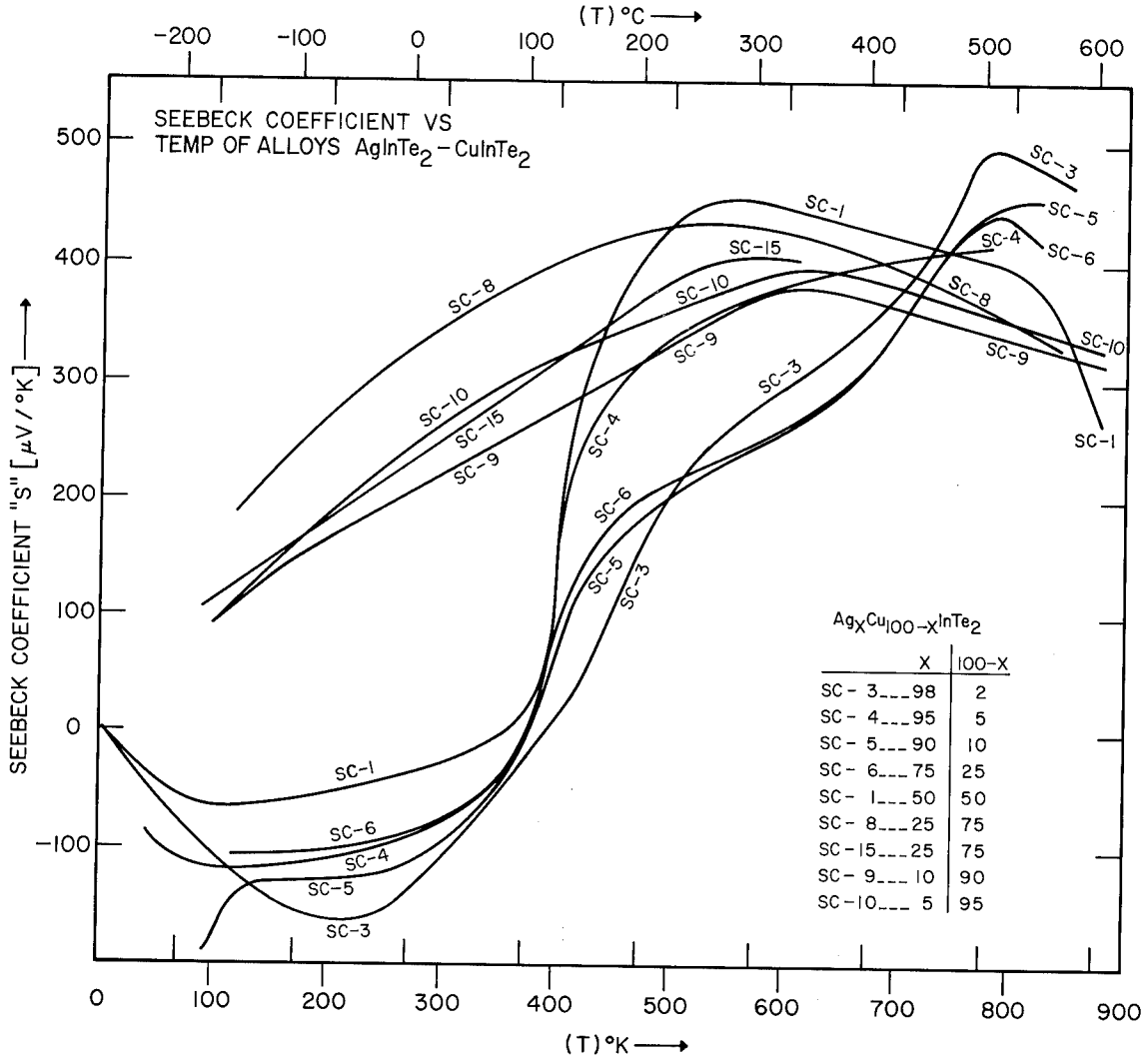

Fig. 63 - Alloys $Ag_x Cu_{100-x} InTe_2$

TABLE XXII

Electrical Resistivity of $CuInTe_2$, $AgInTe_2$ and $Au_{.25}In_{.25}Te_{.50}$

		Electrical Resistivity (ohm-cm)
$CuInTe_2$(H1-2)		1.2×10^{-2}
$CuInTe_2$(C-7)		1.8×10^{-2}
$CuInTe_2$(C-8)	top	6×10^{-2}
	center	22×10^{-2}
	bottom	12×10^{-2}
$CuInTe_2$(C-9)	top	2.2×10^{-2}
	bottom	0.7×10^{-2}
$AgInTe_2$(H2-1)	top	6.25
	center	5.78
	bottom	5.53
$AgInTe_2$(S-9	top	0.86
	center	0.72
	bottom	0.82
$AgInTe_2$(S-8)	top	0.67
	center	0.53
	bottom	0.63
$Au_{.25}In_{.25}Te_{.50}$(H3-4)	top	6.4×10^{-4}
	center	8.3×10^{-4}
	bottom	8.4×10^{-4}

above 200°C, see Figure 64. The transition to intrinsic conduction was shifted to lower temperatures.

$CuInTe_2$ has a figure of merit $Z = 0.265 \times 10^{-3}/°K$, whereas that of $AgInTe_2$ was in the order of $10^{-7}/°K$ due to its high electrical resistivity and low Seebeck coefficient. Table XXIII gives the thermoelectric parameters of $CuInTe_2$ and $AgInTe_2$.

$AgInTe_2$, $CuInTe_2$ and all proportions of $Cu_xAg_{(1-x)}InTe_2$ formed homogeneous single phase alloys after direct solidification from the melt. X-ray analysis indicated a zinc-blende structure typical of the chalcopyrite compounds, and the electrical resistivity and Seebeck coefficient values were in the semiconducting range. $AuInTe_2$ and $Au_xAg_{(1-x)}InTe_2$ formed what appeared to be a peritectic reaction (the thermal analysis curves showing more than one arrest) and were consequently polyphase. Extensive annealing could not convert the polyphase structure to a single phase structure, nor was any indication of the formation of the chalcopyrite structure obtained from X-ray analysis. The electrical resistivity and Seebeck coefficient values for these structures were low, in the metallic range.

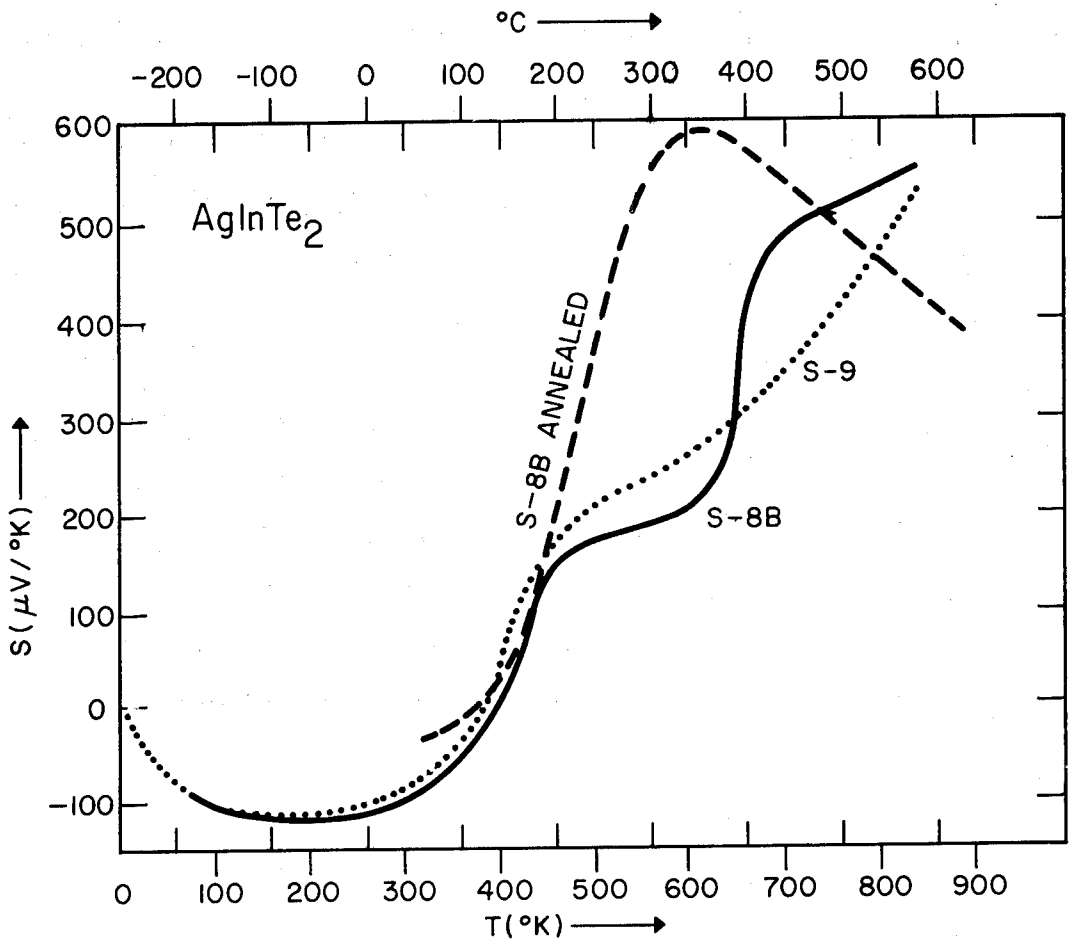

Fig. 64 - $AgInTe_2$

TABLE XXIII

Thermoelectric Parameters of $CuInTe_2$ and $AgInTe_2$ as Measured by the Putley-Harman Technique at 0° C

	$CuInTe_2$ C14(1)	$CuInTe_2$ C14(1)	$AgInTe_2$ S13(3)
Current used, mA	20.45	79.86	4.845
Produced temperature difference, °K	0.379	1.375	0.042
Average temperature of specimen, °K	273.83	276.4	274.5
V_S, microvolts	108.5	458.0	4.545
V_ρ, microvolts	1605.6	6306.4	27599.5
Figure of merit "z", $°K^{-1}$	0.265×10^{-3}	0.260×10^{-3}	5.999×10^{-7}
Thermoelectric power S, $\mu V/°K$	+208.7	+333.1	-108.2
Thermal Conductivity K, Watts/cm, °K	0.06098	0.07395	0.04544
Thermal Conductivity K, cal/sec, cm, °K	0.01457	0.01767	0.01086
Electrical resistivity ρ, ohm-cm	1.214×10^{-2}	1.22×10^{-2}	0.747

The E. I. duPont de Nemours Company, Inc.* is working on a class of silver selenides and tellurides containing di- or multivalent constituents such as Ta, Ti, Nb, Mo, or W. Results of work on $AgTiTe_3$, $AgTiSe_2$, Ag_2NbSe_3, and Ag_2MoSe_3 are presented here. The compositions which are listed are not to be interpreted as representing compounds because X-ray data indicate more than one phase. For each of the above compositions there are shown Z, S, K, and f'. See Figs. 65 through 68.

$AgTiTe_3$ (Fig. 65) possesses a steadily decreasing Seebeck coefficient and resistivity between 100°C and 400°C. The thermal conductivity goes through a minimum value at 200°C and then increases with increasing temperature. The decline of resistivity with increasing temperature is too small to overcome the combined effects of increasing thermal conductivity and falling Seebeck coefficient so that the figure of merit falls from 1.06×10^{-3} at 100°C to 0.62×10^{-3} at 400°C.

$AgTiSe_2$ data runs between 100°C and 600°C (Fig. 66). The Seebeck coefficient remains steady at about 160 microvolts/°C between 100 and 200°C and then it falls almost linearly to 45 microvolts/°C at 600°C. The resistivity falls from 2 milliohm-cm to 0.64 milliohm-cm in the same temperature interval. A minimum in the thermal conductivity occurs at 300°C. The figure of merit has a value of 1.02×10^{-3} at 100°C, peaks at 200°C with a value of 1.6×10^{-3}, and then it falls to 0.2×10^{-3} at 600°C.

Ag_2NbSe_3 data has a more complex structure over the range of 100°C to 700°C (Fig. 67), but the figure of merit is no greater than 1.3×10^{-3}. There is an indication that the figure of merit starts rising again above 600°C but these values were calculated using an assumed value of 0.011 watt/cm°C.

*Pigment Division, E.I. du Pont de Nemours Company, Inc., Wilmington, Delaware.

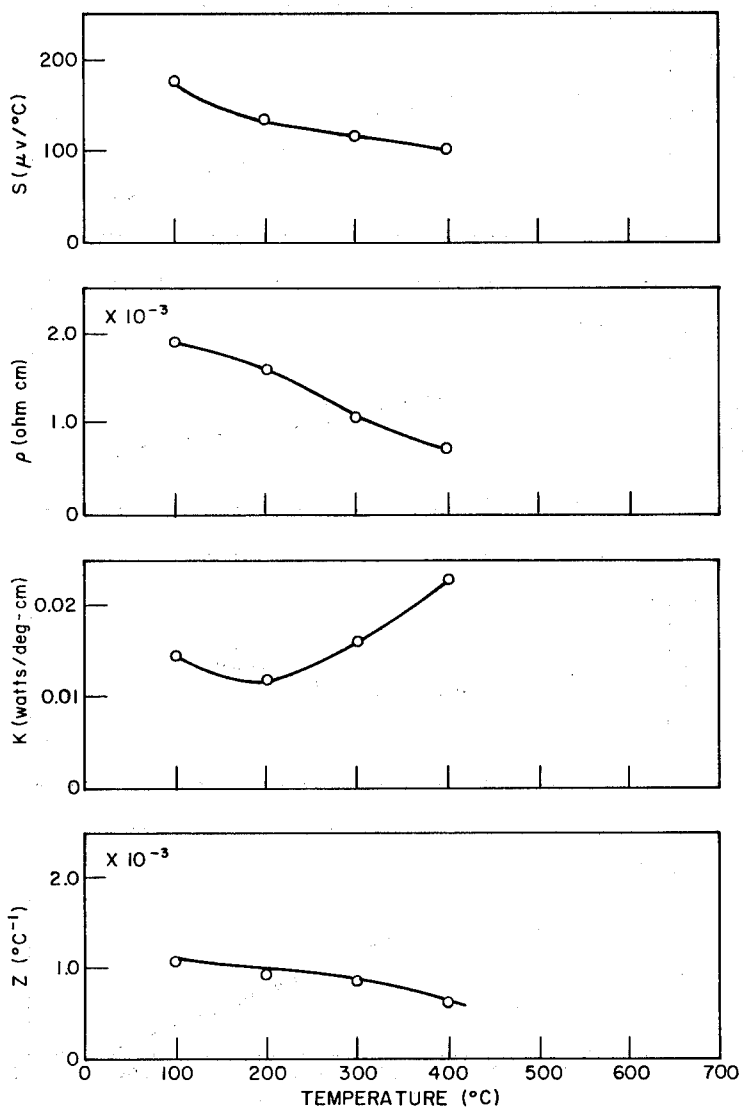

Fig. 65 - $AgTiTe_3$

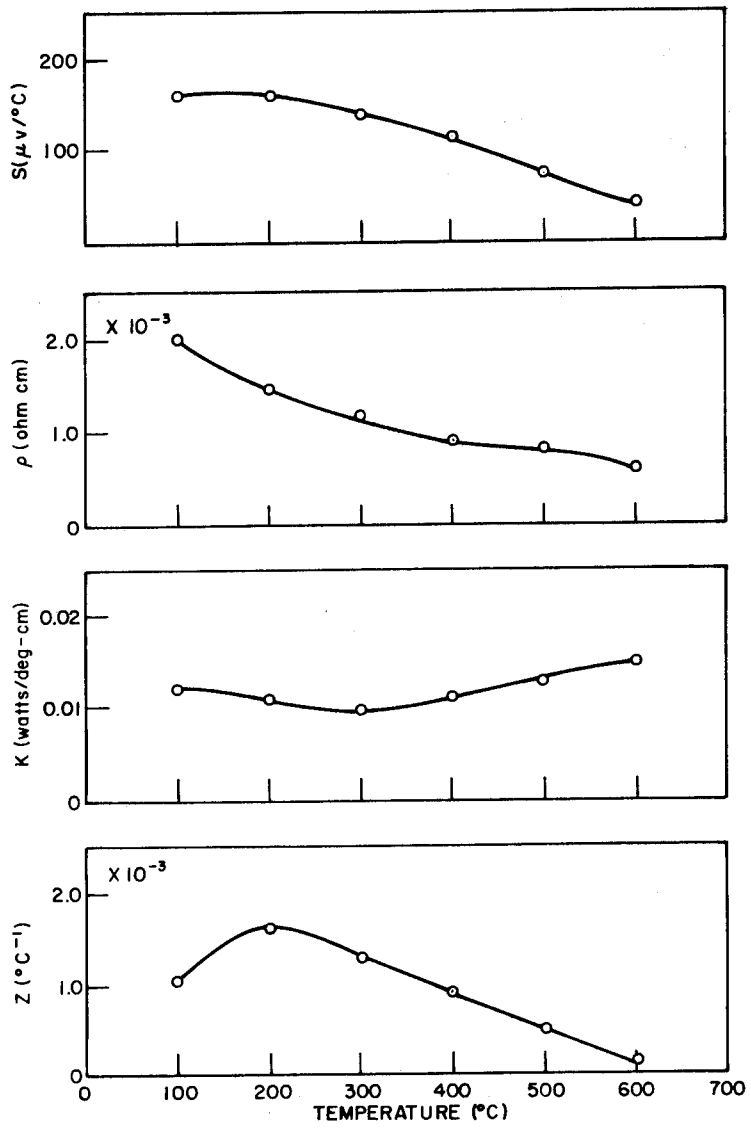

Fig. 66 - $AgTiSe_2$

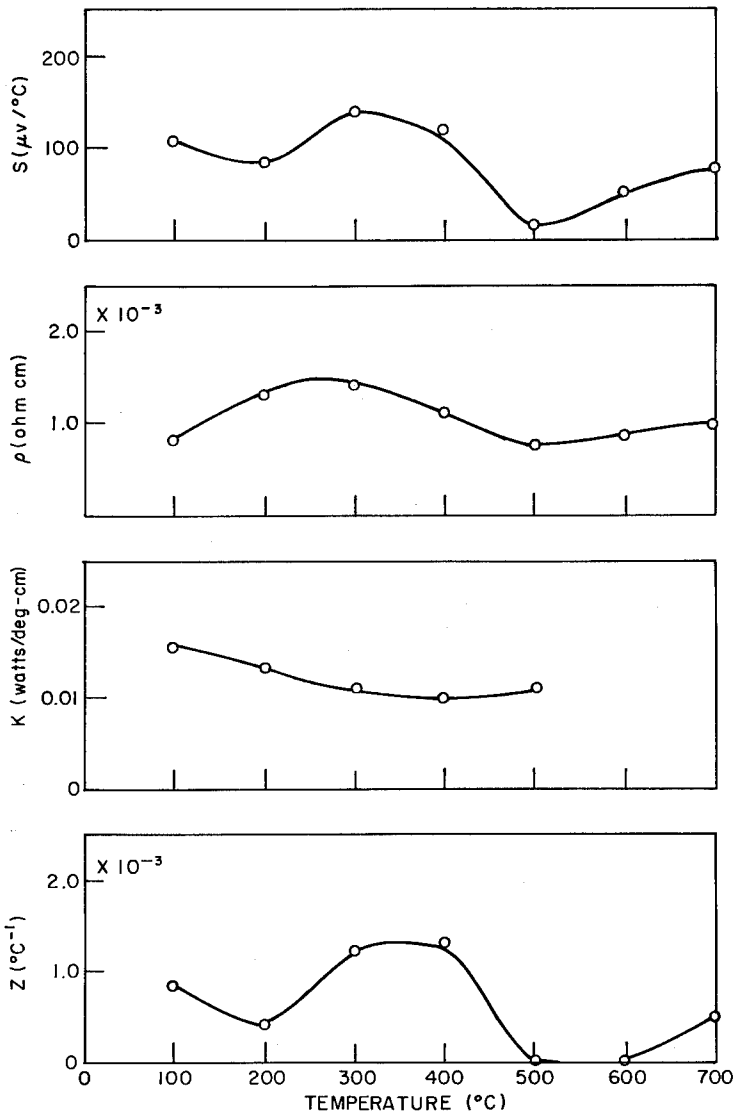

Fig. 67 - $Ag_2 NbSe_3$

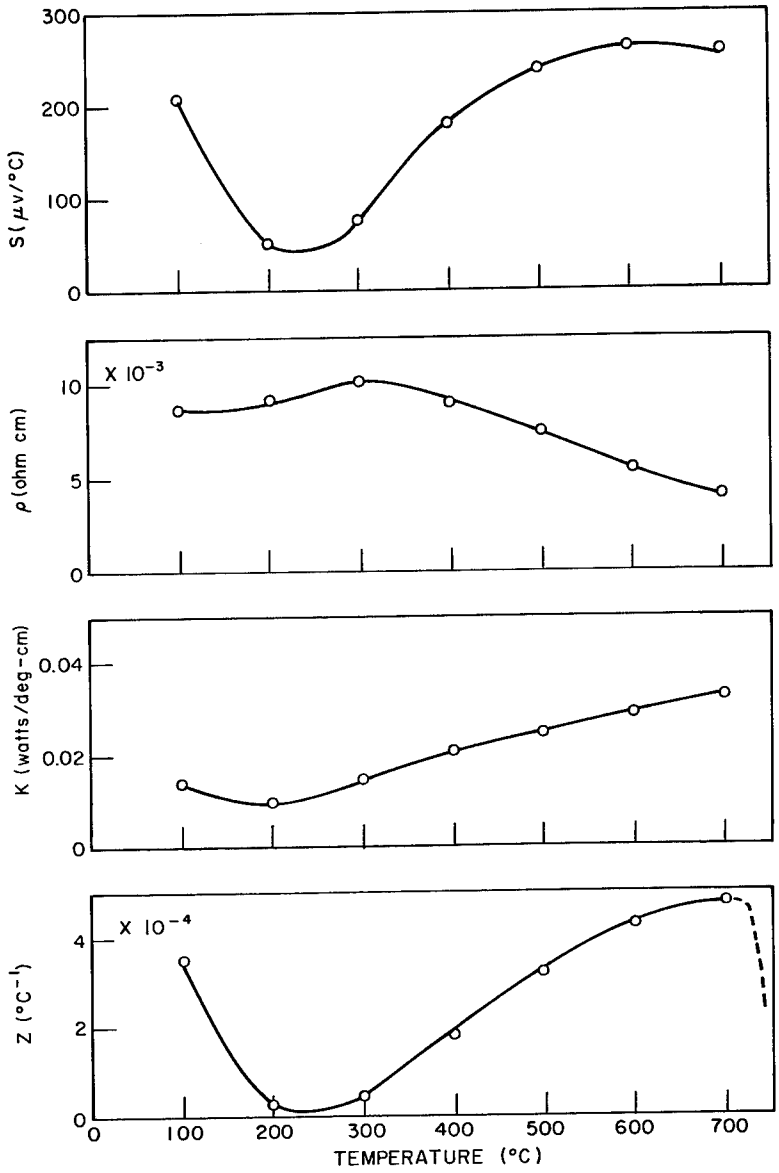

Fig. 68 - $Ag_2 MoSe_3$

Ag_2MoSe_3 (Fig. 68) has a Seebeck coefficient that increases after going through a minimum value of 40 microvolts/°C at 225°C. After reaching a peak value of 260 microvolts/°C at 600°C it starts to fall again. Combining this with the data for the resistivity and thermal conductivity gives a figure of merit which never quite reaches 10^{-3} $(°C)^{-1}$. At the upper limit of measurement (700°C) there are indications that the figure of merit falls with further increase in temperature.

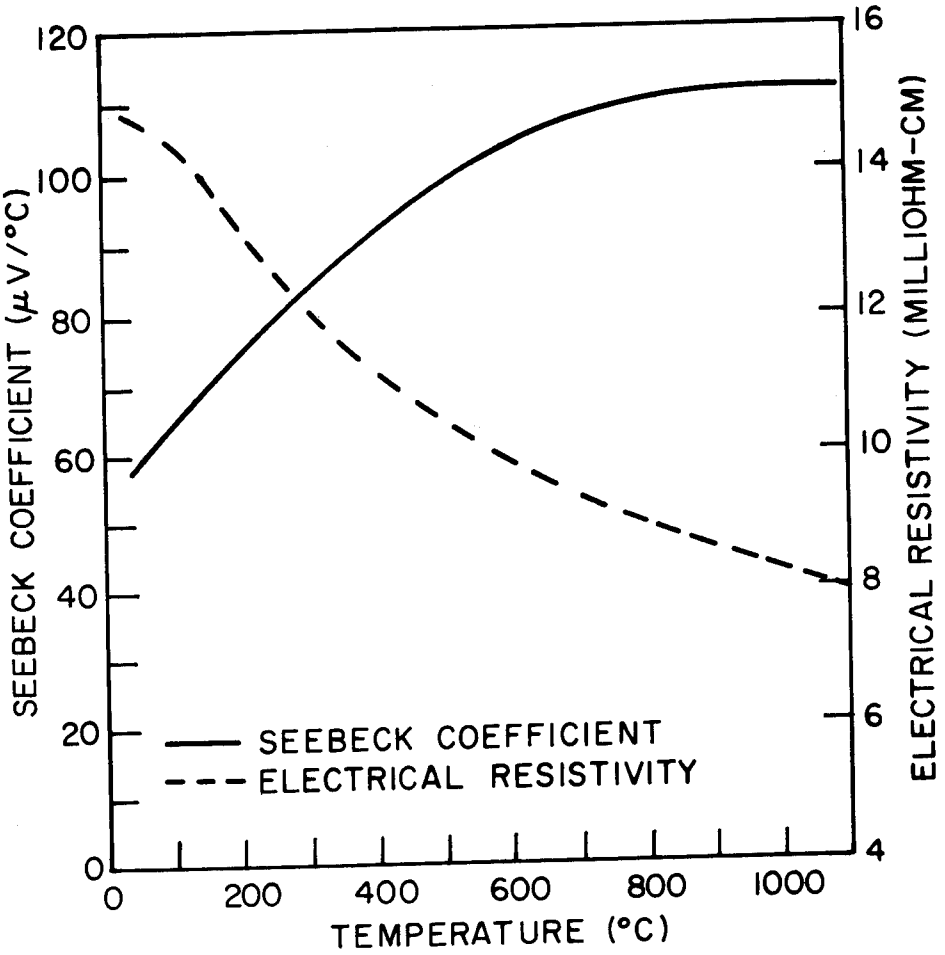

Fig. 69 - Seebeck Coefficient (vs Pt) and Electrical Resistivity Carbon-Boron Carbide (n type)

THERMOELECTRIC MATERIALS

The Parma Research Laboratory, Union Carbide Corporation* describes in this final report their work on carbon and graphite materials, refractory nitrides, and alkali metals in their fused halides. Results of a survey of other intermetallic or inorganic compounds to correlate the desired thermoelectric properties is given.

Both p- and n-type graphite based materials can be produced with reasonable thermoelectric power. Based on graphite, thermoelectric elements were developed which suitably operated at temperatures in excess of 1000°C.

Graphite doped with higher boron content (up to 1.3%) had maxima in their output at higher temperatures. The maximum output for a 1.3% composition occurs at about 1000°C and has a value of about 60 μV/°C relative to pure carbon. A maximum output of 75 μV/°C versus graphite was obtained at room temperature for a 0.04% composition. The electrical properties of a carbon-boron carbide n-type sample are shown in Figure 69. This sample would require a thermal conductivity of 0.015 watt/cm°K at 1000°C in order to have a figure of merit of $Z = 1 \times 10^{-4}$/°K at that temperature.

A small prototype thermoelectric generator was constructed using an n-type silicon carbide-graphite versus a p-type boronated graphite, better materials developed on the contract. The open circuit voltage was 0.94 volt and the resistance 0.475 ohm. This performance is not striking by comparison with those obtained at lower temperatures. Simplicity and economy of the graphite materials offer practical utility in competition with expensive materials of higher efficiency.

*Department of the Navy Contract NObs 77066. Final report covering period 28 January 1959 to 28 July 1960.

Samples were prepared with various additives to determine if increased n- or p-type thermoelectric powers could be obtained. SiC, TiC, Zrc, TaC, Fe_2O_3, and UO_2 were tried but none was found to produce the p-type conduction except boron. Electrical resistivity measurements on a stoichiometric mix of silicon and carbon materials sample were .046 to .053 ohm cm at 1000°C, .095 to .121 at 1900°C, and .051 to .053 at 2000°C. Resistivity measurements on a carbon-boron carbide sample were .070 to .096 ohm cm at 1000°C, .055 to .110 at 1900°C, and .029 to .048 at 2000°C.

Electrical properties of refractory nitrides were determined. Cerium, gadolinium and lanthanum nitrides are essentially metallic with high conductivities and low Seebeck coefficient. Samarium and ytterbium nitrides are n-type conductors with S ≈ 10 to 20 μV/°C. Europium nitride, a semiconduction, is an n-type thermoelectric material with maximum value S = -130 μV/°C at 1150°C and S = -97 μV/°C at 1330°C.

The solution of an alkali metal in its fused halide has potential for thermoelectric application. In one run on cesium dissolved in molten cesium chloride, S ≈ 400 μV/°C.

No striking gaps in the thermoelectric program were revealed in the study of the compounds of the transition metals.

In a survey of vitreous electronic conductors various arsenic, antimony, and thallium tellurides, sulfides, and selenide glasses that were studied had too low electronic conductivities to give a good figure of merit. However, Seebeck coefficients reached values over 1400 μV/°C and thermal conductivities were in the range 10^{-2} to 10^{-3} watt units.

OXIDE THERMOELECTRIC MATERIALS

General Ceramics,* Division of Indiana General Corporation, has obtained dc resistivity measurements for $(Al_2O_3)_x (ZnO)_{100-x}$, $(TiO_2)_x (Fe_2O_3)_{100-x}$, $(V_2O_5)_{3.0} (CeO_2)_{97.0}$ and $(La_2O_3)_{3.0} (CeO_2)_{97.0}$ compounds. New measurements of Seebeck coefficients are being made on $(Al_2O_3)_x (ZnO)_{100-x}$ series, occasioned by detection of a faulty potentiometer. Results on both resistivity and Seebeck coefficients for this series will be presented together in a future summary of progress.

The dc resistivity for four members of $(TiO_2)_x (Fe_2O_3)_{100-x}$ series, wherein "x" was varied from 0.5 to 3.0 in steps of 0.5, decreases continually with increasing temperature from ambient to 1400°C, see Figure 70. At a given temperature, the higher the TiO_2 content, the lower the dc resistivity. The only exception is at the extreme upper end of the temperature range (1427°C) where the composition with the lowest TiO_2 content, $(TiO_2)_{1.5} (Fe_2O_3)_{98.5}$, has the lowest resistivity.

For all compositions, the Seebeck coefficient increases to a maximum as the temperature increases, and then declines as the temperature increases further, see Figure 71. In the 0-900°C range of temperature, the higher the TiO_2 content, the lower the Seebeck coefficient. Above 1200°C the higher the TiO_2 content, the higher the Seebeck coefficient. None of these n-type compositions is particularly promising material.

$(V_2O_5)_{3.0} (CeO_2)_{97.0}$ and $(La_2O_3)_{3.0} (CeO_2)_{97.0}$

*Department of the Navy Contract NObs-78414, General Ceramics Bi-Monthly Progress Report No. 5 covering period 2 October to 1 December 1960.

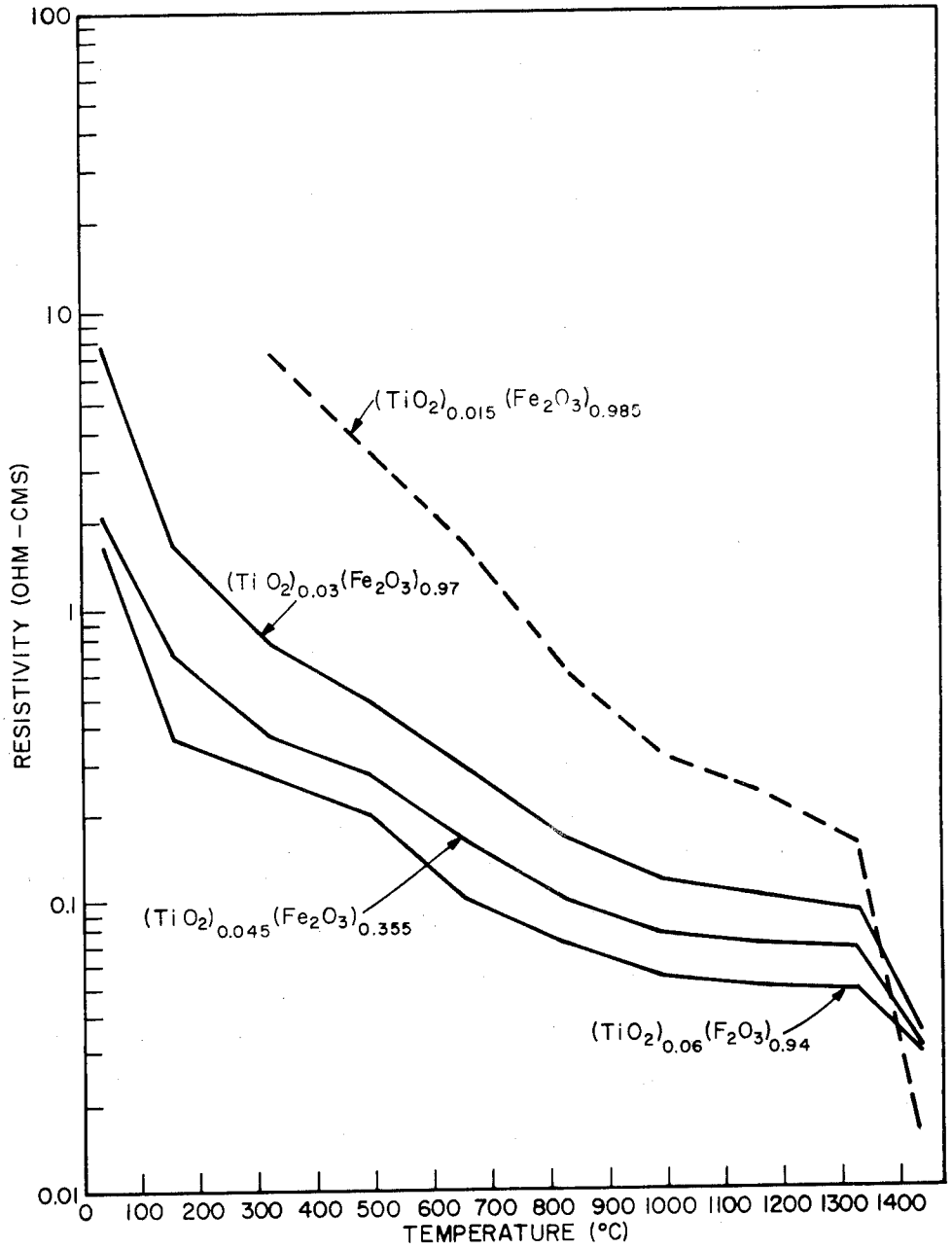

Fig. 70 - $(TiO_2)_x (Fe_2O_3)_{1-x}$ Series

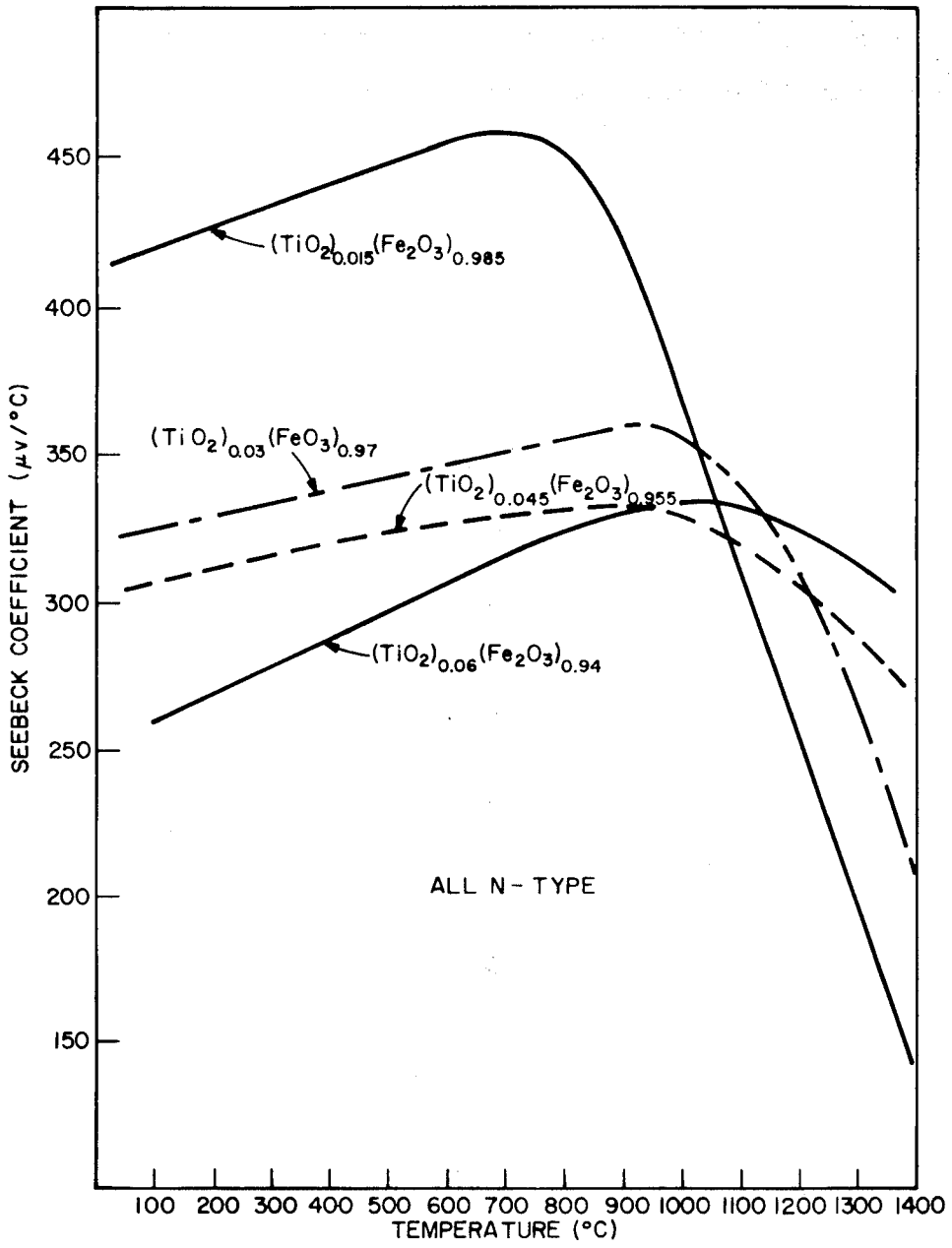

Fig. 71 - $(TiO_2)_x (Fe_2O_3)_{1-x}$ Series

The measured dc resistivities of $(V_2O_5)_{3.0}(CeO_2)_{97.0}$ and $(La_2O_3)_{3.0}(CeO_2)_{97.0}$ throughout the temperature range 0-1400°C were so high that they are unsuitable for power generation purposes.

OXIDE SYSTEMS FOR THERMOELECTRIC POWER GENERATION

Titanium Alloy Manufacturing Division* of National Lead Company is conducting studies in the preparation and evaluation of various oxide-type materials for thermoelectric power generation. The work on ceramic processing presently concerns sintering studies only. Using TiO_2, ZrO_2 and $BaTiO_3$ as base materials, 100 specimens have been prepared. The results of measuring some representative materials similar to, but not identical with, contract materials, were as follows:

Rutile TiO_2 Plus 1% Nb_2O_5

Resistivity was fairly constant at 0.31 ± 0.02 ohm cm from 709°C to 1202°C. Seebeck coefficient varied continuously but irregularly from -536 μV/°C at 368°C to -862 μV/°C at 1122°C.

Lithium Metatitanate, TAM Li_2TiO_3, 71607A

Resistivity decreased continuously from 39 ohm cm at 950°C to 17 ohm cm at 1156°C.

Seebeck coefficient increased irregularly from -766 μV/°C at 704°C to an average of 350 μV/°C at 1223°C.

Barium Titanate, $BaTiO_3$ plus 0.3% La_2O_3

Resistivity decreases continuously from 128 ohm cm at 832°C to 17 ohm cm at 1211°C.

Seebeck coefficient increased irregularly from 195 μV/°C at 704°C to an average of 350 μV/°C at 1223°C.

There was a scatter in Seebeck coefficients attributed to the measuring technique or methods employed.

*Department of the Navy Contract NObs 78326. Titanium Alloy Manufacturing Division Bi-monthly Progress Report No. covering period 1 September to 31 October 1960.

Titanium Alloy Manufacturing Division* of National Lead Company has calculated the formulations for additions to CeO_2 and for synthesis of four ABO_4 niobates. Tables XXIV and XXV give ceramic data on materials of Nb_2O_5 and La_2O_3 additions to cubic ZrO_2 stabilized with 7 mole percent Y_2O_3 and with 15 mole percent CaO, respectively.

The Seebeck coefficient as a function of temperature was determined and is given in Figure 72 for Nb_2O_5 additions to cubic ZrO_2 stabilized with 7 mole percent of Y_2O_3. All these materials are p-type semiconductors. Increased addition of Nb_2O_5 produced a definite increase in Seebeck coefficient. The curve for 2.0 mole percent Nb_2O_5 was suspect and a redetermination was to be made. The specimen with 5.0 mole percent Nb_2O_5 is tetragonal and only it approached a completely sintered state. The others are cubic.

*Department of the Navy Contract NObs 78326. Titanium Alloy Manufacturing Division Bi-Monthly Progress Report No. 6 covering period 1 November to 31 December 1960.

TABLE XXIV

Ceramic Data on Standard Ceramic Bodies of Nb_2O_5 and La_2O_3 Additions to Cubic ZrO_2 Stabilized with 7 m/o Y_2O_3

Addition	Temp.	Time	Bulk Density	Porosity
0.1 m/o Nb_2O_5	3000°F	2 hrs.	4.96 g/cm^3	12.36 %
0.2 m/o Nb_2O_5	3000°F	2 hrs.	4.99	11.51
0.5 m/o Nb_2O_5	3000°F	2 hrs.	5.00	11.92
1.0 m/o Nb_2O_5	3000°F	2 hrs.	5.03	11.26
2.0 m/o Nb_2O_5	3000°F	2 hrs.	5.21	7.38
5.0 m/o Nb_2O_5	3000°F	2 hrs.	5.46	0.013
0.1 m/o La_2O_3	3000°F	2 hrs.	4.86	15.28
0.2 m/o La_2O_3	3000°F	2 hrs.	4.85	15.15
0.5 m/o La_2O_3	3000°F	2 hrs.	4.92	14.85
1.0 m/o La_2O_3	3000°F	2 hrs.	4.96	14.52
2.0 m/o La_2O_3	3000°F	2 hrs.	5.14	12.91
5.0 m/o La_2O_3	3000°F	2 hrs.	5.09	9.54

TABLE XXV

Ceramic Data on Standard Ceramic Bodies of Nb_2O_3 and La_2O_3 Additions to Cubic ZrO_2 Stabilized with 15 m/o CaO

Addition	Sintering Conditions		Bulk Density	Porosity
	Temp.	Time		
0.1 m/o Nb_2O_5	3000°F	2 hrs.	4.58 g/cm^3	17.36 %
0.2 m/o Nb_2O_5	3000°F	2 hrs.	4.59	15.08
0.5 m/o Nb_2O_5	3000°F	2 hrs.	4.57	16.57
1.0 m/o Nb_2O_5	3000°F	2 hrs.	4.68	15.29
2.0 m/o Nb_2O_5	3000°F	2 hrs.	4.88	1.73
5.0 m/o Nb_2O_5	3000°F	2 hrs.	5.05	7.97
0.1 m/o La_2O_3	3000°F	2 hrs.	4.60	15.56
0.2 m/o La_2O_3	3000°f	2 hrs.	4.58	15.51
0.5 m/o La_2O_3	3000°F	2 hrs.	4.59	15.77
1.0 m/o La_2O_3	3000°F	2 hrs.	4.58	16.51
2.0 m/o La_2O_3	3000°F	2 hrs.	4.66	16.04
5.0 m/o La_2O_3	3000°F	2 hrs.	4.32	20.39

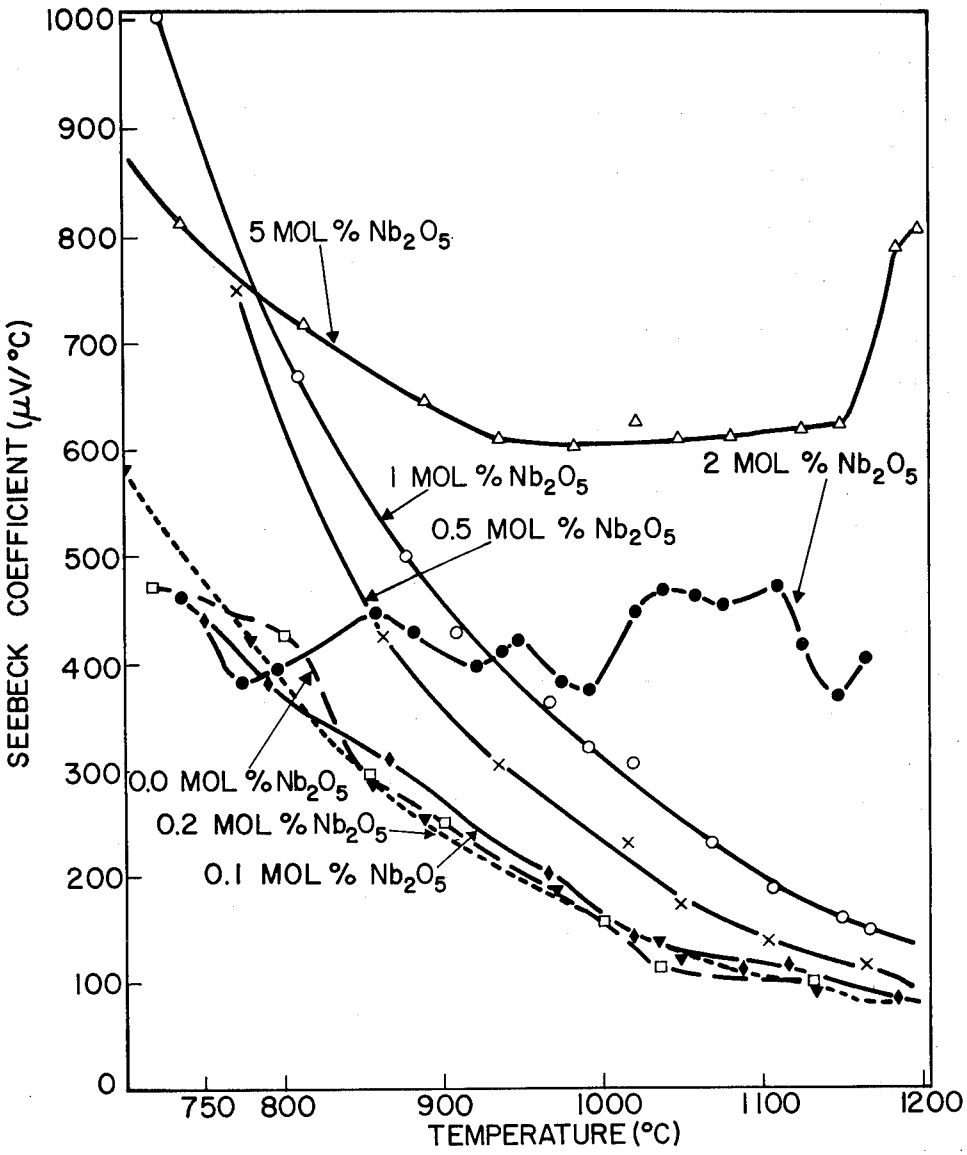

Fig. 72 - Sebeck Coefficient vs Temperature for $Nb_2 O_5$ additions to cubic ZrO_2 stabilized with 7 mol % $Y_2 O_3$

THERMOELECTRIC MATERIALS

Stanford Research Institute* has made thermal conductivity measurements on a cuprous sulfide sample between 24° and 404°C with the conductivity changing from 0.0095 watts/cm-°C at 24°C to 0.022 watts/cm-°C at 404°C. A phase change occurs between 200° to 350°C which is accompanied by a rapid change in resistivity.

They have encountered difficulties such as fracturing during the cutting operations when in preparing cuprous sulfide samples**. Resistivity and Seebeck coefficient obtained on cuprous sulfide with 10 mol % cuprous bromide are given in Table XXVI. Fracturing may account for the change of resistivity at room temperature at the end of the run.

TABLE XXVI

Resistivity and Seebeck Coefficient of Cu_2S-10% CuBr

Temp Range °C	Seebeck Coefficient V/°C	Temp °C	Resistivity ohm-cm
51-55	61	21	1.14×10^{-2}
212-225	131	47	1.12
224-230	149	231	0.49
276-286	143	297	0.53
309-312	186	310	0.54
610-627	250	460	0.62
		622	0.74
		23	1.49

*Department of the Navy contract number NObs 77017. Report No. 11, Bimonthly Progress Report for 1 August to 1 October 1960.

**Department of the Navy Contract NObs-77017. Stanford Research Institute Bimonthly Progress Report No. 12 for period 1 October to 1 December 1960.

Melts containing 50 mol percent cuprous sulfide with nickel sulfide and lead sulfide were prepared, giving p-type material. Lead lowered the melting point and may also decrease the thermal conductivity.

Cuprous telluride had a Seebeck coefficient of 13 μV/°C at 50°C rising to 75 μV/°C at 650°C. The resistivity at room temperature was 1.14×10^{-4} ohm cm., almost a factor of 100 lower than for cuprous sulfide. This is an unsatisfactory material in the pure state but might be attractive as a doping agent for Cu_2S.

Equipment for measuring thermal conductivity at high temperatures is being assembled.

Stanford Research Institute* has examined several compositions of the cuprous sulfide -- cuprous telluride system both in the liquid and solid state. Materials were prepared by heating each of the compositions of 25, 50, and 75 percent cuprous telluride mixed with cuprous sulfide to 1200°C, holding for four hours under a helium atmosphere and then allowing to cool to room temperature. The Seebeck coefficient and the resistivity of these p-type compositions as a function of temperature are shown in Figures 73 and 74, respectively, and cover the liquid as well as the solid phase. The peak in the Seebeck coefficient occurs at the solidification point.

The resisitivity of these compositions, shown in Figure 74, indicate a relatively constant value in the liquid and a decrease as solidification begins.

Adding cuprous telluride to cuprous sulfide lowers the resistivity and the Seebeck coefficient. Since the resistivity is decreased proportionately more than the Seebeck coefficient, there is some improvement of thermoelectric quality.

---

*Department of the Navy Contract NObs-77017. Stanford Research Institute Bimonthly Progress Report No. 13 covering period from 1 December 1960 to 1 February 1961 dated 28 February 1961.

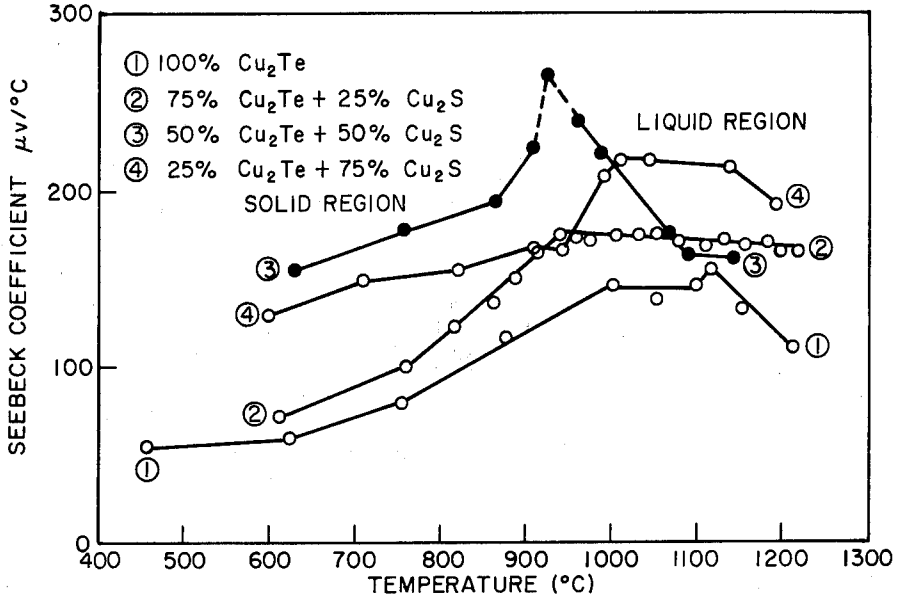

Fig. 73 - Seebeck Coefficient of Various Compositions of Cu_2 Te and C_2 S

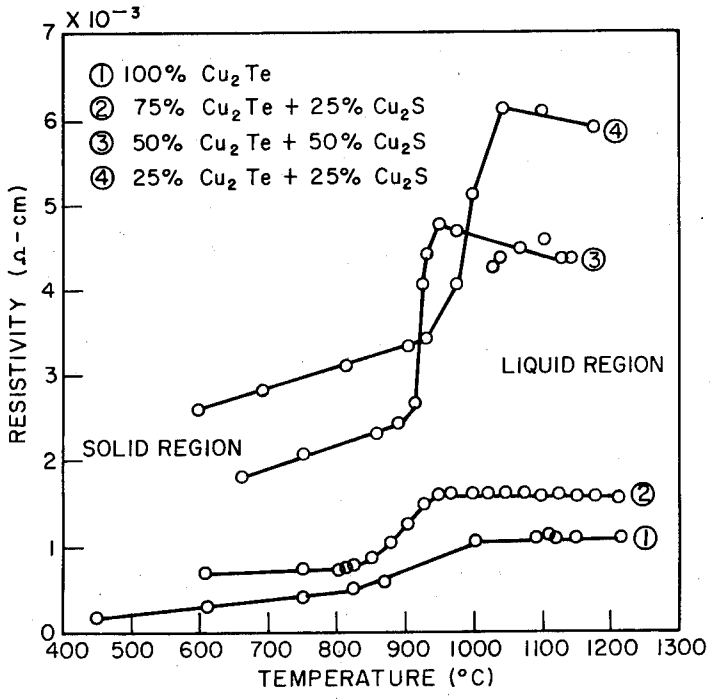

Fig. 74 - Resistivity of Various Compositions of Cu_2 Te and Cu_2 S

Calculated values of thermal conductivity required in the liquid state, assuming that **Z**T equals unity, are shown in Figure 75. In all cases the allowable thermal conductivity is greater than for pure cuprous sulfide. The nominal composition of 75% Cu_2Te + 25% Cu_2S appeared to be the best of those investigated. The temperature range of approximately 250°C which is available for this composition widens the range of applicability.

Thermal conductivities of Cu_2S up to 950°C were obtained using the Peltier method. The thermal conductivity, K, was calculated for two directions of current flow using the relationship,

$$K = \frac{TSIL}{A\Delta T} \quad \text{watts/cm°C}$$

where T is absolute temperature (°K), S is the Seebeck coefficient (volts/°C), I is current (amperes), L is length of sample between thermocouples (cm), A is cross-sectional area of samples (cm^2), and ΔT is temperature differential between the ends of the sample established by passage of current. The calculated values of K were then averaged to give the value of thermal conductivity at the particular temperature. The results are given in Table XXVII. The values are uncorrected as no correction was made for radiation loss, so they are higher than the correct value, the discrepancy increasing with increasing temperature. More accurate high temperature thermal conductivity data is planned to be obtained for the liquid state by using the comparison method with fused quartz in anargon atmosphere of one atmosphere pressure.

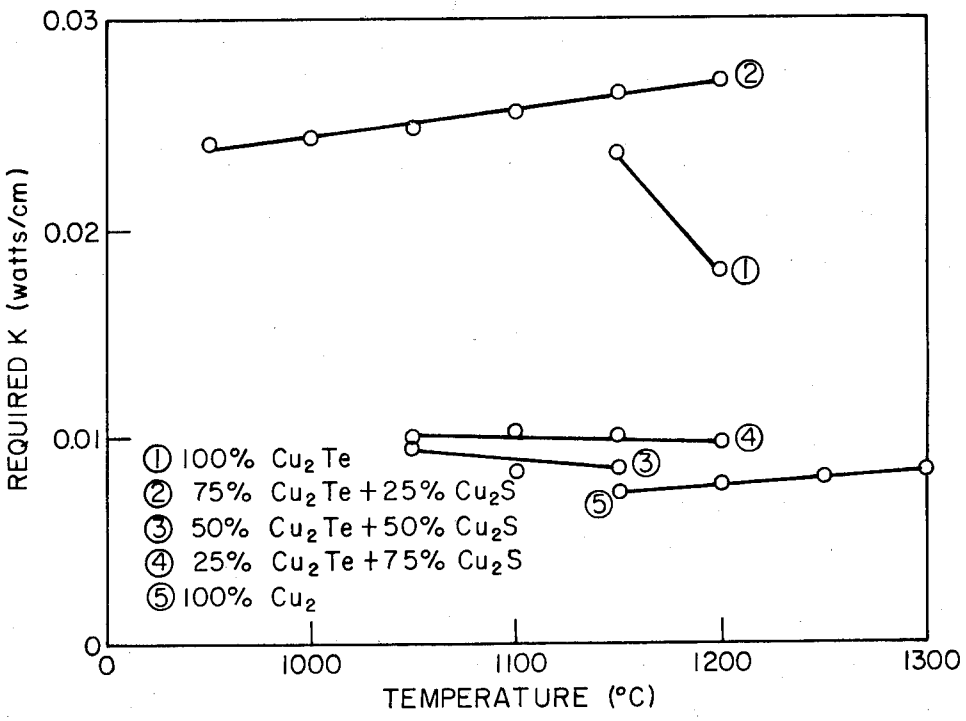

Fig. 75 - Calculated Values of Thermal Conductivity Required for ZT = 1 in the Liquid Range

TABLE XXVII

Thermal Conductivity of Cuprous Sulfide

Temperature (°C)	Uncorrected Thermal Conductivity - [watts/(cm-°C)]
74.5	0.0079
409.4	0.016
626.9	0.051
717.9	0.054
732.7	0.064
758.7	0.075
851.0	0.10
954.0	0.13

PREPARATION AND PROPERTIES OF THERMOELECTRIC MATERIALS

The Institute for Exploratory Research, U. S. Army Signal Research and Development Laboratory* are performing preliminary work in preparing compounds of the Tungsten-Telluride (W-Te) system by (1) direct synthesis and by (2) precipitation by wet process. Only a small number of samples have been prepared. Study of the physical properties of the semi-conducting thermoelectric materials has hardly begun. X-ray analysis on materials obtained by direct synthesis indicated that WTe_2 was probably obtained. The resistivity appeared as varying little versus temperature (10°C to 200°C). In the precipitation method Sodium Telluride (Na_2Te) was first prepared by direct synthesis, then Tungsten-Telluride by precipitation from Sodium Tungstate and Sodium-Telluride solution. It was the more difficult method. The results are under analysis.

*Department of the Army Contract No. DA 91-591-EUC-1505. First Quarterly Progress Report covering period 1 June to 30 October 1960.

RARE EARTH CHALCOGENIDES

The University of Pittsburgh* is performing research on refractory sulfides, selenides, and tellurides of rare earths. The development of suitable thermoelectric materials utilizing ceric oxide proved to be unfeasible. Cerium sulfide, Ce_2S_3, is a semi-conductor and by proper doping becomes a thermoelectric material. Ce_2S_3 has been produced by using carbon disulfide as the reducing agent at 750-850°C. The ceria was heated in a tube furnace. The toxic and explosive CS_2 was handled using argon as a carrier. A very complex reaction product resulted which has not been identified.

*Department of the Navy Contract NObs 77068. University of Pittsburgh Technical Progress Report covering period 1 September to 30 November 1960 dated 1 December 1960.

HIGH TEMPERATURE SEMICONDUCTING COMPOUNDS FOR THERMOELECTRIC POWER GENERATION

The Electro-Optical Systems, Inc.* are preparing to search for high temperature semiconducting compounds for thermoelectric power generation. Their study of systems will include combinations of uranium and/or thorium with sulfur, selenium and/or tellurium. Synthesis of ThS_2, ThS and other stoichometry is being undertaken. Test apparatus and higher purity raw materials are being procured.

*Department of the Navy contract NObs-84327. Electro-Optical Systems, Inc. Bi-monthly Progress Report No. 1 covering period 15 December 1960 15 February 1961.

THERMOELECTRIC GENERATOR MATERIALS*

Some of the best materials known at present which are suitable for use in thermoelectric generators are Bi_2Te_3 and its alloys, PbTe, the III-V compounds, Mn Te, Ge Te, and CeS. The theoretical maximum overall efficiency of an infinite stage generator using these materials and operating between 30°C and 1030°C is 18.3%.

In relation to design considerations a schematic diagram for a thermoelectric generator (Seebeck-effect) and a cooling device (Peltier-effect) T_c and T_h are assumed to have zero electrical resistance. The thermoelectrical materials or arms are p and n. The maximum efficiency of the device, defined as η = $\frac{\text{power dissipated in load R}}{\text{rate of heat removal from hot reservoir}}$

is given by:

$$\eta = \left(1 - \frac{T_e}{T_h}\right) \frac{\sqrt{1 + Z\bar{T}} - 1}{\sqrt{1 + Z\bar{T}} + T_{e/T_h}}$$

where $\bar{T} = 1/2\,(T_c + T_h)$.

If the two arms of the device have the same resistivity ρ, thermal conductivity K, and the same magnitude but opposite sign for their Seebeck coefficients, S, the figure of merit Z, is given by

$$Z = \frac{S^2}{K\rho}$$

---

*Scientific Paper 414 FR 801-P1 of August 1, 1960, by R. C. Miller and R. W. Ure, Jr. Westinghouse Research Laboratories

The only way that the properties of the material effect the efficiency is through this figure of merit. Assumptions made in deriving the efficiency equation which are important for the considerations here are that (1) the contacts between thermoelectric materials and heat reservoirs are of negligible resistance, (2) the ratio of n arm area to p arm area and the load resistance are adjusted to maximize the efficiency, (3) there is perfect thermal insulation, i.e. there is no heat loss from the hot reservoir except through the thermoelectric arms, n and p.

For higher efficiency and greater power per unit weight the hot junction temperature T_h should be as high as possible and the cold junction temperature T_c as low as possible, with the factor of merit of the material as high as possible. Most materials have their high factor of merit over a limited temperature range. Accordingly, a generator working over a wide temperature range would usually use several different materials. Two arrangements for the materials are (1) multistage or cascaded and (2) segmented. These are shown schematically in Figure 77. Referring to the cascade (two couple) scheme, the heat from the cold end of one couple flows into the hot end of the next couple. Straps A and C have high electrical and thermal conductivity. B is an electrically insulating material of high thermal conductivity so there is no temperature drop between A and C. The segmented arrangement shows one couple with two materials in the p arm. Strap D has high electrical and thermal conductivity.

Assuming that there is no temperature drop across the electrical insulation, B, in the cascaded device, then that device is more efficient than the segmented device and its efficiency increases with increase in the number of stages.

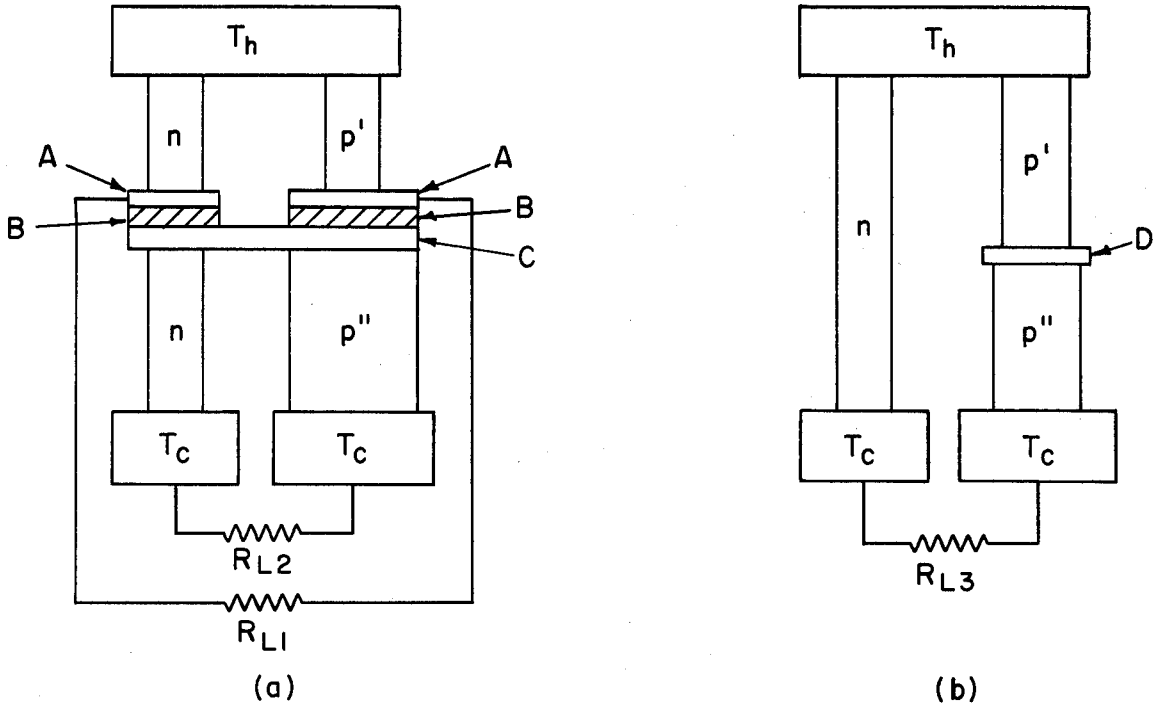

Fig. 77 - Materials in Cascaded (a) and Segmented (b) Arrangements

The figure of merit of a semiconductor is a function of the density of charge carriers in the material. The number of carriers can often be changed by adding suitable impurities to the semiconductor provided the energy gap between the valence and conduction bands is large enough.

Bi_2Te_3 has been used as a thermoelectric refrigerator material. Also, it and its alloys are useful materials for the low temperature end in thermoelectric generators. The electron mobility is 310 cm^2/v sec and the hole mobility is 400 at room temperature. The electron effective mass is $0.45 m_o$, where m_o is the free electron mass, and the hole mass is $0.51 m_o$. Its lattice thermal conductivity is 0.016 w/cm°C at room temperature. The figure of merit of some n-type materials is shown in Figure 78 and of some p-type materials in Figure 79. The figure of merit drops rapidly with increasing temperature because of the small energy gap. The thermoelectric properties of n-type materials $Bi_2Te_{2.4}Se_{0.6}$ + 0.05 wt. % CuBr and Bi_2Te_2Se + 0.10 wt. % CuBr are plotted in Figure 80 and Figure 81, respectively. Those for p-type material are given in Figure 82. PbTe is an intermetallic compound crystallizing with the NaCl structure and melting at 922°C. The electron mobility at room temperature is 1700 cm^2/v sec and the hole mobility is 800. The effective mass is $\sim 0.3 m_o$, assuming acoustic mode lattice scattering. The lattice thermal conductivity is 0.019 w/cm°C at 60°C. The figure of merit of n- and p-type materials from data by R. W. Fritts on cast materials is shown in Figures 83 and 84. Westinghouse Laboratories have produced materials of the same figure of merit by pressing and sintering. The figure of merit for the p-type material decreases more rapidly than that for n-type material as the temperature is raised. Some difficulty is experienced in using these materials at temperatures above 500°C because of their high vapor pressure.

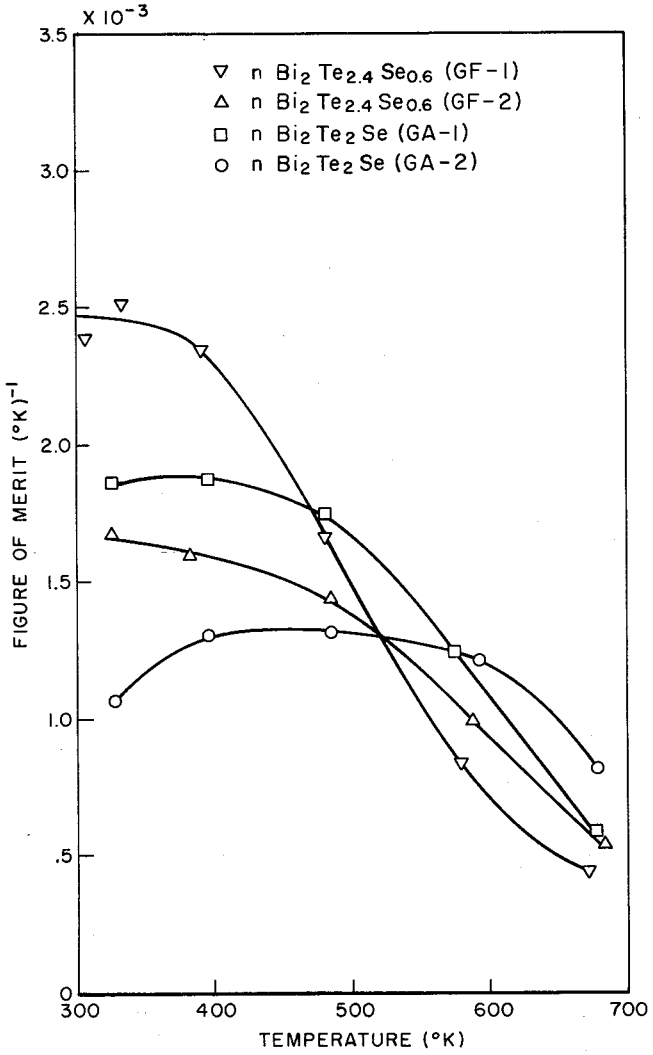

Fig. 78 - Figure of Merit of Some N-Type Materials

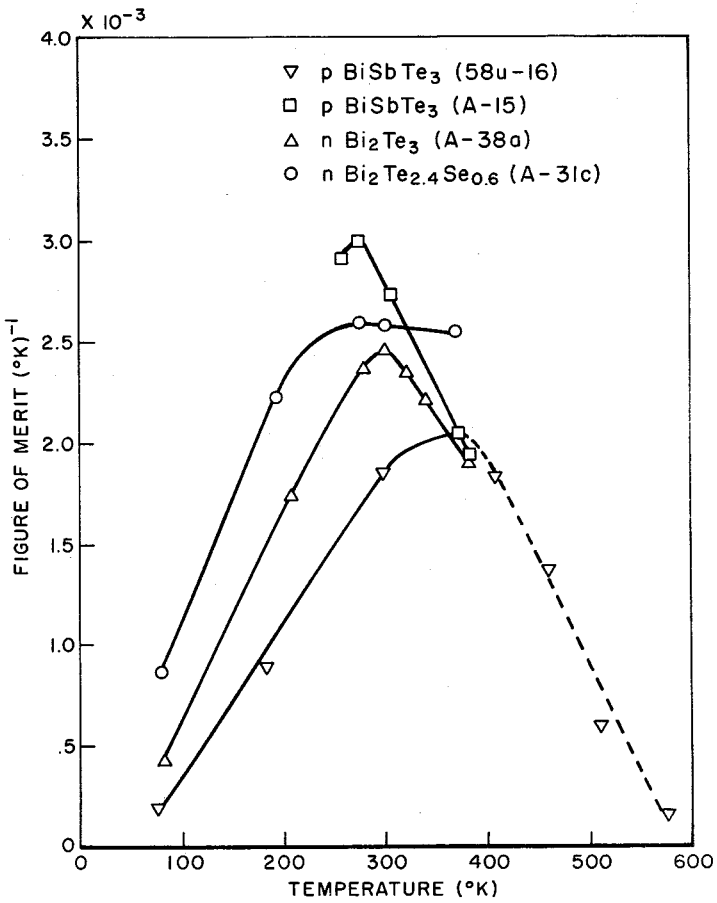

Fig. 79 - Figure of Merit of Some N and P-Type Materials

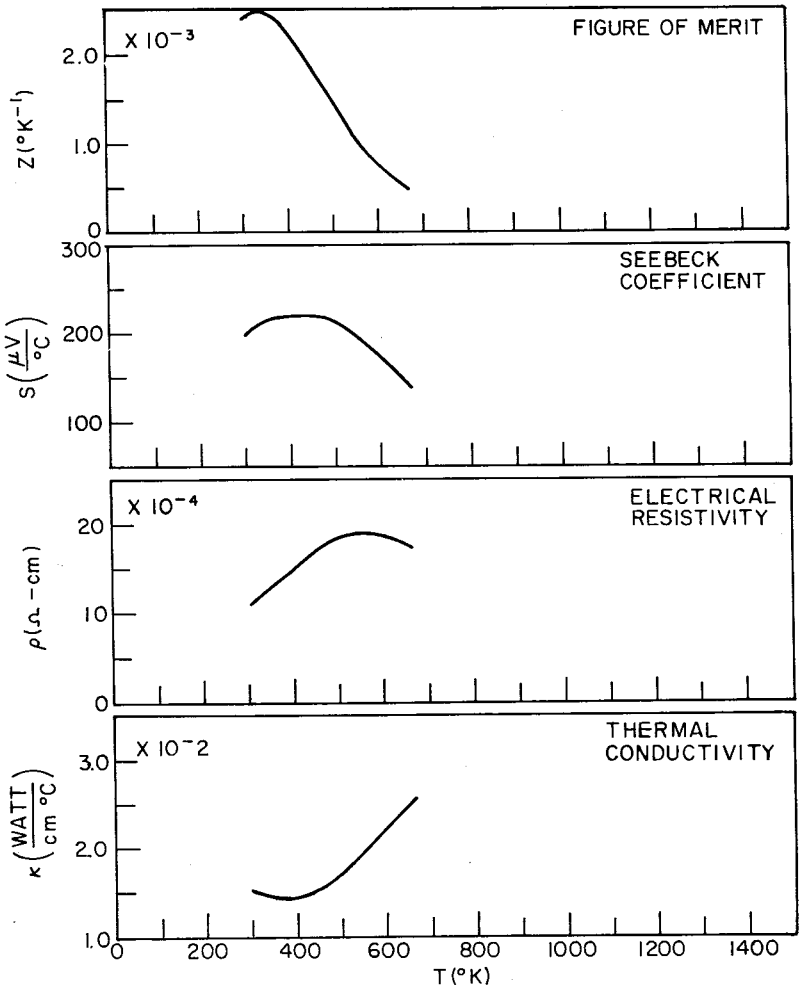

Fig. 80 - $Bi_2 Te_{2.4} Se_{0.6}$ + 0.05 wt. %
CuBr (n type)

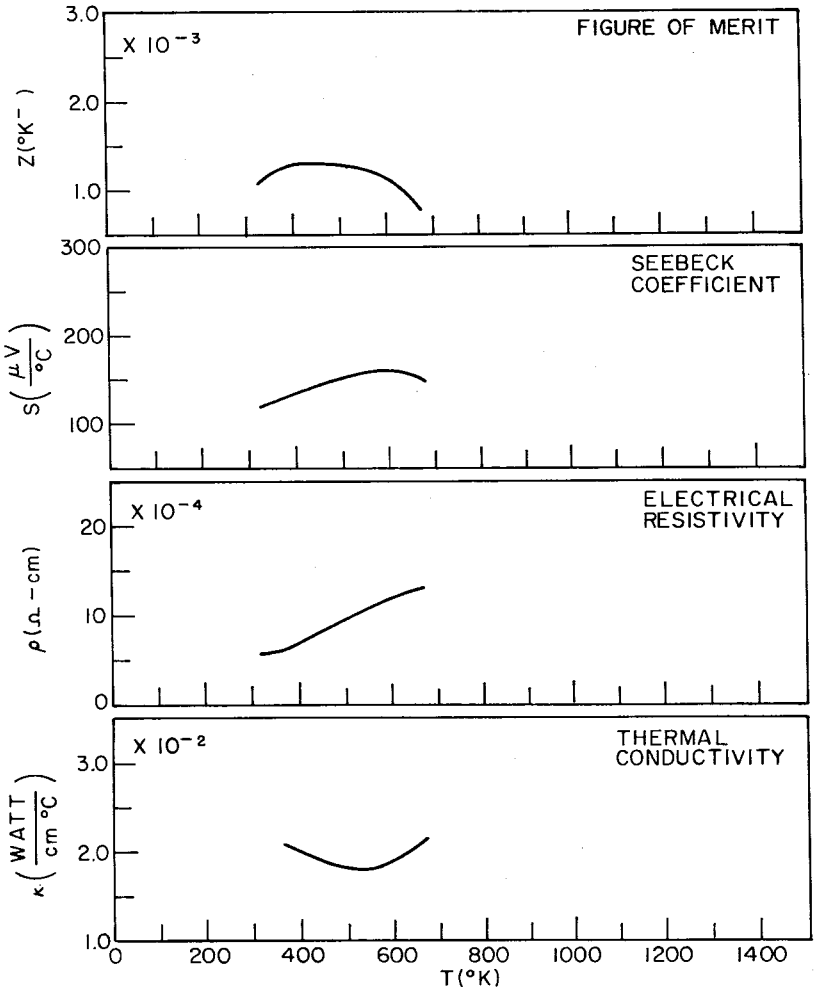

Fig. 81 - $Bi_2 Te_2 Se$ + 0.10 wt. %
CuBr (n type)

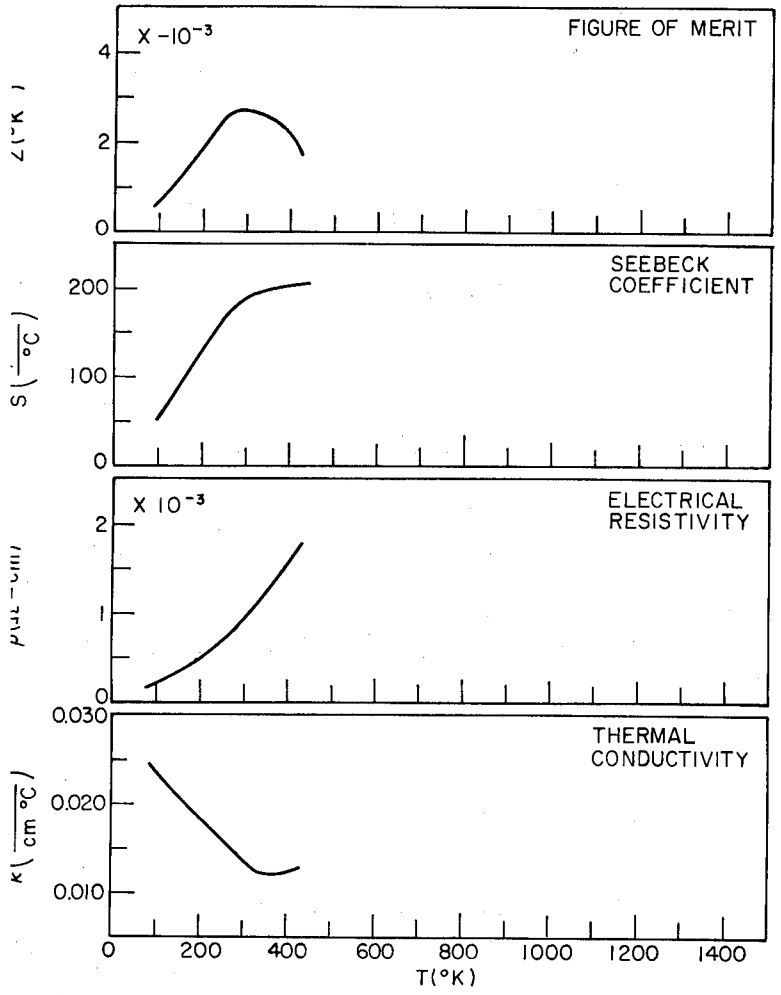

Fig. 82 - $(BiSb)_2 Te$ (p type)

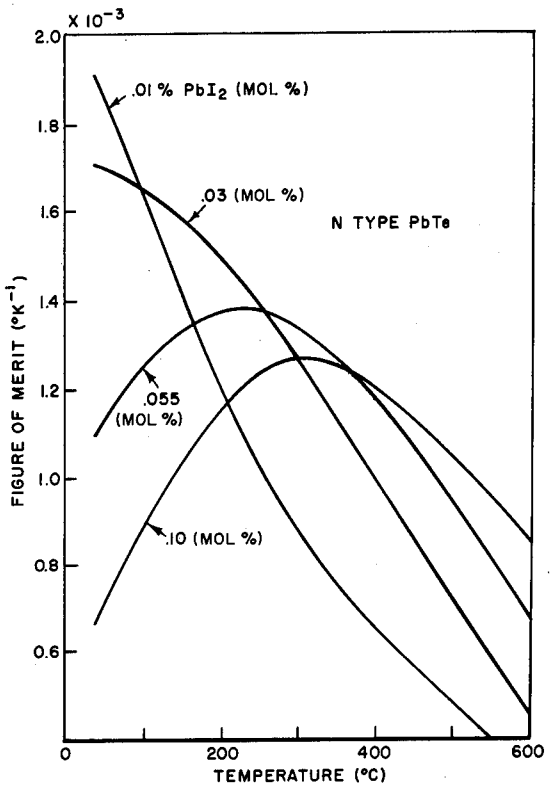

Fig. 83 - Figure of Merit of Some N-Type Lead Tellurides

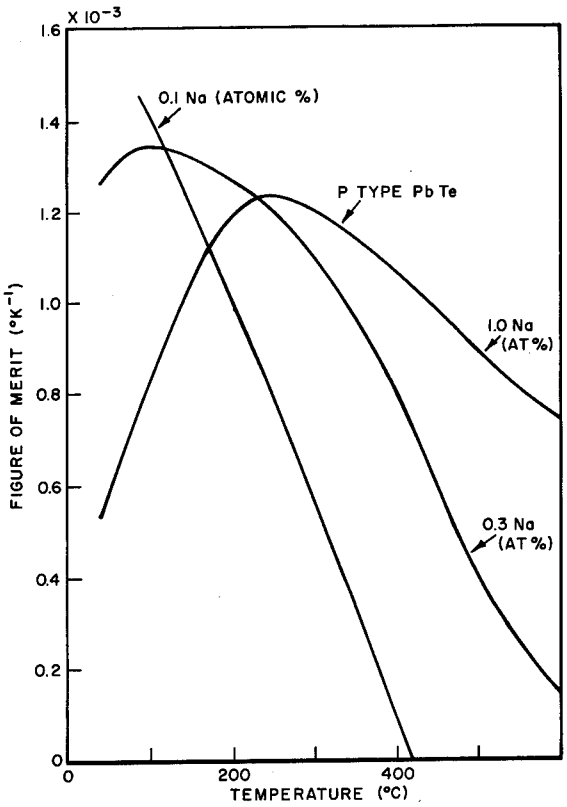

Fig. 84 - Figure of Merit of Some P-Type Lead Tellurides

The III-V compounds are those formed from the elements in the III A (B, Al, Ga, In) and V A (P, As, Sb) columns of the periodic table. Most of them crystallize in the zinc blende structure. Some have very high mobilities and small effective masses. InSb has an electrical mobility of 63,000 cm^2/v sec at room temperature and an electron effective mass of $.014m_o$. The thermal conductivity of InAs is moderately high being 0.26 w/cm°C at 300°K and its effective mass is small. The energy gap is moderately small so the materials are intrinsic over much of their operating temperature range. The hole mobility is much smaller than the electron mobility. In the intrinsic range the Seebeck effect remains large and the ambipolar thermal conduction small. A consequence of the small energy gap is that, as the temperature is raised, the number of carriers increases and soon exceeds the number which optimizes the figure of merit. Because of the small effective mass, the optimum carrier concentration is $10^{18} cm^{-3}$ rather than 10^{19} or greater as in most other thermoelectric materials. These materials are useful only as n-type materials. Figure 85 shows the figure of merit of InAs and $InAs_{1-x}P_x$. Over most of their useful temperature ranges InAs and InSb are intrinsic and hence it is not necessary to dope them in order to get the optimum carrier concentration. However, in order to use InAs below about 600°C, the carrier concentration should be adjusted to approximately $10^{18} cm^{-3}$ by suitable doping. Addition of InP to InAs may increase the figure of merit.

Zinc antimonide, ZnSb, is a useful p-type thermoelectric material and has been used in generators. It is prepared by hot pressing procedure. The compound obtained from the elements alone has a carrier concentration smaller than optimum and a small amount of silver is added to give optimum doping. A further addition of tin increases the mobility without increasing the number of carriers. Properties of a sample of ZnSb are shown in Figure 3.

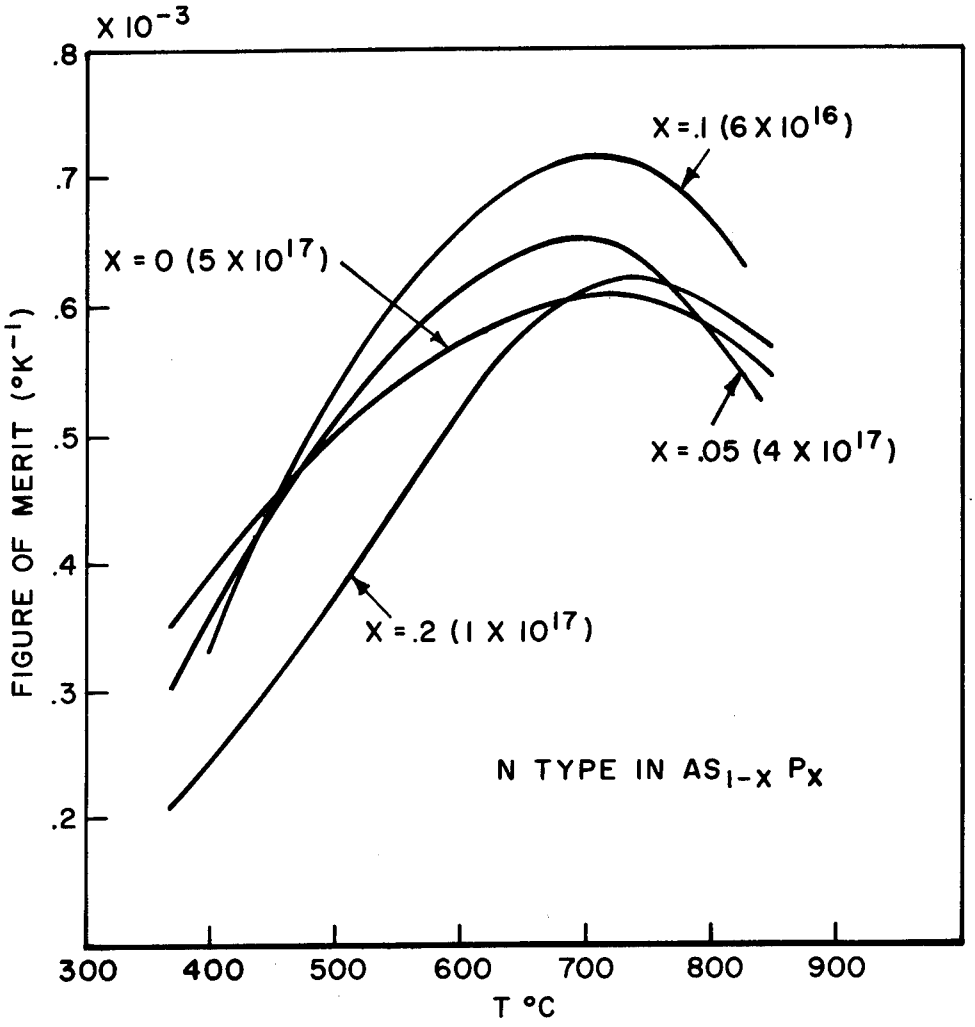

Fig. 85 - $InAs_{1-x}P_x$

Manganese telluride, MnTe, has been proposed as a high temperature (800-1300°K) p-type thermoelectric element. The compound melts at 1440°K and appears to be reasonably stable in the proposed operating range. Figure 14 shows data on a sample doped with 1% Na. From 400 to 800°K the material behaves like a typical semiconductor. The mobility is very low, $\sim$ 2 cm^2/v sec at 400°K. The effective mass appears to be greater than twice the free electron mass. Above 700°K the behavior is complicated and not fully understood. Until a better doping agent is found, MnTe cannot be obtained at its optimum figure of merit.

The phase diagram of the germanium-tellurium system shows only a single compound having the nominal composition GeTe. It melts congruently and is of composition $GeTe_{1.025}$. Above 700°K it has the NaCl type structure while below this temperature there is a rhombohedral distortion of the NaCl lattice which increases with decreasing temperature. The material is always p-type and shows no significant difference in electrical properties between different samples. The mobility is low, $\sim$ 50 cm^2/v sec at room temperature. The lattice thermal conductivity is between .01 and .03 watts/cm°C and not strongly temperature dependent. The electron effective mass is 3.2 m_o if acoustic mode scattering is assumed and 1.75 m_o if optical scattering is assumed. The Hall coefficient has been measured from 78 - 600°K and is roughly 7×10^{-3} coulombs/cm^3. The calculated carrier concentration is 0.9×10^{21} cm^{-3} and too high to give optimum figure of merit. The mobility is low. Optimum doping material has been obtained with Bi. Figure 86 gives the data for a compound having the approximate composition of 95% GeTe and 5% Bi_2Te_3. The figure of merit (maximum) is approximately 1.7×10^{-3} $°C^{-1}$. The figure of merit for GeTe is lower having a maximum of 0.9×10^{-3} $°C^{-1}$ between 800 and 900°K.

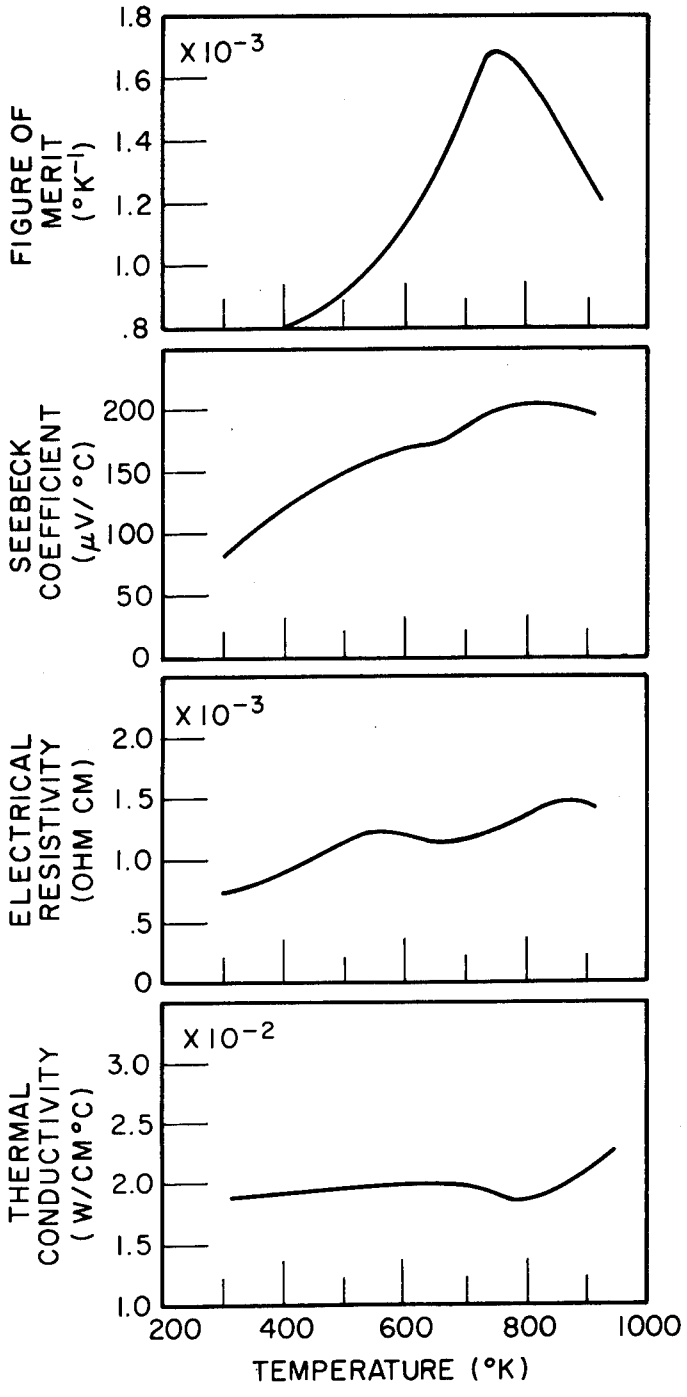

Fig. 86 - 95% GeTe + 5% $Bi_2 Te_3$

In the cerium-sulphur system the compound CeS has the NaCl structure and appears to be a metal. Its Seebeck coefficient never rises above 30 μV. The compounds in the range $CeS_{1.5}$ to $CeS_{1.33}$ all have the Th_3P_4 structure. The composition near $CeS_{1.38}$ appears to have the maximum Z in the range 900 to 1100°C. The properties of $CeS_{1.38}$ and $(CeS)_{1.39}(SrS)_{.07}$ are shown in Figure 10.

Thermoelectric generators have been built having power outputs ranging from 5 watts to 5,000 watts. The power output per unit weight varies from 1 watt/lb (5 watt) to 2.2 watt/lb (100 watt). The measured efficiency varies from 3.7% (neglecting flue losses) to 5.5% (radioisotope heated) or 7%. There are several reasons for the actual efficiency being much lower than the theoretical maximum of 18.3%. Any resistance at the contacts between the materials reduces the performance. It is difficult to make a low resistance contact that will be stable, strong, and not diffuse into or react with the material at high temperature. Most devices have been segmented rather than cascaded (multistaged). If the materials have sufficiently different properties, the segmented device will not have as high efficiency as the corresponding cascaded device. Any temperature drops across the electrical insulation between the stages of the cascaded device will lower the efficiency. In many cases this reduction is sufficient to wipe out the theoretical advantage of the cascaded device. Some materials are difficult to use because of their poor strength at high temperatures, mismatched expansion coefficients, or problems connected with vaporization. Materials have been developed which are capable of giving an efficiency of 18.3% for a thermoelectric generator. Their utilization still offers formidable problems. Materials with higher figure of merit and better mechanical, chemical, and electrical properties which can be used more effectively in actual generators are needed. The electronic properties of some thermoelectric materials are presented in Table No. XXVIII.

TABLE XXVIII

Material	Electron Mobility, μ, cm^2/v sec	Hole Mobility	Electron Effective Mass	Hole Mass	Lattice Thermal conductivity, watts/cm°C
Bi_2Te_3	310 @ rm.temp.	400 @ rm.temp.	0.45 m_o	0.51 m_o	0.016 @ rm.temp.
PbTe	1700 @ rm.temp.	800 @ rm.temp.	~ 0.3 m_o		0.019 @ 65°C
InSb	63,000 @ rm.temp.		0.014 m_o		
InAs	(large)		(small)		0.26 @ 300°K
MnTe (Na doped)	~ .2 @ 400°K				
GeTe	~ 50 @ rm.temp.		3.2 m_o (if acoustic mode scattering) 1.75 m_o (if optical mode scattering)		0.01 - 0.03 @ rm. temp.

Where m_o is the free electron mass

Radio Corporation of America* reports measurements on a thermoelectric power generator having a sandwich construction with two materials in each branch have shown an efficiency of at least 11%. The low temperature side of each arm was of bismuth telluride compounds. For temperatures below 300°C their efficiency was about 6.5%. The high temperature sides of each arm was of GeTe-$AgSbTe_2$ alloy and a PbTe material.

*Department of the Navy Contract No. NObs 77057. RCA Quarterly Progress Report No. 7 covering period 1 August to 31 October 1960 dated 15 November 1960.

5 KILOWATT THERMOELECTRIC GENERATOR

The Westinghouse Electric Corporation, New Products Laboratories*, have tested a full scale thermoelectric generator and an individual module. Some information on the Westinghouse 5-KW experimental thermoelectric generator has been given previously in NRL Memorandum Report 1089 of August 1960. This water cooled generator converts the thermal energy of combustion of kerosene or other fuel oils directly into useful electric power.

The assembled 5-KW generator consists of two units. This was due to the limitations imposed on the present technology in available heat flux density. Each sub-generator consists of 14 thermoelectric generator "side" modules arranged circumferentially about the heat source, which is a fuel oil burner supplemented with radiation baffles to distribute the heat uniformly. Each module is of three sections and consists of a total of 85 thermoelectric couples. There is a four-section "top" module consisting of a total of 136 thermoelectric couples to utilize the heated surface area available at the top of the generator. The hot plate of this module forms the top of the combustion chamber area of the sub-generator. The strap connection (hot junction) between the two thermocouple legs is pressed against the hot side of the module. Short circuiting of the couples is prevented by coating the hot core with an electrical insulation. Each leg of the couple has thermal contact to the water-cooled plate of the module (cold junction) through a flexible copper braid conduction. The couple assembly is kept in compression by means of a coil spring around each braid. All couples are connected in series so that each module has an output of

*Department of the Navy Contract No. NObs 77093. Preliminary Report of August 1960.

approximately 8.5 volts at 200 watts into a matched resistance load of about 0.30 ohms. The modules can be connected in series, series parallel, or parallel as desired. Each module is electrically and mechanically independent of the other assemblies which facilitates removal or replacement.

The couple developed for the generator has an improved p-type material, GeBiTe, perfected for a 400 to 500°C temperature region of operation. It is a pressed composite of GeTe, GeBiTe, and ZnSb. A technique was perfected so that the powdered materials could be used in pressing each leg as a complete unit. Direct contact was made between the GeTe and GeBiTe and a Ni powdered interface was used between GeBiTe and ZnSb. A separately pressed pellet of BiSbTe was soldered on the cold end of the composite pellet to improve the performance in the low temperature region. The n-leg consisted of two pressed pellets. That for the high temperature section was made from powdered PbTe with pressed iron caps as contacts. That for the low temperature action was pressed n-type BiSbTe which was soldered to the cold end of the PbTe pellet.

Various high power burner systems were investigated to determine available heat flux, efficiency, and general over-all characteristics. It was determined that the most practical system was the forced draft atomized fuel burner. The basic components were commercially available and little development work on the burner was necessary. It was a safe and proven system and one without danger of flash back. The oil burner is mounted at the bottom of the unit and fires vertically.

In order to reduce thermal hot spots and large temperature gradients the hot "ball" or core of combustion gases are restricted by a three-pass gas distributor which is a primary combustion chamber located centrally

inside the main combustion area. The distributor's two concentric cylinders topped with a deflection and radiation shield act as baffles to abosrb the heat of combusion. The burner system of the generator is capable of producing heat flux densities as high as 70 watts per square inch with nearly uniform temperature along the walls of the combustion chamber. The vertical and circumferential gradients have been limited to ± 25°C.

Performance test results on the system are shown in Figure 87 for electrical power output versus hot side temperature. A 500 KW output is indicated at 600°C. A total of 5967 watts was generated during full power tests. Module efficiency versus hot junction temperature is shown in Figure 88. At 106°C the efficiency is slightly over 1/2 of 1% whereas for 585°C it is about 4.5%. Module efficiency versus module power output is shown in Figure 89. Module output voltage versus module load current for various constant hot side temperatures, the lowest being 106°C and the highest 585°C, is shown in Figure 90.

The generator represented an increase in power of greater than 50 times that available from any other single thermoelectric source. As short as one year prior to the construction of the generator, 100 watts was the greatest delivered electric power from any thermoelectric device. On the basis of the experienced gained in the construction of their 5-KW generator it was felt that its size and weight could be reduced by a factor of two if built today with present technology and information.

The finished generator was shipped to the U.S. Naval Experiment Station, Annapolis, Maryland, on 19 May 1960.

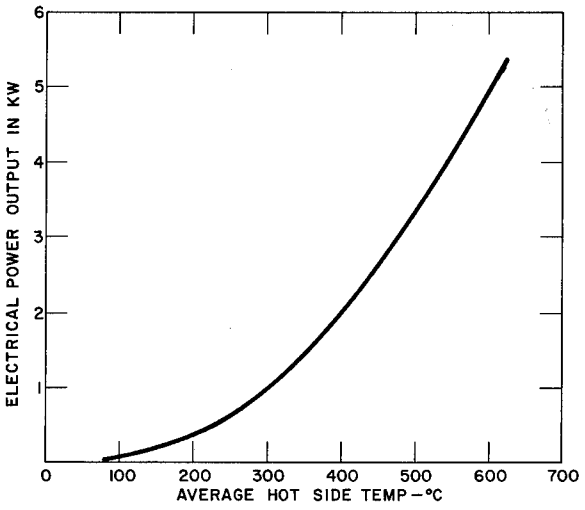

Fig. 87 - Total Generator Power Output vs Average Hot Side Temperature. (Summation of both subgenerators.)

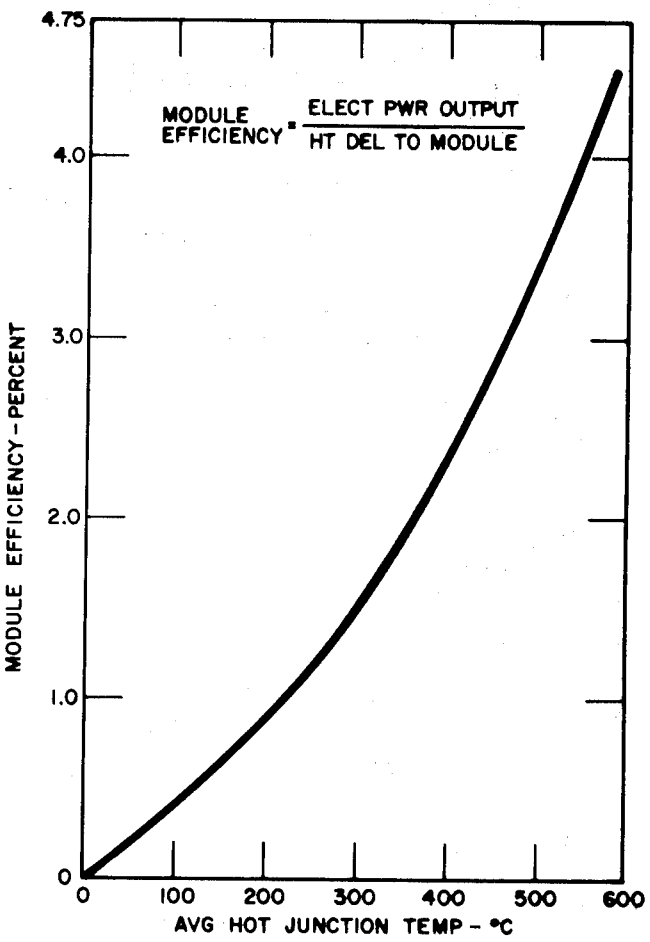

Fig. 88 - Module Efficiency vs Hot Junction Temperature

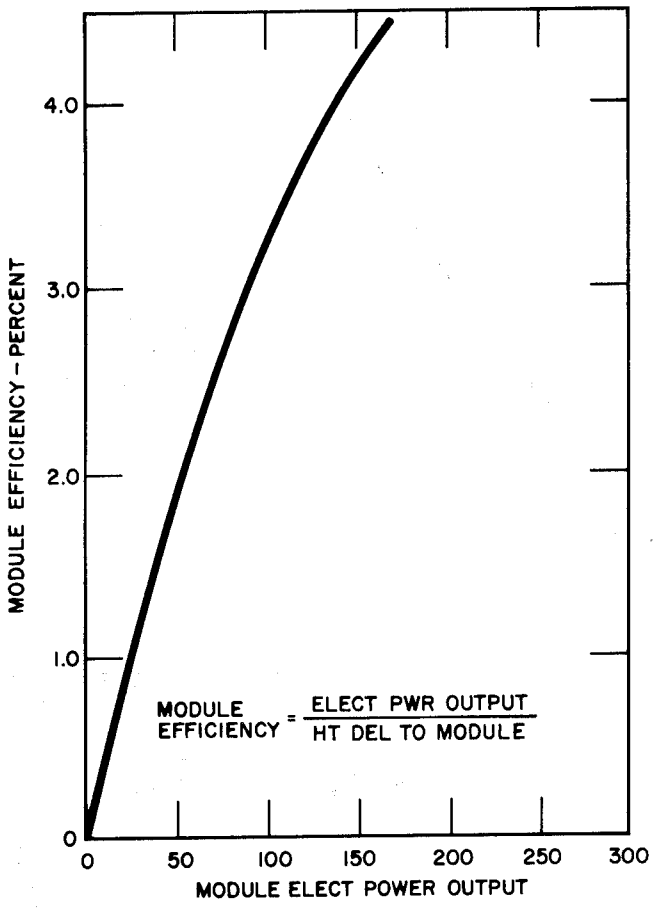

Fig. 89 - Module Efficiency vs Module Electrical Power Output

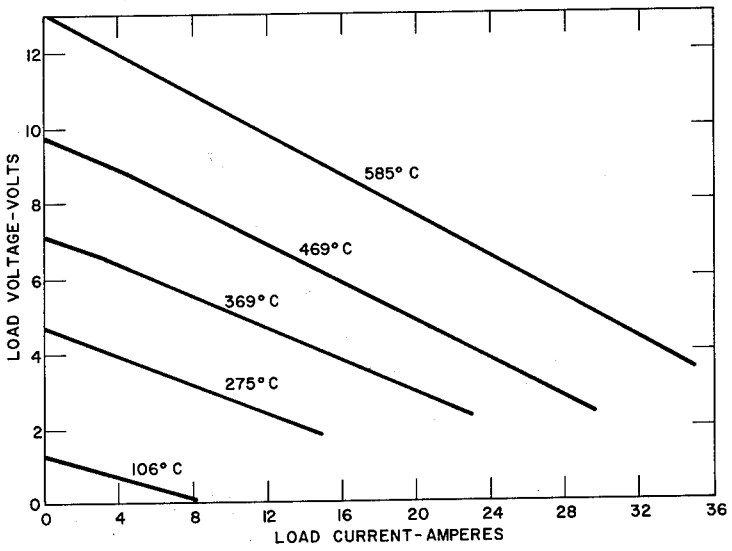

Fig. 90 - Module Output Voltage vs Module Load Current (at constant Hotside Temperature)

FIVE-HUNDRED WATT THERMOELECTRIC GENERATOR

The Minnesota Mining and Manufacturing Company's* report of progress towards the development of a 500-watt thermoelectric generator mainly pertained to thermocouple development and testing, burner system, heat rejection system, thermopile, and test equipment.

The chief problems with the thermoelements were the maintenance of stable, low resistance contacts and overcoming mechanical failure.

Test results on a full-size thermopile, used as an operational tester and employing a gas burner, were:

Power output	202 watts,
Power input	3200 watts,
Efficiency (excluding burner losses)	6% ,

with hot junction temperature 1018°F and cold junction temperature 268°F.

A double-ended burner was developed as a heat source. A test on the burner gave 46% efficiency of heat transfer, 50 watts/in.^{2} heat flux density at the collector wall, and 800°F collector wall temperature.

The heat rejection system included a spine-type heat exchanger.

Based on test results a redesign of the thermopile was considered desirable and new design changes were adopted. On the basis of test results on the new couples it was considered feasible to build a generator having the following specifications:

*Department of the Navy Contract No. NObs 78198. Third Progress Report of 12 December 1960.

Number of couples	279
Weight of generator	35 lbs complete
Power output (total)	300 watts
Fan requirements	50 watts
Useable power output	250 watts
Voltage at matched loads	28 volts
Hot junction temperature	1100 °F
Cold junction temperature	350°F

FIVE HUNDRED WATT PORTABLE THERMOELECTRIC GENERATOR

The Westinghouse Electric Corporation, New Products Laboratories*, are nearing the completion of a 28-volt, d-c, 500-watt thermoelectric generator to be used as a portable power source. The maximum weight of this generator is 35 pounds and its containable volume 20 x 12 x 8 inches by specification. The design uses the heat exchanger as a current carrying member, connecting adjacent couples as strap and braid configurations.

Initially the burner system will use propane gas. The propane aspirates sufficient air for proper combustion, thus eliminating the need for auxiliary power for combustion air. High heat transfer efficiency is obtained and flame instability is reduced. At present, the gasoline-fired system cannot be guaranteed for extended operations due to clogging of the burner nozzle. The effects of lead compounds in the gasoline upon the burner system must be determined.

Module assembly concepts considered were (1) solid aluminum core with pressure contact straps, (2) couples potted in solid modular form, and (3) individually fastened couples in a flexible frame. The pressure contact of straps upon a flat plate assembly technique has been used in previous generators. It provides the simplest reliable construction. The technique of potting the couples eliminates the need for a flat hot core. The couples are set in a frame and rigidly fixed in place by a ceramic-type potting compound. This assembly constitutes a thermoelectric module which may be joined to others to form a core. The individually-fastened couple assemblies, though more complicated to construct, do eliminate the problem of thermal drops and structural failure. The individual couples are fitted over thin rods and

*Department of the Navy Contract No. NObs 78197. Quarterly Progress Letter No. 4 of December 1960.

insulated from each other. The rods are then fastened inside a thin steel frame.

The structure utilizes bases erected on thin rods that are continually in tension. The upper shell of the generator is fabricated of thin, lightweight, honeycomb sandwich material.

RESEARCH AND DEVELOPMENT OF THERMOCOUPLE ENERGY CONVERTER

Servomechanisms, Inc.* have developed a miniature production type modular couple comprised of both "N" and "P" elements of lead telluride. This modular generator element is shown in Figure 91. Steel support rings were used because the green press pressure was sufficient to ensure close to theoretical density. The lead telluride material for the proposed 560 watt generator will be of the alloyed type doped to near optimum levels with bromide for the N-type and sodium for the P-type. The module exploits a simple partial encapsulation process. Miniature test models of single elements were fabricated completely enclosed within iron plated copper and mica containers. Encapsulation was determined to be necessary from results of heat treatments evidencing evaporation or sublimation of the components of the alloy. This was significant above 600°K.

Specimens of a representative engineering grade of lead telluride were used to investigate the effect of post green press sintering. They were cold pressed at 4000 psi and heat treated in a hot press furnace in an argon rich atmosphere. The modules compressing both N and P elements and including the associated contacts have developed electrical resistances very close which would be expected from the resistivity of the lead telluride elements alone.

*U.S. Army Ordnance Corps Picatinny Arsenal Contract No. DA-04-495-501-ORD-1816, Progress Report IV covering period 1 July 1960 to 30 September 1960.

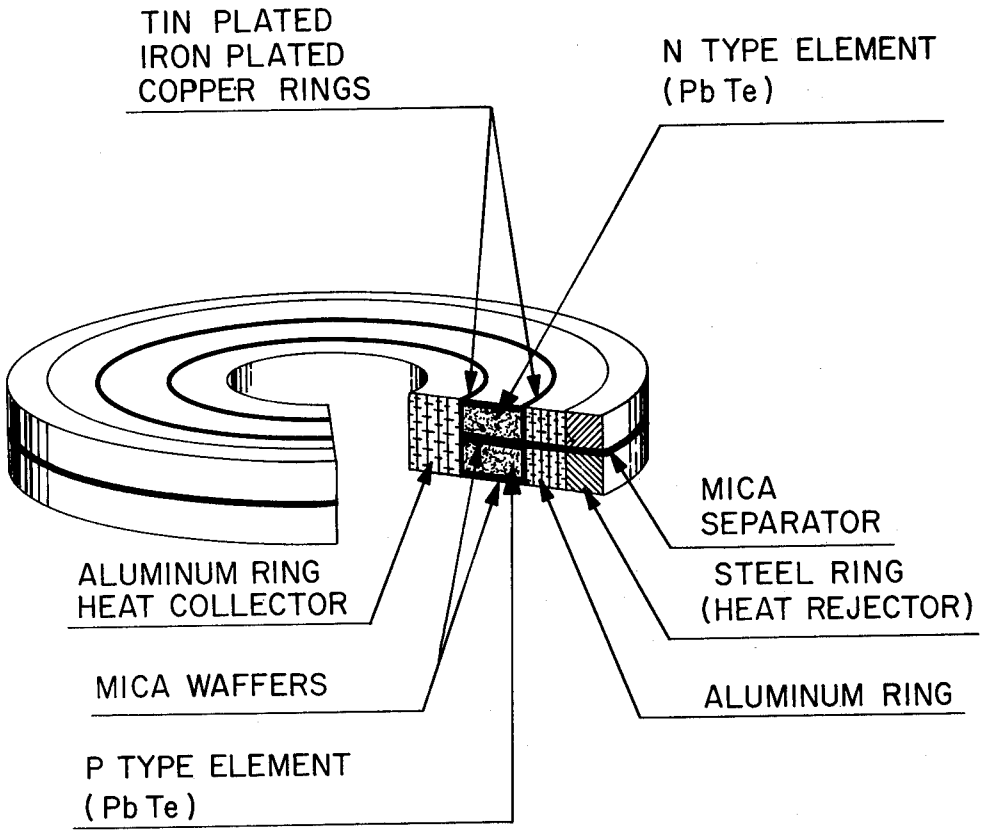

Fig. 91 - Modular Generator Element

PRELIMINARY DESIGN AND PERFORMANCE STUDY OF A SANDWICH THERMOELECTRIC CONVERTER OF SOLAR ENERGY

This paper* was presented at the Symposium on Thermoelectric Energy Conversion, sponsored by the Joint Technical Society and Department of Defense, held in Dallas, Texas, January 8-12, 1961. The converter consists of small thermocouple elements sandwiched between plane solar-energy-collector and space-radiator foils of aluminum. (See Figure 92). The collector absorbs solar energy some of which is converted to electricity by thermocouples. The unusable heat is conducted by the thermocouples to the radiator foil from which it is radiated into space. The thermocouple n-legs are PbTe and p-legs ZnSb. Converter sections are made which permits assembly into panels. The panels may be grouped in series-parallel arrangements. Methods of assembly of panels permit accordion-style folding and unfolding.

The surface of the collector receiving solar energy is covered with layers of vapor-coated SiO_2 and aluminum. The collector surface facing the radiator requires low emissivity at infrared wavelengths as does likewise the radiator surface facing the collector. The space side of the radiator is coated with glass to make it a good emitter.

Based on normal incident solar energy near the earth being 100% at 135 mw/cm^2, the electric output by the converter is 2.67% at 3.61 mw/cm^2.

The converter weight may be computed from the densities and thicknesses of the collector, thermocouples, and radiator. The number of thermocouples per unit of collector and radiator area varies directly with the solar constants and changes inversely with the converter efficiency.

---

*Paper by Robert J. Campana, General Atomic Division of General Dynamics, GA-1922, Project 5.19 of January 9, 1961.

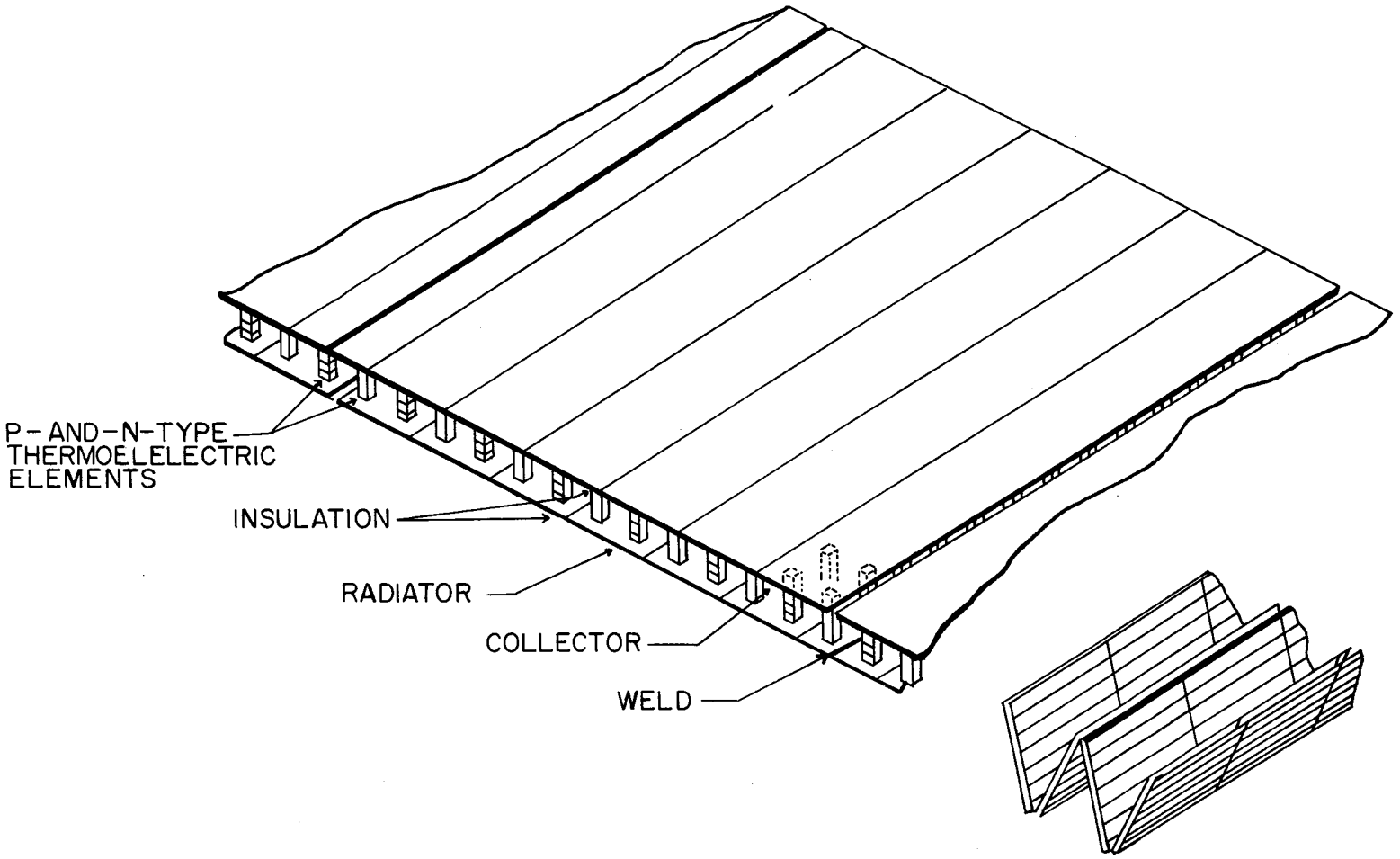

Fig. 92 - Solar Converter Panels

The performance of these generators was compared with other space power-supply systems. The performance of the solar generator is constant over a wide range of power capacities. The deterrent to use of the solar generator is the larger converter areas required because of the low energy-conversion efficiency. The disadvantage is that these areas must be unfolded and maintained in plane geometry in space. Comparison of the solar generator with the silicon-photocell is comparing a system in its early development stages with that of sophisticated operational system. Cost information available is that 0.90 $/watt for semi-conductor material and $\sim$ 1.50 $/watt each for evaporated coatings on the collector and radiator surfaces. The complete estimate of all items amounted to 12 to 16 $/watt based on the following assumptions: (1) 100 KW/yr would be required to power Earth satellites for five years, and (2) the total capacity would support only two manufacturers, sharing production equally.

Silicon-photocell costs based on a vendors price list were given. The cost, including facilities, equipment, and labor, would amount to 130 $/watt, assuming a 10% energy-conversion efficiency. It was stated that the thermocouple converter could produce power for 1/8 to 1/10 the cost of that produced by silicon-photocell conversion.

The thermocouple system is without moving mechanical parts. The conversion elements present very small targets to passing meteorites. Failure of a few cells would result in small decrease in capacity of the multiple cell system. Impairment of a heat flow path would cause a redistribution of the heat flow and its utilization by adjacent legs.

The solar thermocouple concept has potential for use in space-power production. Potential performance is dependent largely on the adequate thickness of the collector and radiator foils and on support and unfolding

mechanism weight. Study results show the potential for thermoelectric conversion of solar energy to be 30 lb/kw(e) for a single generator designed for Earth orbits and as close to the Sun as Venus.

OPTIMIZATION OF THERMOELECTRIC ENERGY CONVERTERS

General Electric Company* is conducting an analysis of a thermoelectric generator in the configuration shown in Figure 93, a planar thermoelectric converter. The study includes computer calculations for the performance of the thermoelectric arms, thermal insulation between the arms, and free-convection heat-rejection. The hot surface temperature was considered to be 533°K (saturated steam) and the cold surface temperature 291°K (salt water). The hot junction temperature, T_1, was assumed to be 505°K to provide an estimate temperature drop between the steam and the converter surface. A value of thermal flux was selected. Using heat transfer relations, the cold-junction temperature was calculated. The thermal resistance was then fixed and considered to remain constant, implying a constant heat flux. The heat leakage was that fraction of the heat flux that goes through the thermal insulating material rather than the semiconductors.

Optimized relations between power per unit weight, power per unit volume, and power per unit area of converter as a function of its efficiency are shown in Figures 94, 95, and 96, respectively.

The following materials properties were selected and used in making the calculations:

*Department of the Navy Contract NObs 78403. General Electric Company Bimonthly Progress Report No. 2 covering the period 15 June to 14 August 1960.

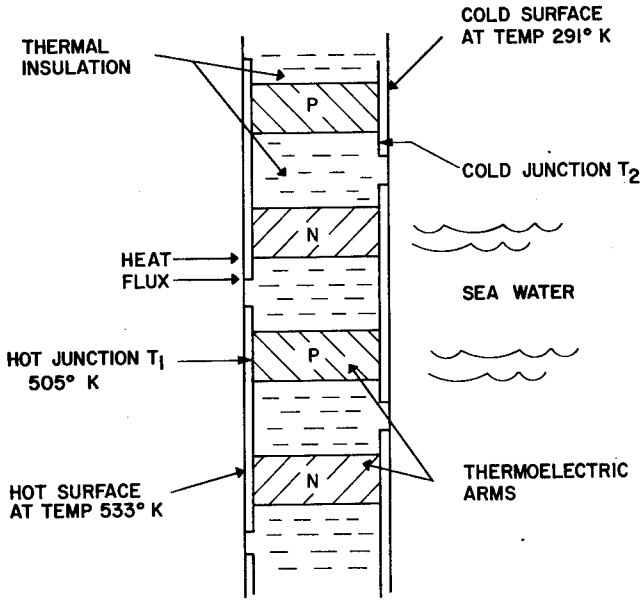

Fig. 93 - Schematic Drawing of Thermoelectric Converter

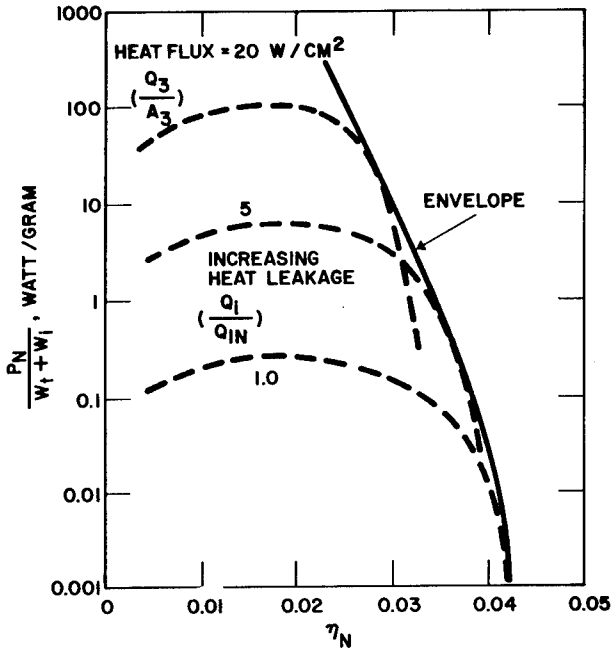

Fig. 94 - Power Output Per Unit Weight of the Converter as a Function of its Efficiency, Indicating the Effects of Heat-Leakage Through the Thermal Insulation for Several Values of Thermal Flux

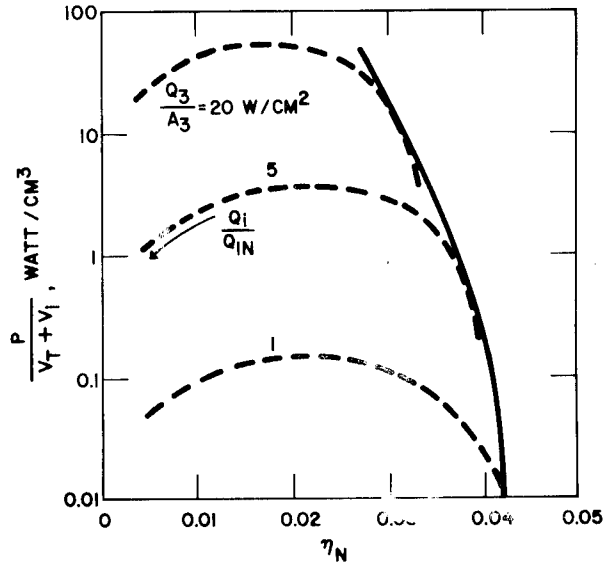

Fig. 95 - Power Output per Unit Volume of Converter Showing Same Parameters as in Fig. 90

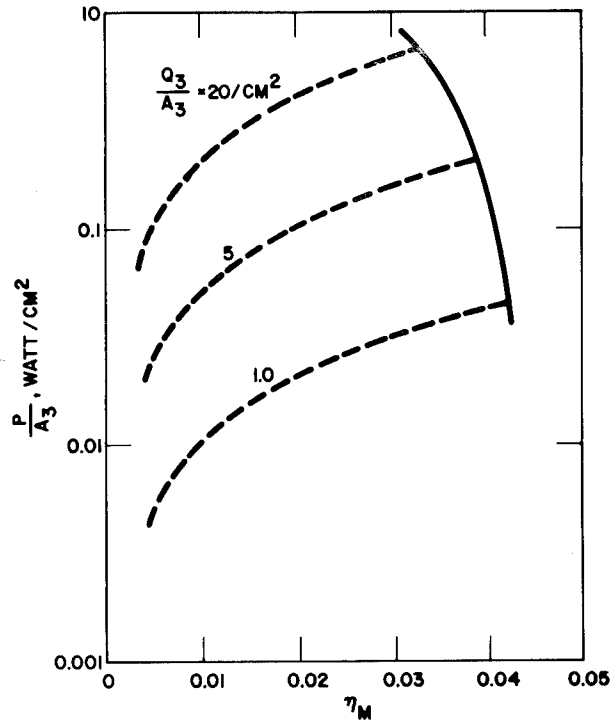

Fig. 96 - Power Output per Unit Area of Converter Showing Same Parameters as in Fig. 90

Thermoelectric Materials

Figure of merit	$1 \times 10^{-3}/°K$
Electrical resistivity, p-type	1×10^{-3} ohm cm
Electrical resistivity, n-type	0.5×10^{-3} ohm cm
Thermal conductivity, p-type	0.020 w/ cm°K
Thermal conductivity, n-type	0.026 w/ cm°K
Density, n and p types	$8.15\ g/cm^3$

Insulation

Thermal conductivity	0.4×10^{-3} w/cm °K
Density	$0.45\ g/cm^3$

The point representing no heat-leakage is the lower right-hand end of a constant-flux curve. In Figure 94 the power per unit weight represent the power output of the converter divided by the total weight of the thermoelectric and thermal insulation materials. Efficiency is the electrical power output divided by the total heat flowing into converter. The envelope curve (solid) shows the maximum power per unit weight for a specified efficiency. The values are limited since only the thermoelectric material and thermal insulation were considered. In Figure 95 the volume is that of the thermoelectric and insulation materials only. In Figure 96 the solid curve is the locus of points where heat leakage is zero.

The thermoelectric arms were assumed to have a rectangular cross-section and with planar conductor plates joining the ends of the arms and extending beyond them to form essentially a continuous surface on both the hot and cold sides of the converter.

Electrical contact resistance was treated as being external to the generator in order to use existing thermoelectric equations. However, for a practical generator it should be included as an additional internal resistance. Results on contact resistance are in considerable error for high flux, high heat-leakage and high contact resistivities (100×10^{-6} ohm cm^2), overemphasizing the effect. With low flux, low heat-leakage, and lower values of contact resistivity (10×10^{-6} ohm cm^2) the results are reasonably accurate and show contact resistance to be a significant factor.

Thermoelectric performance when using forced convection for heat rejection is similar to that of the free-convection case. Pumping power required was found negligible in most cases. Forced convection does not significantly improve efficiency since the cold-junction temperatures for each method are close to the sink temperature. Forced-convection is of interest since space, location, and attitude limitations may make free-convection impractical.

A magnesium oxide-titanium oxide ceramic material was found suitable for high-temperature encapsulation to 1500°C in conjunction with iron end-caps. Its coefficient of thermal expansion more closely approximates that of iron than does forsterite. It may permit reduction of the wall-thickness of encapsulating tubing, reducing thermal losses through the encapsulant. A disadvantage is that $MgO\text{-}TiO_2$ has rather high thermal conductivity around 300°C.

An improved high-temperature sealing apparatus has been constructed which can be operated up to 1700°C and in vacuum.

There are theoretical indications that thermoelectric materials possessing optimum properties at high temperatures, may be produced by allowing two selected high-melting substances, one having no energy gap

and the other a large gap semiconductor. Assumption was made that such a material could be produced by allowing chromium antimonide with manganese antimonide, a small-gap compound. The assumption appears erroneous. Indications are that the band-gap energy of chromium antimonide is lower than had been expected.

U. S. ARMY SIGNAL RESEARCH AND DEVELOPMENT LABORATORY
FORT MONMOUTH, NEW JERSEY

Project No.	:	3A99-20-001-01
Contract No.	:	DA 91-591-EUC-1505
Amount	:	$25,000
Title	:	Preparation and Properties of Thermoelectric Materials
Contractor	:	U.S. Army Signal Research and Development Laboratory, Exploratory Research Division E, Institute for Exploratory Research, Fort Monmouth, New Jersey.
Duration:	:	1 July 1960 - 30 June 1961
Gov't. Project Engineer	:	Dr. I. N. Greenberg, Ft. Monmouth, New Jersey Liberty 2-4000 - Ext. 52814
Principal Investigator	:	Dr. Pierre Aigrain
Purpose	:	Research in: Acquisition through experimental determination and verification of information, not now available, concerning methods of preparation and the physical properties of semi-conducting thermoelectric materials.
Reports to Date	:	First Quarterly Progress Report covering period 6-1-60 to 10-31-60 Second Quarterly Progress Report covering period 11-1-60 to 1-31-61

DEPARTMENT OF THE NAVY
BUREAU OF SHIPS
APPLIED SCIENCE DIVISION
APPLIED RESEARCH BRANCH
DIRECT ENERGY SECTION
(CODE 450)

Index No.	:	SF 013-06-01
Contract No.	:	NObs 84329
Amount	:	$336,900
Title	:	Improved Modules for Thermoelectric Generators
Contractor	:	Westinghouse Electric Corporation, New Products Division, Cheswick, Pennsylvania
Duration	:	1 January 1961 - 1 January 1962
Government Proj. Engineer	:	CDR Peter G. Bierel
Principal Investigator	:	William Evans
Purpose	:	Develop and build new improved modules for use in thermoelectric generators using new fabrication and materials.
Reports to Date	:	None

DEPARTMENT OF THE NAVY
BUREAU OF SHIPS
APPLIED SCIENCE DIVISION
APPLIED RESEARCH BRANCH
DIRECT ENERGY SECTION
(CODE 342B)

Index No.	:	SR 007-12-01
Contract No.	:	NObs 84327
Amount	:	$79,500
Title	:	High Temperature Semiconducting Compounds for Thermoelectric Power Generation
Contractor	:	Electro-Optical Systems, Inc. Pasadena, California
Duration	:	15 December 1960 to 14 December 1961
Government Project Engineer	:	B. B. Rosenbaum
Principal Investigator	:	W. E. Avis, William V. Wright C. B. Jordan (Project Supervisor)
Purpose	:	Research In: Search for high temperature semiconducting compounds for thermoelectric power generation. Systems included in studies are combinations of uranium and/or thorium with sulfur, selenium and/or tellurium.
Reports to Date	:	Bi-monthly Progress Report No. 1 for period 15 December 1960 to 15 February 1961